

Systematics of High Temperature Perturbation Theory: The Two-Loop Electron Self-Energy in QED

Emil Mottola

Theoretical Division

Los Alamos National Laboratory

*Los Alamos, NM 87545 USA**

Zsolt Szép

Statistical and Biological Physics Research Group

of the Hungarian Academy of Sciences,

H-1117 Budapest, Hungary[†]

(Dated: October 30, 2018)

In order to investigate the systematics of the loop expansion in high temperature gauge theories beyond the leading order hard thermal loop (HTL) approximation, we calculate the two-loop electron proper self-energy Σ in high temperature QED. The two-loop bubble diagram of Σ contains a linear infrared divergence. Even if regulated with a non-zero photon mass M of order of the Debye mass, this infrared sensitivity implies that the two-loop self-energy contributes terms to the fermion dispersion relation that are comparable to or even larger than the next-to-leading-order (NLO) contributions of the one-loop Σ . Additional evidence for the necessity of a systematic restructuring of the loop expansion comes from the explicit gauge parameter dependence of the fermion damping rate at both one and two-loops. The leading terms in the high temperature expansion of the two-loop self-energy for all topologies arise from an explicit hard-soft factorization pattern, in which one of the loop integrals is hard ($p \simeq T$), nested inside a second loop integral which is soft ($0 \leq p \lesssim T$ for real parts; $p \simeq eT$ for imaginary parts). There are *no* hard-hard contributions to the two-loop Σ at leading order at high T . Provided the same factorization pattern holds for arbitrary ℓ loops, the NLO high temperature contributions to the electron self-energy come from $\ell - 1$ hard loops factorized with one soft loop integral. This hard-soft pattern is a necessary condition for the resummation over ℓ to coincide with the one-loop self-energy calculated with HTL dressed propagators and vertices, and to yield the complete NLO correction to Σ at scales $\sim eT$, which is both infrared finite and gauge invariant. We employ spectral representations and the Gaudin method for evaluating finite temperature Matsubara sums, which facilitates the analysis of multi-loop diagrams at high T .

PACS numbers: 11.10.Wx, 11.15.Bt, 12.20.Ds

I. INTRODUCTION

The systematics of the usual loop expansion in powers of the weak coupling $e^2 = 1/137 \ll 1$ is well understood in quantum electrodynamics (QED), in perturbation theory about the vacuum state. However, when one considers extreme states of matter at high temperatures or densities, straightforward perturbation theory is of little use, even in a weakly coupled gauge theory like QED. At very high temperatures ($T \gg m_e$) one signal of the failure of the usual loop expansion is the appearance of infrared singularities of the form $(eT/\omega)^{2\ell-2}$, at ℓ loop order, where ω is a characteristic frequency, such as that of an external line in a self-energy diagram. The appearance of such infrared singularities implies that higher order terms in the perturbative series in e^2 are unsuppressed for low energies or momentum scales, and hence the usual perturbative loop expansion fails for $\omega \lesssim eT$.

The singular infrared behavior of perturbation theory at finite temperature can be seen already at the one-loop level. The leading order one-loop singularities arise from the ultraviolet or hard region of the momentum integral, whose power law growth is cut off only by the Bose-Einstein or Fermi-Dirac thermal distribution, so that the loop momentum becomes of order of the temperature T . These leading contributions in the high temperature expansion of one-loop self-energies and vertices are the hard thermal loops (HTL's) [1], studied extensively in the 1990's in both QED and QCD (see [2–5] for reviews). It was found that the leading order (LO) HTL self-energies and proper vertices enjoy some remarkable properties [6–8], among which is that they obey the same Ward identities as those of the exact theory. This enabled Braaten and Pisarski to propose an HTL resummation program [6, 8], in which the LO HTL propagators and vertices are used instead of the bare ones in any diagram in which the loop integration momentum becomes soft ($\sim eT \ll T$). This resummation algorithm was successfully applied to a number of problems, chief among them the first determination of the damping rate of gluons at rest in the high temperature QCD plasma, which is finite and free of any gauge ambiguities [9].

The Ward identities obeyed by the lowest order HTL self-energies and vertices, and the success of HTL resummation in producing gauge invariant physical quantities suggests it should be possible to restructure the perturbative loop expansion of gauge theories at high temperatures or densities in a systematic way. To do so, however, requires a more complete understanding of the infrared singularities of the subleading terms in the high temperature expansion at higher loops. The subleading or next-to-leading order (NLO) terms in the high temperature expansion of the one-loop level fermion self-energy have been computed

*Electronic address: emil@lanl.gov

†Electronic address: szepzs@achilles.elte.hu

[10, 11], but there have been only a few partial calculations of various quantities in different kinematic limits at two-loop order [12–16]. As a consequence, both the nature of the subleading infrared singularities of perturbation theory which HTL resummation includes and those which it does not include, and the general systematics of the reordering of the loop expansion at high temperatures beyond HTL’s, if it exists, has remained relatively unexplored.

The promising beginning of HTL resummation of infrared singularities, and the possibility of extending its success to higher orders in a systematic way is especially interesting in gauge theories. More than just a formal question about the nature of perturbation theory at high temperatures, the lack of systematic expansion methods that can capture both collective behavior and infrared physics in hot or dense matter, and also preserve gauge invariance and the UV renormalization structure of the underlying microscopic theory is a serious obstacle to physical applications in processes from the early universe to heavy-ion collisions, both in and out of equilibrium.

Motivated by these considerations, we present in this paper a calculation of the two-loop electron self-energy Σ in high temperature QED. Our approach is simply to calculate the two-loop self-energy in the high temperature limit, systematically extracting the leading terms at high T , without making any assumptions about the relative importance or unimportance of different contributions or momentum ranges, and without assuming *a priori* how they should be resummed. Once these leading terms in the high temperature expansion of the two-loop self-energy are known, they may be compared then with the known NLO terms of the one-loop self-energy [10, 11]. By explicit calculation we shall find that the *leading* terms in the high temperature expansion of the two-loop self-energy are of the same size, *or even larger* than the NLO terms of the one-loop Σ_1 when evaluated on the fermion mass shell. This is a direct demonstration of the need to take two and higher loops into account in order to obtain the full NLO result.

Dissecting the explicit two-loop self-energy calculation also allows for a more complete understanding of the relative importance of different momentum ranges in the loop integrations. It is already well known that the LO HTL result at one-loop order results from the strictly hard region of the loop integration where $p \sim T$. The NLO terms of the one-loop Σ arise from the region of the loop momentum integral which is parametrically less than T . For the case of the imaginary part of Σ , the relevant momentum scale is $p \sim eT \ll T$, while the real part of the self-energy receives contributions from the entire range of loop momentum $0 \leq p \lesssim T$, and give rise to $\ln(T/\omega)$ weak dependence upon the temperature. Although momenta up to T do play a role in the real parts, unlike the purely hard contributions which grow as a power of T , logarithms are a signal of sensitivity to the low momentum, infrared region of the loop integration as well. Following the convention in the field [1, 6], we term all such contributions where internal momenta of

order eT or less play an important role, *soft* loop integrals. We shall see that the leading order terms at two loops which are comparable to the NLO terms at one loop all come from momentum integrations where one of the loops is hard, while the other is soft, in the sense just described. Thus these comparable terms coming from one- and two-loop diagrams have in common that they arise from *exactly one soft internal momentum loop*.

An additional signal of the need for a reordering of perturbation theory comes from the gauge dependence of the one-loop self-energy, even when evaluated on the fermion mass shell. In the LO HTL limit, *i.e.* when the loop momentum is hard, the one-loop electron dispersion relation is independent of the gauge fixing parameter ξ . However at NLO in the high temperature expansion coming from the soft region of the loop momentum integral, the one-loop dispersion relation becomes dependent upon ξ [10, 11]. This is sufficient proof that the NLO one loop calculation is incomplete and physically meaningless by itself, and a systematic resummation method to obtain gauge invariant results for physical quantities such as the fermion damping rate at order e^2T is necessary. Our calculation will show that this gauge dependence is not cured at two-loops, and a full resummation of higher loops is necessary in order to arrive at the full NLO gauge invariant decay rate of an on-shell fermion in the plasma of order e^2T .

When higher numbers of loops are considered, we encounter a new phenomenon not present at one loop. At two-loop order in addition to gauge parameter dependence of the on-shell dispersion relation, we encounter uncanceled true infrared and/or collinear divergences, not regulated even at finite values of the soft external energy ω , or momentum \mathbf{q} . In particular, a linear infrared divergence appears in the bubble diagram Fig. 2 of the two-loop fermion self-energy, arising from the double photon massless propagator pole in this diagram. Quite apart from dependence upon the gauge parameter ξ , the appearance of such unregulated divergences from massless, unscreened photons is itself also sufficient evidence for the breakdown of the loop expansion at high temperatures, and the need for a resummation of diagrams with still larger numbers of loops.

In order to regulate the divergences in the two-loop fermion self-energy, we introduce a photon mass M in the evaluation of the bubble diagram of Fig. 2. In the usual perturbative expansion, the formal limit $M \rightarrow 0$ should be taken. Since this limit does not exist at two-loop order, we may anticipate the result that after HTL resummation of the photon self-energy the photon acquires a non-zero Debye screening mass of order eT . Taking $M \sim eT$ allows us to characterize the order of all the two-loop contributions to Σ , and compare finite contributions from different loop orders in a meaningful way. In other words, when the formal photon regulator mass is replaced by the physical Debye screening mass, by a partial resummation of the photon propagator for soft momenta, there are neither infrared nor collinear divergences in the

two-loop dressed self-energy, and all NLO contributions to the fermion self-energy are estimated correctly in powers of e . The photon mass M thus plays a dual role in our considerations, first as a regulator of infrared divergences in bare loop diagrams, and second, as a parameter whose finite value of order eT after resummation of higher loop diagrams enables us to estimate the finite magnitude of resummed amplitudes.

Both the gauge parameter dependence and the explicit infrared divergences as $M \rightarrow 0$ in the bare loop expansion can be cured only by systematically including the contributions from higher numbers of loops $\ell > 2$, despite the fact that these contain additional explicit powers of the coupling. This HTL improved resummation leads finally to the complete order e^2T corrections to the fermion dispersion relation in the plasma for both its real and imaginary parts, compared to the LO result for the fermion thermal mass, $eT/\sqrt{8}$ which is purely real. Thus the reordering of perturbation theory in the plasma is decidedly non-analytic in $\alpha = e^2/4\pi$.

The structure of the explicit two-loop calculation of Σ shows that the leading contributions at high temperatures arise entirely from momentum integrals which *factorize* into one momentum integral which is hard ($p \sim T$), and a second one which is soft (in the sense defined above). Overlapping two-loop momentum integrals which violate this hard-soft pattern can be shown explicitly to be suppressed by additional powers of e , thus justifying their neglect, in $\mathcal{O}(e^2T)$ calculation of the self-energy and damping rate. In particular, the detailed analysis of the two-loop self-energy shows that there are *no* contributions at this order coming from both loops hard, which naive power counting would apparently allow [3, 8]. That such hard-hard contributions from two-loop diagrams at this order in e^2T are completely absent is in accordance with the an earlier result by Schulz for the two-loop gluon polarization in QCD at next to leading order [14]. A fact apparently not widely recognized is that the contribution at two-loop order of only hard-soft integrals to terms of order e^2T in the fermion self-energy and the complete absence of hard-hard contributions is exactly what is *required* by the HTL resummation program, when HTL propagators and vertices are re-expanded in primitive bare loops of perturbation theory, a point which we elaborate in some detail in Sec. V. Thus one result of our detailed evaluation of the two-loop self-energy is a refinement of naive power counting rules, and a clarification of the hard-soft factorization structure of the high temperature expansion of perturbation theory, which underpins resummation of one-loop diagrams with HTL dressed propagators and vertices.

The factorization pattern should be expected to continue at $\ell > 2$ loops as well, namely all the order e^2T corrections to the fermion dispersion relation should arise from $\ell - 1$ hard loops inside only one soft loop. This HTL reordering of the ordinary loop expansion is necessary to collect all the infrared sensitive terms of relative order $(eT/\omega)^{2\ell-2}$ from ℓ loops, which make equally important contributions to

the fermion dispersion relation and damping rate, when $\omega \sim eT$. When all these subleading contributions are summed over all ℓ loops by the HTL resummation of propagators and vertices in an HTL dressed one-loop diagram, the gauge parameter dependence at subleading e^2T order is eliminated. The curing of both the infrared divergences, and the gauge parameter dependence of the ordinary bare loop expansion by the same resummation in HTL propagators and vertices, when calculating damping rates and plasma frequencies, represents an important check on its physical consistency [9, 14, 17–21].

The technical evaluation of the two-loop diagrams in the imaginary time formalism [3, 5] is facilitated considerably by using Gaudin’s method [22, 23], which we review in Appendix A. This very efficient method of performing the frequency sums makes calculations of diagrams involving many finite temperature propagators feasible. The Gaudin method also makes the hard-soft factorization pattern at two-loops more evident, and makes feasible the analysis of dressed and/or even higher loop diagrams, at least for the purpose of extracting their leading order behavior in the high temperature limit.

The outline of the paper is as follows. In Section II we review the one-loop finite temperature electron self-energy, including both the LO HTL and NLO terms, and the latter’s dependence upon the gauge fixing parameter ξ . In Section III we present the basic calculation of the three diagrams of two different topologies in the two-loop electron self-energy by the Gaudin method in the Feynman gauge, introducing the photon mass regulator for the most infrared sensitive bubble diagram. In Section IV we present the detailed analysis of the two-loop integrals obtained in Section III, for a fermion at rest $\mathbf{q} = 0$. We show that the leading contributions in the high temperature expansion of the two-loop diagrams of both topologies come from one loop hard, the other soft, thus demonstrating explicitly that there are no hard-hard contributions, and the soft-soft contributions are subleading at this order. In Section V we compare our results with the insertions of effective HTL self-energies and vertices in the one-loop Σ , explicitly verifying the equivalence of these insertions for both the real and imaginary parts to order e^2T , which is necessary for the HTL resummation program to work. In Section VI we study the gauge parameter dependence of the two-loops self-energy, and show that it does not cancel even on shell, in neither its real or imaginary parts. Section VII contains a summary of the main results for the two-loop self-energy to order e^2T , concluding with a discussion of the lessons for a systematic reorganization of the loop expansion in high temperature gauge theories to higher orders.

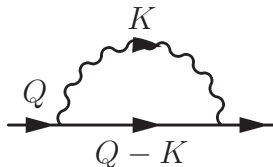


FIG. 1: One-loop contribution to the fermion self-energy.

II. THE ONE-LOOP ELECTRON SELF-ENERGY

We begin by setting our conventions and reviewing the existing leading order (LO) [3, 24] and NLO [10, 11] calculations of the one-loop QED electron finite temperature self-energy,

$$\Sigma_1(Q) = -ie^2 \int_K \gamma_\mu G(Q-K) \gamma_\nu D^{\mu\nu}(K) \quad (2.1)$$

represented in Fig. 1. For the purposes of this paper, we use the Feynman rule conventions of [25] wherein the tree-level electron-photon vertex is $-ie\gamma_\mu$. In (2.1) the tree-level fermion propagator is given by

$$G(K) = \frac{i}{\not{K}} = \not{K} \tilde{D}(K), \quad \tilde{D}(K) = i/(K^2 + i\epsilon), \quad (2.2)$$

with $\not{K} = \gamma^\mu K_\mu = k_0\gamma_0 - \mathbf{k} \cdot \boldsymbol{\gamma}$. The tree-level photon propagator in the one-parameter family of covariant ξ -gauges is

$$D^{\mu\nu}(K) = - \left(g^{\mu\nu} - (1-\xi) \frac{K^\mu K^\nu}{K^2} \right) D(K), \quad D(K) = i/(K^2 + i\epsilon). \quad (2.3)$$

We employ the somewhat redundant notation of $\tilde{D}(K)$ and $D(K)$ for the same function of K^2 in order to distinguish propagators with fermionic Matsubara frequencies from those with bosonic Matsubara frequencies in the imaginary time formalism of finite temperature field theory [3, 5]. Thus, in imaginary time where the generic four-momentum becomes $K^\mu = (i\omega_n, \mathbf{k})$,

$$D(i\omega_n, \mathbf{k}) = -i\Delta(i\omega_n, \mathbf{k}) = \frac{-i}{-(i\omega_n)^2 + \mathbf{k}^2}, \quad \omega_n = 2\pi nT; \quad (2.4a)$$

$$\tilde{D}(i\omega_n, \mathbf{k}) = -i\tilde{\Delta}(i\omega_n, \mathbf{k}) = \frac{-i}{-(i\omega_n)^2 + \mathbf{k}^2}, \quad \omega_n = (2n+1)\pi T, \quad (2.4b)$$

The indices of the four-momentum are raised and lowered with the metric tensor $g^{\mu\nu} = \text{diag}(1, -1, -1, -1)$. The Dirac γ -matrices satisfy the anticommutation relation $\{\gamma_\mu, \gamma_\nu\} = 2g_{\mu\nu}$, so that $(\gamma^0)^\dagger = \gamma^0$ is Hermitian.

For evaluation of loop integrals such as that in (2.1) we use the convention

$$\int_K \longrightarrow iT \sum_n \int_{\mathbf{k}} \equiv iT \sum_n \int \frac{d^3\mathbf{k}}{(2\pi)^3}. \quad (2.5)$$

Moreover, our conventions are such that the electron and photon proper self-energies, Σ and $\Pi_{\mu\nu}$, contribute to the full inverse propagators in the form

$$i\mathcal{G}^{-1}(Q) = iG^{-1}(Q) - \Sigma(Q), \quad iD_{\mu\nu}^{-1}(Q) = iD_{\mu\nu}^{-1}(Q) - \Pi_{\mu\nu}(Q), \quad (2.6)$$

for the electron and photon respectively. The sign convention for Σ here is the opposite of that of [11].

It will also be convenient to work with the spectral representation of the propagators, which is given by

$$D^{\mu\nu}(i\omega_n, \mathbf{k}) = -i \int_{-\infty}^{\infty} \frac{dk_0}{2\pi} \frac{\rho^{\mu\nu}(k_0, \mathbf{k})}{k_0 - i\omega_n} = -i\Delta^{\mu\nu}(i\omega_n, \mathbf{k}), \quad (2.7a)$$

$$G(i\omega_n, \mathbf{k}) = -i \int_{-\infty}^{\infty} \frac{dk_0}{2\pi} \frac{\rho_F(k_0, \mathbf{k})}{k_0 - i\omega_n} = -i\Delta_F(i\omega_n, \mathbf{k}), \quad (2.7b)$$

where

$$\rho^{\mu\nu}(k_0, \mathbf{k}) \equiv - \left(g^{\mu\nu} + (1 - \xi) K^\mu K^\nu \frac{\partial}{\partial k_0^2} \right) \rho(k_0, \mathbf{k}), \quad (2.8a)$$

$$\rho_F(k_0, \mathbf{k}) \equiv \not{K} \rho(k_0, \mathbf{k}). \quad (2.8b)$$

Here $\rho(k_0, \mathbf{k})$ is the spectral function of a free massless boson,

$$\rho(K) \equiv \rho(k_0, \mathbf{k}) = 2\pi \varepsilon(k_0) \delta(k_0^2 - \mathbf{k}^2), \quad (2.9)$$

and $\varepsilon(k_0) = \theta(k_0) - \theta(-k_0)$ is the sign function. Accordingly, the spectral representation of $\Delta(i\omega_n, \mathbf{k})$ is

$$\Delta(i\omega_n, \mathbf{k}) = -\frac{1}{K^2} = \int_{-\infty}^{\infty} \frac{dk_0}{2\pi} \frac{\rho(k_0, \mathbf{k})}{k_0 - i\omega_n}, \quad (2.10)$$

and similarly for $\tilde{\Delta}(i\omega_n, \mathbf{k})$, with the only difference that in this latter case ω_n is fermionic.

A. Feynman Gauge Evaluation

We consider first the Feynman gauge condition ($\xi = 1$). In this case, using the spectral representation of the propagators, the self-energy (2.1) for a fermion with external Matsubara frequency ν_q becomes

$$\Sigma_1(i\nu_q, \mathbf{q}) = -2e^2 \int_{\mathbf{k}} \int_{-\infty}^{\infty} \frac{dk_0}{2\pi} \int_{-\infty}^{\infty} \frac{dp_0}{2\pi} \rho(k_0, \mathbf{k}) \rho_F(p_0, \mathbf{q} - \mathbf{k}) T \sum_n \left[\frac{1}{k_0 - i\omega_n} \right] \left[\frac{1}{p_0 - i(\nu_q - \omega_n)} \right]. \quad (2.11)$$

The frequency sum can be performed using Gaudin's method [22], reviewed recently in [23] and in Appendix A.

Gaudin's method relies first on the spectral representation of finite temperature propagators in the imaginary time formalism (2.10), and second, on a graphical representation of a particular partial fractioning decomposition of the products of denominators that arise in finite temperature perturbation theory into

a sum of products, in each of which the only Matsubara frequencies which appear are the *independent* ones to be summed. Since an ℓ -loop finite temperature diagram contains ℓ independent Matsubara sums, this means that it can be written as a sum of terms each of which contains exactly ℓ independent frequency sums, which can be performed simply, no matter how many propagators or vertices the original Feynman diagram contains. This disentangling of the independent and dependent Matsubara frequencies greatly facilitates the computation of multi-loop finite temperature diagrams, or even one-loop finite temperature diagrams with multiple vertex insertions.

For the one-loop diagram of Fig. 1 the Gaudin decomposition into terms with the one independent Matsubara frequency to be summed amounts to the simple partial fraction identity,

$$\begin{aligned} & T \sum_n \left[\frac{e^{i\omega_n \tau_1}}{k_0 - i\omega_n} \right] \left[\frac{e^{i(\nu_q - \omega_n)\tau_2}}{p_0 - i(\nu_q - \omega_n)} \right] \\ &= \frac{e^{i\nu_q \tau_2}}{k_0 + p_0 - i\nu_q} \left[T \sum_n \frac{e^{i\omega_n(\tau_1 - \tau_2)}}{k_0 - i\omega_n} \right] + \frac{e^{i\nu_q \tau_1}}{k_0 + p_0 - i\nu_q} \left[T \sum_n \frac{e^{i(\nu_q - \omega_n)(\tau_2 - \tau_1)}}{p_0 - i(\nu_q - \omega_n)} \right], \end{aligned} \quad (2.12)$$

so that only one denominator in each term now contains the Matsubara frequency to be summed. Each of the τ_k are infinitesimals, assumed positive, assigned to each line; for example $\tau_k = k\epsilon$ with $\epsilon \rightarrow 0^+$, so that $\tau_1 - \tau_2$ has a definite sign. Shifting then the summation over the bosonic frequency $\omega_n = 2\pi nT$ in the second term of (2.12) to the fermionic frequency $\tilde{\omega}_n \equiv \nu_q - \omega_n = (2n+1)\pi T$, and applying the fundamental summation formulas (A3) and (A4) for bosonic and fermionic frequencies respectively, we obtain for the sum in (2.11) or (2.12) the result

$$T \sum_n \frac{1}{(k_0 - i\omega_n)[p_0 - i(\nu_q - \omega_n)]} = -\frac{n_F(p_0) + n_B(-k_0)}{k_0 + p_0 - i\nu_q}, \quad (2.13)$$

in the limit $\tau_i \rightarrow 0^+$ with $\tau_1 - \tau_2 \rightarrow 0^-$. Here $n_B(E), n_F(E)$ are the Bose-Einstein and Fermi-Dirac distribution functions given by

$$n_B(E) \equiv \frac{1}{\exp(E/T) - 1}, \quad n_F(E) \equiv \frac{1}{\exp(E/T) + 1}. \quad (2.14)$$

The power of the Gaudin method lies in the fact that once the propagator denominators with independent Matsubara frequencies are isolated, as in (2.12), one never needs any other Matsubara frequency sums other than the fundamental ones (A3) and (A4), no matter how many propagators or vertices the original Feynman diagram contains. This advantage becomes more and more evident at higher loop orders, or in diagrams with larger numbers of finite temperature propagators.

We remark also that had we assigned the τ_i differently, so that, *e.g.* $\tau_1 - \tau_2 \rightarrow 0^+$, we would have obtained $+[n_F(-p_0) + n_B(k_0)]$ instead of $-[n_F(p_0) + n_B(-k_0)]$ in the numerator of (2.13). However these

two expressions are equal, by use of the identities

$$n_B(-E) = -1 - n_B(E), \quad n_F(-E) = 1 - n_F(E), \quad (2.15)$$

for the Bose-Einstein and Fermi-Dirac statistical distributions. Hence although one needs *some* regulator to define the frequency sums (A3) and (A4), appearing in intermediate steps in the Gaudin method, one can check that the results for any diagram containing at least two Matsubara propagators (whose frequency sums converge absolutely) are in fact independent of the regulator used.

Performing next the frequency integrals over k_0 and p_0 in (2.11), by making use of the δ -functions in the spectral representations (2.8) and (2.9), and using the first identity in (2.15), we obtain

$$\Sigma_1(i\nu_q, \mathbf{q}) = 2e^2 \int \frac{d^3\mathbf{k}}{(2\pi)^3} \frac{1}{4E_1E_2} \sum_{s_1, s_2 = \pm 1} \left[(\gamma^0 E_2 s_1 - (\mathbf{q} - \mathbf{k}) \cdot \boldsymbol{\gamma} s_1 s_2) \frac{1 + n_B(s_1 E_1) - n_F(s_2 E_2)}{i\nu_q - s_1 E_1 - s_2 E_2} \right], \quad (2.16)$$

where $E_1 = k$, $E_2 = |\mathbf{q} - \mathbf{k}|$. For each particular value of s_1 and s_2 the terms in the sum can be associated with physical processes like pair creation and annihilation or scattering off of particles in the heat bath [26].

Examining (2.16) one sees that for soft external four-momentum there are two types of terms: one with $s_2 = -s_1$ and the other with $s_2 = s_1$. In the first case the energy denominator is small for $|\mathbf{q}| \ll |\mathbf{k}|$, since $E_1 - E_2 \simeq \mathbf{k} \cdot \mathbf{q}/k$, and the \mathbf{k} integration is dominated by hard $k = |\mathbf{k}| \sim T$. These hard momentum integrals are proportional to T^2 and give the LO result in the HTL approximation. Physically these terms correspond to Landau damping in the plasma, which includes processes possible only at nonzero temperature: particle absorption from the heat bath and emission into the heat bath.

In the second case, that is with $s_2 = s_1 = \pm 1$, the two energies E_1 and E_2 add rather than cancel for large k in the denominator of (2.16), and hence there are additional powers of k in the denominator which makes the integral over \mathbf{k} more sensitive to its small k range. Since $1 + n_B(s_1 E_1) - n_F(s_1 E_2) = \varepsilon(s_1)(1 + n_B(E_1) - n_F(E_2))$, the appearance of the “1” shows that here one encounters processes which are possible also at zero temperature, *e.g.* pair creation. The NLO terms in the high temperature expansion of the one-loop self-energy come from these types of processes.

Focusing on a fermion with vanishing spatial three-momentum ($\mathbf{q} = 0$) one has $E_1 = E_2 = k$ and the above two possibilities give

$$\text{LO HTL:} \quad \text{from} \quad \sum_{s_2 = -s_1 = \pm 1} \longrightarrow -\frac{1}{2k} [n_B(k) + n_F(k)] \frac{1}{i\nu_q}, \quad (2.17)$$

$$\text{NLO HTL:} \quad \text{from} \quad \sum_{s_2 = s_1 = \pm 1} \longrightarrow -\frac{1}{4k} [1 + n_B(k) - n_F(k)] \left(\frac{1}{i\nu_q - 2k} + \frac{1}{i\nu_q + 2k} \right). \quad (2.18)$$

Using (2.17) and (2.18) one obtains then

$$\Sigma_1(i\nu_q, \mathbf{q} = \mathbf{0}) = \frac{e^2}{2\pi^2 i\nu_q} \gamma_0 \int_0^\infty dk k [n_B(k) + n_F(k)] - \frac{e^2 i\nu_q}{8\pi^2} \gamma_0 \int_0^\infty dk \frac{k}{k^2 - (i\nu_q)^2/4} [1 + n_B(k) - n_F(k)]. \quad (2.19)$$

In the last expression the “1” in square brackets is the logarithmically UV divergent vacuum contribution, which must be renormalized in the standard manner. Since we are interested only in the high T dependence of the self-energy in the hot plasma, we may discard such vacuum contributions. It is important to point out that because of the identities (2.15), identifying the vacuum contribution unambiguously requires first expressing all statistical distributions as functions of energy arguments which are *positive*. This can be done most conveniently before doing the frequency integrals by using the following expressions:

$$\begin{aligned} n_B(E) &= -\theta(-E) + \varepsilon(E)n_B(|E|), & n_B(-E) &= -\theta(E) - \varepsilon(E)n_B(|E|), \\ n_F(E) &= \theta(-E) + \varepsilon(E)n_F(|E|), & n_F(-E) &= \theta(E) - \varepsilon(E)n_F(|E|). \end{aligned} \quad (2.20)$$

Clearly the k integral in the first term of (2.19) is hard in the sense that a positive power of k in the integrand is cut off only by a statistical distribution function n_B or n_F at $k \sim T$, and we obtain

$$\int_0^\infty dk k [n_B(k) + n_F(k)] = \frac{\pi^2 T^2}{6} + \frac{\pi^2 T^2}{12} = \frac{\pi^2 T^2}{4}. \quad (2.21)$$

In contrast, in the second integral of (2.19) the integrand is a decreasing function of k for large k , even without the statistical distribution functions. Integrals of this kind are soft, in the sense that the small k range is important, and the n_B or n_F thermal functions serve only to cut off at most an otherwise logarithmically diverging integral at large k , in which the argument of the logarithm is sensitive to the soft momentum region. The high temperature limit of the second soft term in (2.19) is evaluated in Appendix B, where it is shown that

$$\int_0^\infty dk \frac{k}{k^2 - (i\nu_q)^2/4} n_B(k) \Big|_{i\nu_q = \omega + i0^+} = \frac{i\pi T}{\omega} - \frac{1}{2} \ln \left(\frac{T}{\omega} \right) + \dots, \quad (2.22a)$$

$$\int_0^\infty dk \frac{k}{k^2 - (i\nu_q)^2/4} n_F(k) \Big|_{i\nu_q = \omega + i0^+} = 0 + \frac{1}{2} \ln \left(\frac{T}{\omega} \right) + \dots, \quad (2.22b)$$

where only the high temperature asymptotic values of the integrals are displayed, neglecting terms that do not grow with T . Thus, in Feynman gauge,

$$\Sigma_1(\omega, \mathbf{0}) \simeq \frac{e^2 T^2}{8\omega} \gamma_0 + \frac{e^2}{8\pi^2} \gamma_0 \left(\omega \ln \frac{T}{\omega} - i\pi T \right), \quad (\xi = 1). \quad (2.23)$$

The first term is the leading order (LO) HTL result, which receives contributions from both the electron and photon thermal distributions in (2.21). It is purely real, and in fact, independent of the gauge parameter

ξ . The second two terms in (2.23) are the next-to-leading order (NLO) or subleading terms in the high temperature expansion, which come from the soft momentum region in the integrals (2.22), and yield both a real and imaginary part. The contribution of the Fermi-Dirac statistical factor to the imaginary part and of the zero temperature vacuum part are subleading to this (NNLO) in the high temperature expansion.

The real part of the off-shell one-loop self-energy Σ_1 in (2.23) illustrates the infrared divergence at small external frequencies $\omega \rightarrow 0$. The on-shell condition at LO is obtained by finding the zeroes of the one-loop corrected inverse propagator $iG^{-1}(Q) - \Sigma_1(Q)$ in (2.6). For vanishing spatial momentum $\mathbf{q} = 0$, this on-shell condition is

$$\omega\gamma_0 = \Sigma(\omega, \mathbf{q} = 0) \quad (2.24)$$

or to leading order,

$$\omega = \frac{e^2 T^2}{8\omega} + \dots \quad (2.25)$$

where the ellipsis denotes the NLO terms. Thus on the fermion mass shell the tree level inverse Dirac propagator is set equal to the one-loop result and $\omega \simeq eT/\sqrt{8}$ [3, 27, 28]. It is the fact that $\omega \sim eT$ on-shell owing to the infrared enhancement of the one-loop self-energy at small ω that leads to inverse powers of the coupling at higher loop orders, re-ordering of the perturbative expansion, and eventually the need for further resummation.

B. Gauge Parameter Dependence of Σ_1

The general expression for the one-loop self-energy at NLO in the HTL approximation and for $\mathbf{q} \neq 0$, in a general $\xi \neq 1$ gauge can be found in [10] (real part) and [11] (both real and imaginary parts). Explicitly, the ξ dependent term is

$${}^\xi\Sigma_1(Q) = (1 - \xi)ie^2 \int_K \gamma_\mu \frac{1}{\mathcal{Q} - \mathcal{K}} \gamma_\nu \frac{K^\mu K^\nu}{(K^2)^2}. \quad (2.26)$$

Making the substitution $\mathcal{K} = -(\mathcal{Q} - \mathcal{K}) + \mathcal{Q}$ we can rewrite this as

$${}^\xi\Sigma_1(Q) = (1 - \xi)ie^2 \int_K \frac{1}{(K^2)^2} \left[\mathcal{Q} \frac{1}{\mathcal{Q} - \mathcal{K}} \mathcal{Q} - (\mathcal{Q} + \mathcal{K}) \right]. \quad (2.27)$$

Since the very last term here involving only \mathcal{K} vanishes by symmetry, in this form one can see that if the lowest order tree level on-shell condition for a massless fermion $\mathcal{Q} = 0$ is used, the gauge parameter dependence of the one-loop self-energy vanishes, provided that there are no infrared divergences in this

limit. This is indeed the result that one obtains in the well-known QED perturbation theory at zero temperature with a finite electron mass.

At high temperatures, the existence of the ω^{-1} infrared behavior of the LO HTL self-energy in (2.23), and imposition of the modified HTL on-shell condition (2.25) implies that $\mathcal{Q} = \omega\gamma_0 \neq 0$ for a fermion at rest in the plasma. Hence (2.27) no longer vanishes for HTL dressed fermions and the gauge parameter independence of the modified fermion dispersion relation at any given loop order is no longer guaranteed, even on-shell. This is clearly the result of using an on-shell condition such as (2.25) which mixes loop orders.

To evaluate ${}^\xi\Sigma_1(Q)$ explicitly in the high temperature limit, we group the terms in a somewhat different way. Using the fact that $\mathcal{K}(\mathcal{Q} - \mathcal{K})\mathcal{K} = Q^2\mathcal{K} - K^2\mathcal{Q} - (Q - K)^2\mathcal{K}$, and that $\frac{\partial}{\partial M^2} \int_K \mathcal{K} D_{M^2}(K)$ vanishes, we may also write ${}^\xi\Sigma_1(Q)$ in the form

$${}^\xi\Sigma_1(Q) = (1 - \xi)e^2 \left\{ -iQ^2 \frac{\partial}{\partial M^2} \int_K \mathcal{K} D_{M^2}(K) \tilde{D}(Q - K) \Big|_{M^2=0} + i\mathcal{Q} \int_K D(K) \tilde{D}(Q - K) \right\}, \quad (2.28)$$

where

$$D_{M^2}(K) \equiv \frac{i}{K^2 - M^2} \quad (2.29)$$

is the bosonic propagator with finite M^2 . The corresponding spectral representation is

$$D_{M^2}(K) = -i \int_{-\infty}^{\infty} \frac{dk_0}{2\pi} \frac{\rho_{M^2}(k_0, \mathbf{k})}{k_0 - i\omega_n}, \quad (2.30)$$

with

$$\rho_{M^2}(k_0, \mathbf{k}) = 2\pi\varepsilon(k_0)\delta(k_0^2 - \mathbf{k}^2 - M^2). \quad (2.31)$$

The technique of introducing a photon mass M , differentiating with respect to it, and taking the $M \rightarrow 0$ limit at the end of the calculation is a useful method for defining the double pole term, $(K^2)^{-2}$ appearing in both ${}^\xi\Sigma_1$ and the two-loop self-energy bubble diagram of the next section. At this point the photon mass M is introduced as a mathematical convenience and infrared regulator only, and the limit $M \rightarrow 0$ should be taken at the end of the calculation. A finite photon self-energy of order $M \sim eT$ is obtained only after HTL resummation.

The reason for the rearrangement of ${}^\xi\Sigma_1$ into the form (2.28) is that each of the terms in (2.28) are finite in the limit $M \rightarrow 0$, whereas as we shall show in Sec. VI, each of the terms in (2.27) is M dependent and divergent in this limit, with the sum of terms in ${}^\xi\Sigma_1$ finite. In imaginary time, using the spectral representation of the propagators (2.10) and (2.30) we have

$${}^\xi\Sigma_1(i\nu_q, \mathbf{q}) = (1 - \xi)e^2\gamma_0 \times$$

$$\left\{ -Q^2 \frac{\partial}{\partial M^2} \int_{\mathbf{k}} \int_{-\infty}^{\infty} \frac{dk_0}{2\pi} k_0 \rho_{M^2}(k_0, \mathbf{k}) \int_{-\infty}^{\infty} \frac{dp_0}{2\pi} \rho(p_0, \mathbf{q} - \mathbf{k}) T \sum_n \frac{1}{(k_0 - i\omega_n)[p_0 - i(\nu_q - \omega_n)]} \right\}_{M^2=0} \\ + \mathcal{Q} \int_{\mathbf{k}} \int_{-\infty}^{\infty} \frac{dk_0}{2\pi} \int_{-\infty}^{\infty} \frac{dp_0}{2\pi} \rho(k_0, \mathbf{k}) \rho(p_0, \mathbf{q} - \mathbf{k}) T \sum_n \frac{1}{(k_0 - i\omega_n)[p_0 - i(\nu_q - \omega_n)]} \Bigg\}. \quad (2.32)$$

Since ω_n is bosonic and $\nu_q - \omega_n$ is fermionic, the Matsubara sum here is identical to that given in (2.13). One next performs the frequency integrals over k_0 and p_0 in (2.32). For the integrals over the frequencies which are *not* arguments of the statistical factors, the spectral decomposition (2.10) may be undone, re-obtaining Matsubara propagators. The remaining frequency integrals are performed using the Dirac δ functions in the spectral functions after using the relations (2.20), which allows the separation of the vacuum and thermal pieces by making the arguments of the statistical distributions explicitly positive. Keeping only the thermal part and taking $\mathbf{q} = 0$, in this way one obtains

$$\xi \Sigma_1(i\nu_q, \mathbf{q} = \mathbf{0}) = \frac{(1 - \xi)e^2}{8\pi^2} \gamma_0 \left\{ (i\nu_q)^2 \frac{\partial}{\partial M^2} \left[\frac{2}{i\nu_q} \mu_- \mu_+ \int_0^\infty dk \frac{k n_F(k)}{k^2 - \mu_-^2} - \frac{2}{i\nu_q} \int_0^\infty dk \frac{k^2 E_k n_B(E_k)}{E_k^2 - \mu_+^2} \right] \right\}_{M^2=0} \\ + i\nu_q \int_0^\infty dk \frac{k}{k^2 - (i\nu_q)^2/4} [n_B(k) - n_F(k)], \quad (2.33)$$

where $E_k^2 \equiv k^2 + M^2$ and $\mu_\pm = ((i\nu_q)^2 \pm M^2)/(2i\nu_q)$. We have omitted from the square bracket terms independent of M^2 which give a vanishing contribution upon differentiation.

The last integral in (2.33) is the same one obtained in the Feynman gauge calculation, *c.f.* (2.19). After analytical continuation ($i\nu_q \rightarrow \omega + i0^+$), the ξ -dependent real part of the self-energy comes only from this term. From (2.22) it also contributes to the imaginary part. The first integral of (2.33) is of the form given in (B1) with the replacement $ia \rightarrow \mu_-/T$. Using (B10a) one can readily check that the term containing this integral will give a contribution which is subleading to (2.34). The second integral in (2.33) contributes to the imaginary part of $\xi \Sigma_1$ as shown by (B24). All these ξ dependent terms arise from the soft momentum region. The final result for the high temperature expansion of the ξ dependent part of the one-loop fermion self-energy is

$$\xi \Sigma_1(\omega, \mathbf{0}) = (1 - \xi) \frac{e^2}{8\pi^2} \gamma_0 \left(-\omega \ln \frac{T}{\omega} + \frac{3\pi iT}{2} \right). \quad (2.34)$$

Unlike the LO HTL result, the NLO terms and therefore the imaginary part of the one-loop self-energy for a fermion at rest in the plasma is gauge-parameter dependent, even after the LO HTL on-shell condition (2.25) has been utilized. This clearly indicates that the imaginary part obtained from the NLO one-loop self-energy calculation alone cannot be the full answer for the dressed quasi-particle damping rate, and both the real and imaginary parts of Σ should receive additional contributions of the same magnitude in

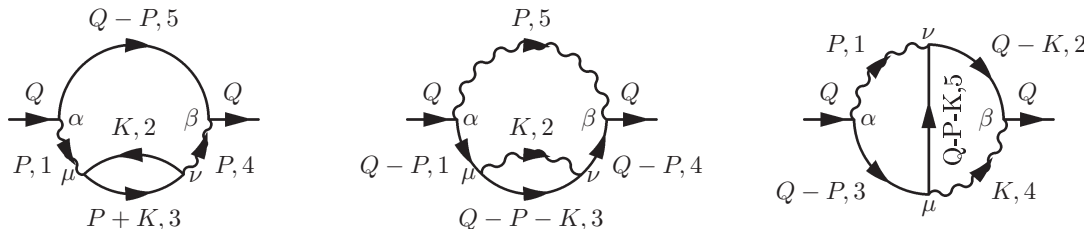


FIG. 2: Two-loop contributions to the fermion self-energy: from left to right, the bubble (B) diagram, rainbow (R) diagram, and the crossed photon (C) diagram.

the weak coupling e at higher loops, in order to obtain a physical result independent of ξ . We show next that terms of the same or larger magnitude to (2.34) are indeed generated at two-loop order, for $\omega \sim eT$ due to increased sensitivity to the infrared of the two-loop self-energy.

III. THE TWO-LOOP ELECTRON SELF-ENERGY

In this section we compute the two-loop electron self-energy in the Feynman gauge $\xi = 1$, perform the Matsubara sums in the imaginary time formalism by Gaudin's method, and reduce the expressions to integrals over two spatial loop momenta \mathbf{k} and \mathbf{p} , for general external electron energy and momentum $(i\nu_q, \mathbf{q})$. The leading terms in the high temperature expansion arise from only those terms with two statistical factors, n_B or n_F . The analysis of the integrals, the explicit extraction of their leading high temperature, most infrared sensitive terms, and the analytic continuation to real electron energies $i\nu_q \rightarrow \omega + i0^+$ for $\mathbf{q} = 0$ electrons at rest in the plasma are performed in the next section.

At two-loops the electron self-energy is composed of the three diagrams pictured in Fig. 2, which we call the bubble (B) diagram, the rainbow (R) diagram, and the crossed photon (C) diagram. The corresponding contributions to Σ will be denoted by Σ_B , Σ_R and Σ_C respectively.

An earlier partial calculation of the two-loop electron self-energy at finite temperatures has been given in the literature in Ref. [12]. The authors of this work were interested in the ultraviolet renormalizability of QED and electron mass renormalization at finite temperatures. For that reason they used real time Feynman propagators (rather than the appropriate causal real time Schwinger-Keldysh formalism), and did not calculate the imaginary parts of any of the two-loop diagrams. They also did not calculate the contribution of the bubble diagram (B), which turns out to give the dominant contribution to the real part at leading order in the high temperature expansion, in which we are interested.

The calculation of such multi-loop diagrams in the imaginary time formalism is greatly facilitated by Gaudin's method for performing the Matsubara sums [22]. Since each of the two-loop self-energy

diagrams contains five finite temperature propagators, finding the appropriate partial fraction identity analogous to (2.12) for disentangling the two independent Matsubara frequencies is already quite non-trivial. Gaudin's method for doing this involves a graphical decomposition of each original two-loop Feynman diagram in Σ into a sum of tree diagrams, each containing three propagators, and the complement of the tree containing the other two propagators which carry the two independent Matsubara frequencies. This graphical decomposition is illustrated in Fig. 3, for the case of the bubble (B) self-energy diagram. Calculations in scalar field theory using Gaudin's method were presented in [23] on a two-loop diagram having the topology of diagram (C). Diagrams of type (R) or (B) were outside the interest of the authors of [23] because, having a self-energy insertion on an internal line, they are not in the class of two-particle irreducible (2PI) diagrams. The method works equally well on diagrams of all topologies. However, since two fermion propagators (diagram R) or two photon propagators (diagram B) have the same four-momentum, the two diagrams suffer from a double pole problem (in any method). In Gaudin's method this problem manifest itself in two different ways, as one sees from the Gaudin tree graphs of Fig. 3. The first way is illustrated by the first four graphs, where one encounters the product of a spectral function corresponding to a line which acquires a statistical factor and a Matsubara propagator with the same four-momentum, that is $\delta(p_0^2 - \mathbf{p}^2)/(\mathbf{p}^2 - p_0^2)$. The second way in which the double pole problem arises is found in the last three Gaudin tree graphs, where one encounters the product of two Matsubara propagators sharing the same 4-momentum. In both cases the expressions can be regularized by a massive regulator, which effectively defines ill-defined double pole quantities by the replacements

$$\rho(p^0, \mathbf{p})\Delta(p^0, \mathbf{p}) \rightarrow \frac{1}{2} \frac{\partial}{\partial M^2} \rho_{M^2}(p^0, \mathbf{p}) \equiv \frac{1}{2} \frac{\partial}{\partial M^2} \left\{ 2\pi\epsilon(p^0)\delta\left((p^0)^2 - \mathbf{p}^2 - M^2\right) \right\}, \quad (3.1a)$$

$$[\Delta(p^0, \mathbf{p})]^2 \rightarrow -\frac{\partial}{\partial M^2} \Delta_{M^2}(p^0, \mathbf{p}) \equiv -\frac{\partial}{\partial M^2} \left\{ \frac{1}{-(p^0)^2 + \mathbf{p}^2 + M^2} \right\}. \quad (3.1b)$$

The $M^2 \rightarrow 0$ limit can be examined then at the end of the calculation. As a technical remark, M^2 may be considered to have an infinitesimal negative imaginary part $M^2 \rightarrow M^2 - i0^+$, if necessary in any intermediate steps of the calculation.

A. The Bubble Diagram

The contribution of the bubble graph of Fig. 2 reads

$$\Sigma_B(Q) = -ie^4 \int_K \int_P \gamma_\alpha G(Q - P) \gamma_\beta D^{\alpha\mu}(P) \text{tr} [\gamma_\mu G(P + K) \gamma_\nu G(K)] D^{\nu\beta}(P). \quad (3.2)$$

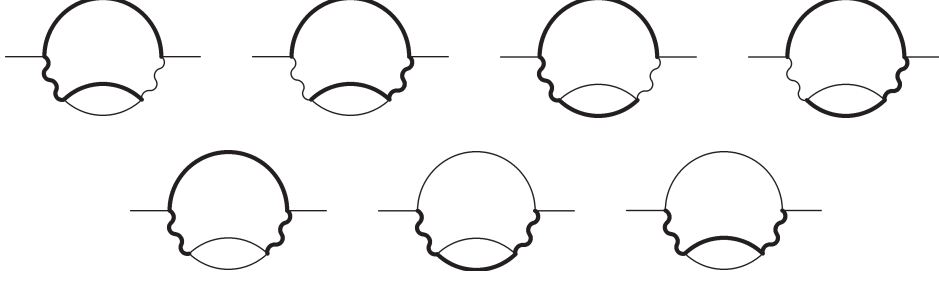


FIG. 3: The Gaudin tree graphs corresponding to the bubble diagram of Fig. 2. The thin lines carry the independent Matsubara frequencies while the thick lines belong to the tree (see Appendix A). The assignment of the momenta of the lines are the same as in the corresponding bubble Feynman diagram of Fig. 2.

The double pole of this diagram leads both to possible infrared and collinear divergences (see e.g. [29] and references therein), which requires regularization. For this reason we introduce a mass M for the photon which will be kept to the end of the calculation, in order both to regulate the divergences of the perturbative two-loop self-energy and also to estimate the coupling and temperature dependence of the resummed electron self-energy when M is replaced by the Debye screening mass $\sim eT$.

In imaginary time, using the spectral representation of the propagators, we have

$$\begin{aligned} \Sigma_B(i\nu_q, \mathbf{q}) = e^4 \int_{\mathbf{k}} \int_{\mathbf{p}} \left(\prod_{i=1}^5 \int \frac{dp_i^0}{2\pi} \right) \gamma_\alpha \rho_F(P_5) \gamma_\beta \rho^{\alpha\mu}(P_1) \rho^{\nu\beta}(P_4) \text{tr} \{ \gamma_\mu \rho_F(P_3) \gamma_\nu \rho_F(P_2) \} \\ \times \left(T^2 \sum_{n,m} \prod_{i=1}^5 \frac{1}{p_i^0 - i\omega_i} \right), \end{aligned} \quad (3.3)$$

where $P_1 = P_4 = P$, $P_2 = K$, $P_3 = P + K$, and $P_5 = Q - P$ with $Q = (i\nu_q, \mathbf{q})$, $P = (i\omega_n, \mathbf{p})$, and $K = (i\omega_m, \mathbf{k})$. The Matsubara sums performed with Gaudin's method gives for the last factor of (3.3),

$$\begin{aligned} T^2 \sum_{n,m} \prod_{i=1}^5 \frac{1}{p_i^0 - i\omega_i} &= T^2 \sum_{n,m} \left(\frac{1}{p_1^0 - i\omega_n} \right) \left(\frac{1}{p_2^0 - i\omega_m} \right) \left(\frac{1}{p_3^0 - i\omega_m - i\omega_n} \right) \left(\frac{1}{p_4^0 - i\omega_n} \right) \left(\frac{1}{p_5^0 - i\nu_q + i\omega_n} \right) \\ &= \frac{1}{(p_1^0 - p_4^0)(p_5^0 + p_4^0 - i\nu_q)} \left[\frac{n_F(p_3^0) n_B(-p_4^0)}{p_2^0 + p_4^0 - p_3^0} \right] + \frac{1}{(p_4^0 - p_1^0)(p_5^0 + p_1^0 - i\nu_q)} \left[\frac{n_B(-p_1^0) n_F(p_3^0)}{p_2^0 + p_1^0 - p_3^0} \right] \\ &\quad - \frac{1}{(p_1^0 - p_4^0)(p_5^0 + p_4^0 - i\nu_q)} \left[\frac{n_F(p_2^0) n_B(p_4^0)}{p_3^0 - p_2^0 - p_4^0} \right] - \frac{1}{(p_4^0 - p_1^0)(p_5^0 + p_1^0 - i\nu_q)} \left[\frac{n_B(p_1^0) n_F(p_2^0)}{p_3^0 - p_1^0 - p_2^0} \right] \\ &\quad + \frac{n_F(p_2^0) n_F(p_3^0)}{(p_1^0 + p_2^0 - p_3^0)(p_4^0 + p_2^0 - p_3^0)(p_5^0 + p_3^0 - p_2^0 - i\nu_q)} \\ &\quad + \frac{1}{(p_1^0 + p_5^0 - i\nu_q)(p_4^0 + p_5^0 - i\nu_q)(p_2^0 - p_3^0 - p_5^0 + i\nu_q)} \left[n_F(p_2^0) n_F(-p_5^0) + n_F(p_3^0) n_F(p_5^0) \right], \end{aligned} \quad (3.4)$$

where each of the seven terms corresponds respectively to each of the seven Gaudin tree graphs shown in Fig. 3.

For each of these terms two of the lines (the thin lines in Fig. 3) have associated statistical factors n_B or n_F , while the remaining three lines (the thick lines in Fig. 3) have no statistical factors associated with them. The integrations over the p_i^0 for these latter three propagators can be performed simply by undoing the substitution of the spectral representation (2.7a) and (2.7b) in favor of the original imaginary time propagators, $\Delta^{\mu\nu}$ or Δ_F . Then the first and second of the seven terms give identical contributions with p_1^0 replaced by p_4^0 , as do the third and fourth terms with the same replacement. Dropping the 0 superscript on the remaining integration variables p_i^0 to simplify the notation, we obtain then from (3.3) and (3.4)

$$\begin{aligned}
\Sigma_B(i\nu_q, \mathbf{q}) = & e^4 \int_{\mathbf{k}} \int_{\mathbf{p}} \left\{ 2 \int \frac{dp_3}{2\pi} \int \frac{dp_4}{2\pi} n_F(p_3) n_B(-p_4) \times \right. \\
& \gamma_\alpha \Delta_F(i\nu_q - p_4, \mathbf{q} - \mathbf{p}) \gamma_\beta \Delta^{\alpha\mu}(p_4, \mathbf{p}) \rho^{\nu\beta}(p_4, \mathbf{p}) \text{tr} \{ \gamma_\mu \rho_F(p_3, \mathbf{p} + \mathbf{k}) \gamma_\nu \Delta_F(p_3 - p_4, \mathbf{k}) \} \\
& - 2 \int \frac{dp_2}{2\pi} \int \frac{dp_4}{2\pi} n_F(p_2) n_B(p_4) \times \\
& \gamma_\alpha \Delta_F(i\nu_q - p_4, \mathbf{q} - \mathbf{p}) \gamma_\beta \Delta^{\alpha\mu}(p_4, \mathbf{p}) \rho^{\nu\beta}(p_4, \mathbf{p}) \text{tr} \{ \gamma_\mu \Delta_F(p_2 + p_4, \mathbf{p} + \mathbf{k}) \gamma_\nu \rho_F(p_2, \mathbf{k}) \} \\
& + \int \frac{dp_2}{2\pi} \int \frac{dp_3}{2\pi} n_F(p_2) n_F(p_3) \times \\
& \gamma_\alpha \Delta_F(i\nu_q + p_2 - p_3, \mathbf{q} - \mathbf{p}) \gamma_\beta \Delta^{\alpha\mu}(p_3 - p_2, \mathbf{p}) \Delta^{\nu\beta}(p_3 - p_2, \mathbf{p}) \text{tr} \{ \gamma_\mu \rho_F(p_3, \mathbf{p} + \mathbf{k}) \gamma_\nu \rho_F(p_2, \mathbf{k}) \} \\
& - \int \frac{dp_2}{2\pi} \int \frac{dp_5}{2\pi} n_F(p_2) n_F(-p_5) \times \\
& \gamma_\alpha \rho_F(p_5, \mathbf{q} - \mathbf{p}) \gamma_\beta \Delta^{\alpha\mu}(i\nu_q - p_5, \mathbf{p}) \Delta^{\nu\beta}(i\nu_q - p_5, \mathbf{p}) \text{tr} \{ \gamma_\mu \Delta_F(i\nu_q + p_2 - p_5, \mathbf{p} + \mathbf{k}) \gamma_\nu \rho_F(p_2, \mathbf{k}) \} \\
& + \int \frac{dp_3}{2\pi} \int \frac{dp_5}{2\pi} n_F(p_3) n_F(p_5) \times \\
& \left. \gamma_\alpha \rho_F(p_5, \mathbf{q} - \mathbf{p}) \gamma_\beta \Delta^{\alpha\mu}(i\nu_q - p_5, \mathbf{p}) \Delta^{\nu\beta}(i\nu_q - p_5, \mathbf{p}) \text{tr} \{ \gamma_\mu \rho_F(p_3, \mathbf{p} + \mathbf{k}) \gamma_\nu \Delta_F(p_3 + p_5 - i\nu_q, \mathbf{k}) \} \right\}. \quad (3.5)
\end{aligned}$$

Expressing the fermionic and gauge Euclidean propagators Δ_F and $\Delta^{\mu\nu}$, and the spectral densities ρ_F and $\rho^{\mu\nu}$ in terms of the bosonic forms Δ and ρ defined in (2.10) and (2.9), and evaluating the expression (3.5) in the $\xi = 1$ gauge, we obtain the covariant form for the bubble diagram,

$$\begin{aligned}
\Sigma_B(i\nu_q, \mathbf{q})|_{\xi=1} = & e^4 \int_{\mathbf{k}} \int_{\mathbf{p}} \int_{-\infty}^{\infty} \frac{dk^0}{2\pi} \int_{-\infty}^{\infty} \frac{dp^0}{2\pi} \rho(K) \rho(P) \times \\
& \left\{ 2 \left[n_F(-k^0) n_B(-p^0) + n_F(k^0) n_B(p^0) \right] B(K; K + P; Q - P) \Delta(P) \Delta(K + P) \Delta(Q - P) \right. \\
& \quad + n_F(k^0) n_F(p^0) B(K; P; K + Q - P) \Delta^2(K - P) \Delta(K + Q - P) \\
& \quad \left. - \left[n_F(k^0) n_F(-p^0) + n_F(-k^0) n_F(p^0) \right] B(K; K + Q - P; P) \Delta^2(Q - P) \Delta(K + Q - P) \right\}, \quad (3.6)
\end{aligned}$$

where we have defined the factor arising from the Dirac algebra,

$$B(P_2; P_3; P_5) \equiv B(p_2^0, \mathbf{p}_2; p_3^0, \mathbf{p}_3; p_5^0, \mathbf{p}_5) \equiv \gamma^\mu \mathcal{P}_5 \gamma^\nu \text{tr} \{ \gamma_\mu \mathcal{P}_3 \gamma_\nu \mathcal{P}_2 \} = 8[\mathcal{P}_2(P_3 \cdot P_5) + \mathcal{P}_3(P_2 \cdot P_5)], \quad (3.7)$$

and relabeled in the first term of (3.5) $p_3 \rightarrow -k^0, p_4 \rightarrow p^0, \mathbf{k} \rightarrow -\mathbf{k} - \mathbf{p}$; in the second term of (3.5) $p_2 \rightarrow k^0, p_4 \rightarrow p^0$; in the third term of (3.5) $p_2 \rightarrow k^0, p_3 \rightarrow p^0, \mathbf{p} \rightarrow \mathbf{p} - \mathbf{k}$; in the fourth term of (3.5)

$p_2 \rightarrow k^0, p_5 \rightarrow p^0, \mathbf{p} \rightarrow -\mathbf{p} + \mathbf{q}$; and finally in the fifth term of (3.5), $p_3 \rightarrow -k^0, p_5 \rightarrow p^0, \mathbf{p} \rightarrow -\mathbf{p} + \mathbf{q}, \mathbf{k} \rightarrow -\mathbf{k} + \mathbf{p} - \mathbf{q}$, in order to arrive at (3.6).

From the form of (3.6) we observe the double pole structure of the bubble diagram as discussed at the beginning of this section. The first term of (3.6) within curly brackets contains the singular product $\rho(P)\Delta(P)$, which is regulated by the replacement (3.1a). This term will turn out to give the most singular contribution to the two-loop Σ in this limit. The second and third terms of (3.6) within the curly brackets involve the square of a zero temperature bosonic propagator $\Delta^2(K - P)$ or $\Delta^2(Q - P)$, both of which are regulated by the replacement (3.1b).

In order to perform the detailed analysis of the integrals appearing (3.6) and exhibit explicitly their hard-soft pattern, it turns out to be more convenient to express (3.6) in a slightly different form. Leaving the first term as it is, in the second term of (3.6) we shift $P \rightarrow P + K$ (*i.e.* $p^0 \rightarrow p^0 + k^0$ and $\mathbf{p} \rightarrow \mathbf{p} + \mathbf{k}$), while in the third term of (3.6) we undo the shifts defined in the passage from (3.5) to (3.6) which were necessary in order to express (3.5) in the compact covariant form (3.6), that is, simply relabel $p_2 = k^0, p_5 = p^0$ and $p_3 = k^0, p_5 = p^0$ in the last two terms of (3.5), without changing the integration variables \mathbf{p} and \mathbf{k} . After introducing the M^2 regulator (3.1a) of the double pole terms, and evaluating the k^0 integrals, one obtains from either (3.5) or (3.6) the three terms

$$\Sigma_{\text{B}}(i\nu_q, \mathbf{q})|_{\xi=1} = \Sigma_{\text{B1}}(i\nu_q, \mathbf{q}) + \Sigma_{\text{B2}}(i\nu_q, \mathbf{q}) + \Sigma_{\text{B3}}(i\nu_q, \mathbf{q}), \quad (3.8)$$

with

$$\begin{aligned} \Sigma_{\text{B1}}(i\nu_q, \mathbf{q}) = e^4 \lim_{M^2 \rightarrow 0} \frac{\partial}{\partial M^2} \int_{\mathbf{k}} \int_{\mathbf{p}} \int_{-\infty}^{\infty} \frac{dp^0}{2\pi} \frac{1}{2k} \Delta(i\nu_q - p^0, \mathbf{q} - \mathbf{p}) \rho_{M^2}(p^0, \mathbf{p}) \sum_{r=\pm 1} r \left\{ \Delta(rk + p^0, \mathbf{k} + \mathbf{p}) \right. \\ \left. \left[n_F(-rk) n_B(-p^0) + n_F(rk) n_B(p^0) \right] B(rk, \mathbf{k}; rk + p^0, \mathbf{k} + \mathbf{p}; i\nu_q - p^0, \mathbf{q} - \mathbf{p}) \right\}, \end{aligned} \quad (3.9a)$$

$$\begin{aligned} \Sigma_{\text{B2}}(i\nu_q, \mathbf{q}) = -e^4 \lim_{M^2 \rightarrow 0} \frac{\partial}{\partial M^2} \int_{\mathbf{k}} \int_{\mathbf{p}} \int_{-\infty}^{\infty} \frac{dp^0}{2\pi} \frac{1}{2k} \Delta(i\nu_q - p^0, \mathbf{q} - \mathbf{p}) \Delta_{M^2}(p^0, \mathbf{p}) \sum_{r=\pm 1} r \left\{ \rho(p^0 + rk, \mathbf{p} + \mathbf{k}) \right. \\ \left. n_F(rk) n_F(p^0 + rk) B(rk, \mathbf{k}; p^0 + rk, \mathbf{p} + \mathbf{k}; i\nu_q - p^0, \mathbf{q} - \mathbf{p}) \right\}, \end{aligned} \quad (3.9b)$$

$$\begin{aligned} \Sigma_{\text{B3}}(i\nu_q, \mathbf{q}) = e^4 \lim_{M^2 \rightarrow 0} \frac{\partial}{\partial M^2} \int_{\mathbf{k}} \int_{\mathbf{p}} \int_{-\infty}^{\infty} \frac{dp^0}{2\pi} \rho(p^0, \mathbf{q} - \mathbf{p}) \Delta_{M^2}(i\nu_q - p^0, \mathbf{p}) \sum_{r=\pm 1} r \left\{ \right. \\ \frac{n_F(rk)}{2k} n_F(-p^0) B(rk, \mathbf{k}; i\nu_q + rk - p^0, \mathbf{p} + \mathbf{k}; p^0, \mathbf{q} - \mathbf{p}) \Delta(i\nu_q + rk - p^0, \mathbf{p} + \mathbf{k}) \\ \left. - \frac{n_F(r|\mathbf{p} + \mathbf{k}|)}{2|\mathbf{p} + \mathbf{k}|} n_F(p^0) B(rk + p^0 - i\nu_q, \mathbf{k}; rk, \mathbf{p} + \mathbf{k}; p^0, \mathbf{q} - \mathbf{p}) \Delta(rk + p^0 - i\nu_q, \mathbf{k}) \right\}, \end{aligned} \quad (3.9c)$$

where $k \equiv |\mathbf{k}|, p \equiv |\mathbf{p}|$. We will evaluate the leading order terms in the high temperature expansion of (3.9) for $\mathbf{q} = \mathbf{0}$ in the next section.

B. The Rainbow Diagram

The contribution of the rainbow (R) graph of Fig. 2 is given by

$$\Sigma_{\text{R}}(Q) = ie^4 \int_K \int_P \gamma_\alpha G(P_1) \gamma_\mu G(P_3) \gamma_\nu D^{\nu\mu}(P_2) G(P_4) \gamma_\beta D^{\beta\alpha}(P_5), \quad (3.10)$$

where we have introduced the labels, P_i for the five different four-momenta, $P_1 = P_4 = Q - P$, $P_2 = K$, $P_3 = Q - P - K$, and $P_5 = P$, with $Q = (i\nu_q, \mathbf{q})$, $P = (i\omega_n, \mathbf{p})$, and $K = (i\omega_m, \mathbf{k})$, as in the previous B diagram.

It is possible to evaluate this rainbow diagram in a completely analogous manner as the bubble diagram. Since the topology of the two graphs is the same, one will obtain seven tree diagrams by the Gaudin method for the rainbow self-energy, analogous to the seven tree diagrams of Fig. 3. In the case of the rainbow diagram the differing Dirac structure allows for some simplification. In the Feynman gauge $\xi = 1$, we have

$$\gamma_\alpha \not{P}_1 \gamma_\mu \not{P}_3 \gamma^\mu \not{P}_4 \gamma^\alpha = 4 \not{P}_4 \not{P}_3 \not{P}_1 = 4 \{ [P_1^2 + P_3^2 - (P_1 - P_3)^2] \not{P}_4 - P_1^2 \not{P}_3 \}, \quad (3.11)$$

since $P_1 = P_4$. Using also that $P_1 - P_3 = P_2$ we have

$$\frac{\gamma_\alpha \not{P}_1 \gamma_\mu \not{P}_3 \gamma^\mu \not{P}_4 \gamma^\alpha}{P_1^2 P_2^2 P_3^2 P_4^2 P_5^2} = 4 \left[\frac{\not{P}_4}{P_2^2 P_3^2 P_4^2 P_5^2} - \frac{\not{P}_3}{P_2^2 P_3^2 P_4^2 P_5^2} \right] + 4 \frac{\not{P}_4}{(P_4^2)^2} \frac{1}{P_5^2} \left(\frac{1}{P_2^2} - \frac{1}{P_3^2} \right). \quad (3.12)$$

As in the bubble diagram there is a potential double pole problem which shows up only in the second set of terms in (3.12), and can most conveniently be handled by introducing a fermion mass m , and making the replacement

$$\frac{i \not{P}_4}{(P_4^2)^2} \rightarrow \frac{\partial}{\partial m^2} \left(\frac{i \not{P}_4}{P_4^2 - m^2} \right) \equiv \frac{\partial G_{m^2}(P_4)}{\partial m^2}, \quad (3.13)$$

and taking the limit $m^2 \rightarrow 0$ at the end of the calculation. Because this is a fermionic double pole rather than the bosonic one in the bubble diagram, the limit will be less singular, and in fact not give rise to divergences in the leading order of the high temperature expansion.

The two sets of terms in (3.12), denoted by R1 and R2 give for the full rainbow two-loop self-energy the expression

$$\Sigma_{\text{R}}(Q) \Big|_{\xi=1} = \Sigma_{\text{R1}}(Q) + \Sigma_{\text{R2}}(Q), \quad (3.14)$$

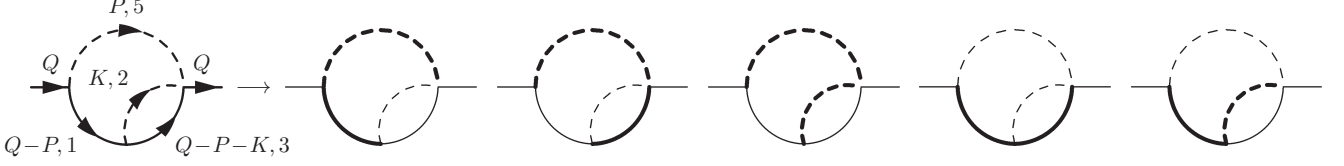


FIG. 4: The diagrammatic representation of the integrals in (3.15a) obtained by reducing the original rainbow diagram and its decomposition in Gaudin tree graphs. The dashed (solid) line means bosonic (fermionic) propagator. As in Fig. 3 the two thin lines carry the two independent Matsubara frequencies to be summed, while the thick lines belong to the Gaudin tree and represent propagators that contain the time component variable of the appropriate momenta p_i^0 in place of the Matsubara frequencies.

with

$$\Sigma_{R1}(Q) = -4e^4 \int_K \int_P \left[D(P_2) \tilde{D}(P_3) G(P_4) D(P_5) - D(P_2) G(P_3) \tilde{D}(P_4) D(P_5) \right], \quad (3.15a)$$

$$\Sigma_{R2}(Q) = 4ie^4 \left(\int_K \tilde{D}(K) - \int_K D(K) \right) \frac{\partial}{\partial m^2} \int_P G_{m^2}(P) D(Q-P) \Big|_{m^2=0}. \quad (3.15b)$$

To obtain the second R2 term we have used for the last term inside the parentheses of (3.12) the shift $K \rightarrow Q - P - K$ and then for both terms within the parentheses the shift $P \rightarrow Q - P$. The advantage of the form (3.15) is that whereas the original expression (3.10) has five propagators, the R1 terms have only four propagators, and the R2 terms factorize into the product of a difference of two tadpoles and a derivative of a one-loop self-energy with only two propagators. In these expressions it is important to keep track of which momenta are bosonic and which are fermionic. The latter propagators are denoted with a tilde.

In imaginary time, using the spectral representation of the propagators, we have for the two contributions

$$\begin{aligned} \Sigma_{R1}(i\nu_q, \mathbf{q}) &= 4e^4 \int_{\mathbf{k}} \int_{\mathbf{p}} \left(\prod_{i=2}^5 \int \frac{dp_i^0}{2\pi} \right) [\rho(p_3^0, \mathbf{p}_3) \rho_F(p_4^0, \mathbf{p}_4) - \rho_F(p_3^0, \mathbf{p}_3) \rho(p_4^0, \mathbf{p}_4)] \times \\ &\quad \rho(p_2^0, \mathbf{p}_2) \rho(p_5^0, \mathbf{p}_5) \left(T^2 \sum_{n,m} \prod_{i=2}^5 \frac{1}{p_i^0 - i\omega_i} \right), \end{aligned} \quad (3.16a)$$

$$\begin{aligned} \Sigma_{R2}(i\nu_q, \mathbf{q}) &= 4e^4 T \int_{\mathbf{k}} \left(\sum_m \tilde{\Delta}(i\omega_m, \mathbf{k}) - \sum_m \Delta(i\omega_m, \mathbf{k}) \right) \times \\ &\quad \frac{\partial}{\partial m^2} \int_{\mathbf{p}} \int_{-\infty}^{\infty} \frac{dp^0}{2\pi} \int_{-\infty}^{\infty} \frac{dk^0}{2\pi} \rho_F(p^0, E_{\mathbf{p}}) \rho(k^0, \mathbf{q} - \mathbf{p}) T \sum_n \frac{1}{(p^0 - i\omega_n)(k^0 - i(\nu_q - \omega_n))} \Big|_{m^2=0}. \end{aligned} \quad (3.16b)$$

The Matsubara frequency sums in the R1 terms may now be performed by Gaudin's method. The Gaudin relevant tree diagrams represented diagrammatically in Fig. 4. Having one propagator less compared to

the original graph, it is somewhat easier to compute the sums, and we obtain

$$\begin{aligned}
T^2 \sum_{n,m} \prod_{i=2}^4 \frac{1}{p_i^0 - i\omega_i} &= -\frac{n_B(-p_2^0)n_F(-p_3^0)}{(p_4^0 - p_2^0 - p_3^0)(p_5^0 + p_2^0 + p_3^0 - i\nu_q)} - \frac{n_F(-p_4^0)n_B(-p_2^0)}{(p_3^0 - p_4^0 + p_2^0)(p_5^0 + p_4^0 - i\nu_q)} \\
&- \frac{n_F(-p_4^0)n_F(p_3^0)}{(p_2^0 - p_4^0 + p_3^0)(p_5^0 + p_4^0 - i\nu_q)} - \frac{n_B(-p_2^0)n_B(p_5^0)}{(p_4^0 + p_5^0 - i\nu_q)(p_3^0 + p_2^0 + p_5^0 - i\nu_q)} \\
&- \frac{n_F(p_3^0)n_B(p_5^0)}{(p_4^0 + p_5^0 - i\nu_q)(p_2^0 + p_3^0 + p_5^0 - i\nu_q)}, \tag{3.17}
\end{aligned}$$

with each term corresponding to a Gaudin tree graph of Fig. 4. In (3.16b), ω_n is fermionic and $\nu_q - \omega_n$ is bosonic, and we obtain

$$T \sum_n \frac{1}{(p^0 - i\omega_n)(r^0 - i(\nu_q - \omega_n))} = \frac{n_F(-p^0) + n_B(r^0)}{p^0 + r^0 - i\nu_q} \tag{3.18}$$

for the Matsubara sum.

Substituting (3.17) into (3.16a), the integrations over the two p_i^0 which do not appear in the statistical distributions can be performed simply by using the definition (2.10) of the spectral representation of the Euclidean propagator function Δ . By relabeling $p_2^0 \rightarrow k^0, p_3^0 \rightarrow p^0, \mathbf{p} \rightarrow -\mathbf{p} + \mathbf{q} - \mathbf{k}$ in the first of the five terms arising from (3.17), $p_2^0 \rightarrow k^0, p_4^0 \rightarrow p^0, \mathbf{p} \rightarrow -\mathbf{p} + \mathbf{q}$ in the second term, $p_3^0 \rightarrow k^0, p_4^0 \rightarrow p^0, \mathbf{k} \rightarrow -\mathbf{k} + \mathbf{p}, \mathbf{p} \rightarrow -\mathbf{p} + \mathbf{q}$ in the third term, $p_2^0 \rightarrow k^0, p_5^0 \rightarrow p^0$ in the fourth term, and $p_3^0 \rightarrow k^0, p_5^0 \rightarrow p^0, \mathbf{k} \rightarrow -\mathbf{k} + \mathbf{q} - \mathbf{p}$ in the fifth term arising from (3.17), we arrive at the covariant form,

$$\begin{aligned}
\Sigma_{R1}(i\nu_q, \mathbf{q}) &= -4e^4 \int_{\mathbf{k}} \int_{\mathbf{p}} \int_{-\infty}^{\infty} \frac{dk^0}{2\pi} \int_{-\infty}^{\infty} \frac{dp^0}{2\pi} \left\{ \mathbb{K} n_B(-k^0) n_F(-p^0) [\Delta(K+P)\Delta(Q-K-P) \right. \\
&+ \Delta(P-K)\Delta(Q-P)] + (\mathbb{P} - \mathbb{K}) n_F(k^0) n_F(-p^0) \Delta(P-K)\Delta(Q-P) \\
&+ n_B(p^0) \Delta(Q-P)\Delta(Q-P-K) [\mathbb{P} n_B(-k^0) + (\mathbb{Q} - \mathbb{P} - \mathbb{K}) n_F(k^0)] \left. \right\} \rho(k^0, \mathbf{k}) \rho(p^0, \mathbf{p}), \tag{3.19}
\end{aligned}$$

for (3.16a).

For (3.16b), we evaluate first

$$T \sum_n \int_{\mathbf{k}} \left(\tilde{\Delta}(i\omega_n, \mathbf{k}) - \Delta(i\omega_n, \mathbf{k}) \right) = -\frac{1}{2\pi^2} \int_0^\infty dk k [n_B(k) + n_F(k)] = -\frac{T^2}{8}. \tag{3.20}$$

Then using (3.18), we obtain

$$\Sigma_{R2}(i\nu_q, \mathbf{q}) = -\frac{e^4 T^2}{2} \frac{\partial}{\partial m^2} \int_{\mathbf{p}} \int_{-\infty}^{\infty} \frac{dp^0}{2\pi} \left\{ \mathbb{P} n_F(-p^0) \rho_{m^2}(P) \Delta(Q-P) + (\mathbb{Q} - \mathbb{P}) n_B(p^0) \rho(P) \Delta_{m^2}(Q-P) \right\} \Big|_{m^2=0}, \tag{3.21}$$

where the substitutions $r^0 \rightarrow p^0$ and $\mathbf{p} \rightarrow \mathbf{q} - \mathbf{p}$ have been made in the second term to arrive at (3.21).

Finally one may perform the k^0 and p^0 integrations in (3.19) and the p^0 integration in (3.21) by using the δ functions in the spectral representations to obtain

$$\Sigma_{R1}(i\nu_q, \mathbf{q}) = -e^4 \int_{\mathbf{k}} \int_{\mathbf{p}} \sum_{r,s=\pm 1} \left\{ \frac{n_B(k) n_F(p)}{kp} (kr\gamma_0 - \mathbf{k} \cdot \boldsymbol{\gamma}) \times \right.$$

$$\begin{aligned}
& [\Delta(kr + ps, \mathbf{k} + \mathbf{p})\Delta(i\nu_q - kr - ps, \mathbf{q} - \mathbf{k} - \mathbf{p}) + \Delta(ps - kr, \mathbf{p} - \mathbf{k})\Delta(i\nu_q - ps, \mathbf{q} - \mathbf{p})] \\
& + \frac{n_F(k)n_F(p)}{kp} [(ps - kr)\gamma_0 - (\mathbf{p} - \mathbf{k}) \cdot \boldsymbol{\gamma}] \Delta(ps - kr, \mathbf{p} - \mathbf{k})\Delta(i\nu_q - ps, \mathbf{q} - \mathbf{p}) \\
& + \left[\frac{n_B(k)n_B(p)}{kp} (ps\gamma_0 - \mathbf{p} \cdot \boldsymbol{\gamma}) + \frac{n_F(k)n_B(p)}{kp} [(i\nu_q - ps - kr)\gamma_0 + (\mathbf{q} - \mathbf{p} - \mathbf{k}) \cdot \boldsymbol{\gamma}] \right] \times \\
& \Delta(i\nu_q - ps, \mathbf{q} - \mathbf{p})\Delta(i\nu_q - ps - kr, \mathbf{q} - \mathbf{p} - \mathbf{k}) \Big\} + \dots
\end{aligned} \tag{3.22}$$

and

$$\begin{aligned}
\Sigma_{\text{R2}}(i\nu_q, \mathbf{q}) = & -\frac{e^4 T^2}{4} \frac{\partial}{\partial m^2} \int_{\mathbf{p}} \sum_{s=\pm 1} \left\{ [(i\nu_q - sp)\gamma_0 - (\mathbf{q} - \mathbf{p}) \cdot \boldsymbol{\gamma}] \Delta_{m^2}(i\nu_q - sp, \mathbf{q} - \mathbf{p}) \frac{n_B(p)}{p} \right. \\
& \left. - (sE_p\gamma_0 - \mathbf{p} \cdot \boldsymbol{\gamma}) \Delta(i\nu_q - sE_p, \mathbf{q} - \mathbf{p}) \frac{n_F(E_p)}{E_p} \right\} \Big|_{m^2=0} + \dots,
\end{aligned} \tag{3.23}$$

where the ellipsis in each case denotes the terms with fewer than two statistical factors, which are subleading in the high temperature limit. We again postpone to the next section the detailed evaluation of (3.22) and (3.23) in Feynman gauge for a fermion at rest.

C. The Crossed Photon Diagram

The third and final two-loop diagram is the crossed photon diagram of Fig. 2, which topologically has the form of a vertex correction. The contribution of this crossed diagram to the two-loop electron self-energy is

$$\Sigma_{\text{C}}(Q) = ie^4 \int_K \int_P \gamma_\alpha G(Q - P) \gamma_\mu G(Q - P - K) \gamma_\nu D^{\nu\alpha}(P) G(Q - K) \gamma_\beta D^{\beta\mu}(K). \tag{3.24}$$

In imaginary time, using the spectral representation of the propagators, this becomes

$$\Sigma_{\text{C}}(i\nu_q, \mathbf{q}) = -e^4 \int_{\mathbf{k}} \int_{\mathbf{p}} \left(\prod_{i=1}^5 \int \frac{dp_i^0}{2\pi} \right) \gamma_\alpha \rho_F(P_3) \gamma_\mu \rho_F(P_5) \gamma_\nu \rho^{\nu\alpha}(P_1) \rho_F(P_2) \gamma_\beta \rho^{\beta\mu}(P_4) \left(T^2 \sum_{n,m} \prod_{i=1}^5 \frac{1}{p_i^0 - i\omega_i} \right), \tag{3.25}$$

where $P_1 = P$, $P_2 = Q - K$, $P_3 = Q - P$, $P_4 = K$ and $P_5 = Q - P - K$ with again $Q = (i\nu_q, \mathbf{q})$, $P = (i\omega_n, \mathbf{p})$, and $K = (i\omega_m, \mathbf{k})$. The Matsubara sums performed with Gaudin's method gives for the last factor of (3.25),

$$\begin{aligned}
& T^2 \sum_{n,m} \prod_{i=1}^5 \frac{1}{p_i^0 - i\omega_i} = \\
& \frac{1}{(p_1^0 + p_3^0 - i\nu_q)(p_2^0 + p_4^0 - i\nu_q)} \left[\frac{n_B(-p_1^0)n_F(p_2^0)}{p_5^0 + p_1^0 - p_2^0} + \frac{n_B(-p_4^0)n_F(p_3^0)}{p_5^0 + p_4^0 - p_3^0} \right]
\end{aligned}$$

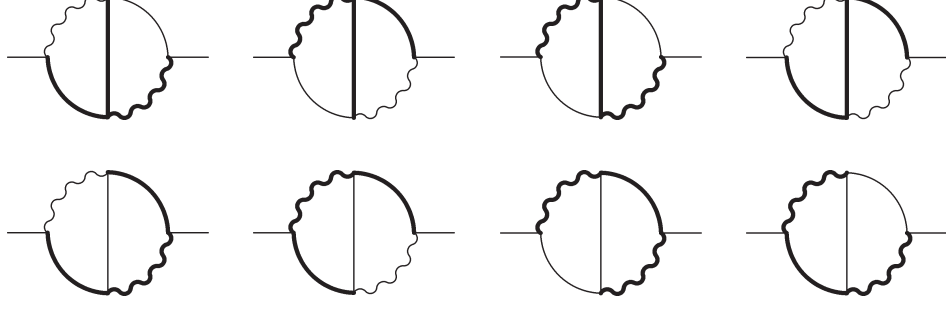


FIG. 5: The Gaudin tree graphs corresponding to the crossed photon diagram of Fig. 2. A tree is represented by thick lines. As in Figs. 3 and 4 the two thin lines carry the two independent Matsubara frequencies to be summed, while the thick lines belong to the Gaudin tree and contain no Matsubara frequencies.

$$\begin{aligned}
& + \frac{1}{(p_1^0 + p_3^0 - i\nu_q)(p_2^0 + p_4^0 - i\nu_q)} \left[\frac{n_F(p_2^0)n_F(p_3^0)}{p_5^0 - p_2^0 - p_3^0 + i\nu_q} + \frac{n_B(-p_1^0)n_B(-p_4^0)}{p_5^0 + p_1^0 + p_4^0 - i\nu_q} \right] \\
& + \frac{1}{p_1^0 + p_4^0 + p_5^0 - i\nu_q} \left[\frac{n_B(-p_1^0)n_F(p_5^0)}{(p_2^0 - p_1^0 - p_5^0)(p_3^0 + p_1^0 - i\nu_q)} - \frac{n_B(p_4^0)n_F(p_5^0)}{(p_2^0 + p_4^0 - i\nu_q)(p_3^0 - p_4^0 - p_5^0)} \right] \\
& + \frac{1}{p_2^0 + p_3^0 - p_5^0 - i\nu_q} \left[\frac{n_F(p_3^0)n_F(p_5^0)}{(p_4^0 + p_5^0 - p_3^0)(p_1^0 + p_3^0 - i\nu_q)} - \frac{n_F(-p_2^0)n_F(p_5^0)}{(p_1^0 + p_5^0 - p_2^0)(p_4^0 + p_2^0 - i\nu_q)} \right], \quad (3.26)
\end{aligned}$$

where the corresponding eight Gaudin tree graphs are depicted in Fig. 5.

Substituting (3.26) into (3.25), the integrations over the three p_i^0 which do not involve the statistical factors n_B or n_F in each of the eight terms can be performed using the definition, Eqs. (2.7a) and (2.7b), simply undoing the spectral decomposition in favor of the Matsubara propagator (2.4). The first and second of the eight terms are identical after a relabeling of momenta, while the fifth and sixth terms and the seventh and eighth terms can also be grouped together. Suppressing the 0 superscript on the timelike integration variables, we obtain

$$\begin{aligned}
\Sigma_C(i\nu_q, \mathbf{q}) = & -e^4 \int_{\mathbf{k}} \int_{\mathbf{p}} \left\{ 2 \int \frac{dp_1}{2\pi} \int \frac{dp_2}{2\pi} n_B(-p_1)n_F(p_2) \times \right. \\
& \gamma_\alpha \Delta_F(i\nu_q - p_1, \mathbf{q} - \mathbf{p}) \gamma_\mu \Delta_F(p_2 - p_1, \mathbf{q} - \mathbf{p} - \mathbf{k}) \gamma_\nu \rho^{\nu\alpha}(p_1, \mathbf{p}) \rho_F(p_2, \mathbf{q} - \mathbf{k}) \gamma_\beta \Delta^{\beta\mu}(i\nu_q - p_2, \mathbf{k}) \\
& + \int \frac{dp_2}{2\pi} \int \frac{dp_3}{2\pi} n_F(p_2)n_F(p_3) \times \\
& \gamma_\alpha \rho_F(p_3, \mathbf{q} - \mathbf{p}) \gamma_\mu \Delta_F(i\nu_q - p_2 - p_3, \mathbf{q} - \mathbf{p} - \mathbf{k}) \gamma_\nu \Delta^{\nu\alpha}(i\nu_q - p_3, \mathbf{p}) \rho_F(p_2, \mathbf{q} - \mathbf{k}) \gamma_\beta \Delta^{\beta\mu}(i\nu_q - p_2, \mathbf{k}) \\
& + \int \frac{dp_1}{2\pi} \int \frac{dp_4}{2\pi} n_B(-p_1)n_B(-p_4) \times \\
& \gamma_\alpha \Delta_F(i\nu_q - p_1, \mathbf{q} - \mathbf{p}) \gamma_\mu \Delta_F(i\nu_q - p_1 - p_4, \mathbf{q} - \mathbf{p} - \mathbf{k}) \gamma_\nu \rho^{\nu\alpha}(p_1, \mathbf{p}) \Delta_F(i\nu_q - p_4, \mathbf{k}) \gamma_\beta \rho^{\beta\mu}(p_4, \mathbf{k}) \\
& + \int \frac{dp_1}{2\pi} \int \frac{dp_5}{2\pi} n_B(-p_1)n_F(-p_5) \times \\
& \gamma_\alpha \Delta_F(i\nu_q - p_1, \mathbf{q} - \mathbf{p}) \gamma_\mu \rho_F(p_5, \mathbf{q} - \mathbf{p} - \mathbf{k}) \gamma_\nu \rho^{\nu\alpha}(p_1, \mathbf{p}) \Delta_F(p_1 + p_5, \mathbf{q} - \mathbf{k}) \gamma_\beta \Delta^{\beta\mu}(i\nu_q - p_1 - p_5, \mathbf{k}) \\
& \left. - \int \frac{dp_4}{2\pi} \int \frac{dp_5}{2\pi} n_B(p_4)n_F(p_5) \times \right.
\end{aligned}$$

$$\begin{aligned}
& \gamma_\alpha \Delta_F(p_4 + p_5, \mathbf{q} - \mathbf{p}) \gamma_\mu \rho_F(p_5, \mathbf{q} - \mathbf{p} - \mathbf{k}) \gamma_\nu \Delta^{\nu\alpha}(i\nu_q - p_4 - p_5, \mathbf{p}) \Delta_F(i\nu_q - p_4, \mathbf{q} - \mathbf{k}) \gamma_\beta \rho^{\beta\mu}(p_4, \mathbf{k}) \\
& + \int \frac{dp_3}{2\pi} \int \frac{dp_5}{2\pi} n_F(p_3) n_F(p_5) \times \\
& \gamma_\alpha \rho_F(p_3, \mathbf{q} - \mathbf{p}) \gamma_\mu \rho_F(p_5, \mathbf{q} - \mathbf{p} - \mathbf{k}) \gamma_\nu \Delta^{\nu\alpha}(i\nu_q - p_3, \mathbf{p}) \Delta_F(i\nu_q + p_5 - p_3, \mathbf{q} - \mathbf{k}) \gamma_\beta \Delta^{\beta\mu}(p_3 - p_5, \mathbf{k}) \\
& - \int \frac{dp_2}{2\pi} \int \frac{dp_5}{2\pi} n_F(-p_2) n_F(p_5) \times \\
& \gamma_\alpha \Delta_F(i\nu_q + p_5 - p_2, \mathbf{q} - \mathbf{p}) \gamma_\mu \rho_F(p_5, \mathbf{q} - \mathbf{p} - \mathbf{k}) \gamma_\nu \Delta^{\nu\alpha}(p_2 - p_5, \mathbf{p}) \rho_F(p_2, \mathbf{q} - \mathbf{k}) \gamma_\beta \Delta^{\beta\mu}(i\nu_q - p_2, \mathbf{k}) \Big\}. \tag{3.27}
\end{aligned}$$

Expressing the fermionic and gauge Euclidean propagators Δ_F and $\Delta^{\mu\nu}$, and the spectral densities ρ_F and $\rho^{\mu\nu}$ in terms of the bosonic forms Δ and ρ defined in (2.10) and (2.9), and evaluating the expression (3.28) in the $\xi = 1$ Feynman gauge, we get the covariant form for the crossed photon diagram,

$$\begin{aligned}
\Sigma_C(i\nu_q, \mathbf{q})|_{\xi=1} &= -e^4 \int_{\mathbf{k}} \int_{\mathbf{p}} \int_{-\infty}^{\infty} \frac{dk^0}{2\pi} \int_{-\infty}^{\infty} \frac{dp^0}{2\pi} \rho(K) \rho(P) \times \\
& \left\{ 2n_F(k^0) n_B(-p^0) C(K; Q - P; K - P) \Delta(Q - P) \Delta(Q - K) \Delta(K - P) \right. \\
& + n_F(k^0) n_F(p^0) C(K; P; K + P - Q) \Delta(Q - P) \Delta(Q - K) \Delta(K + P - Q) \\
& + n_B(-k^0) n_B(-p^0) C(Q - K; Q - P; Q - P - K) \Delta(Q - P) \Delta(Q - K) \Delta(K + P - Q) \\
& + \left[n_F(k^0) n_B(-p^0) - n_F(k^0) n_B(p^0) \right] C(K + P; Q - P; K) \Delta(K + P) \Delta(Q - P) \Delta(Q - K - P) \\
& \left. + \left[n_F(k^0) n_F(p^0) - n_F(k^0) n_F(-p^0) \right] C(Q - P + K; P; K) \Delta(Q - P) \Delta(Q - P + K) \Delta(K - P) \right\}, \tag{3.28}
\end{aligned}$$

where we have defined the factor arising from the Dirac algebra,

$$C(P_2; P_3; P_5) \equiv C(p_2^0, \mathbf{p}_2; p_3^0, \mathbf{p}_3; p_5^0, \mathbf{p}_5) \equiv \gamma_\alpha \not{P}_3 \gamma_\mu \not{P}_5 \gamma^\alpha \not{P}_2 \gamma^\mu = -8(P_2 \cdot P_3) \not{P}_5, \tag{3.29}$$

and relabeled $p_2 \rightarrow k^0, p_1 \rightarrow p^0, \mathbf{k} \rightarrow -\mathbf{k} + \mathbf{q}$ in the first term of (3.27), $p_2 \rightarrow k^0, p_3 \rightarrow p^0, \mathbf{k} \rightarrow -\mathbf{k} + \mathbf{q}, \mathbf{p} \rightarrow \mathbf{p} + \mathbf{q}$ in the second term, $p_4 \rightarrow k^0, p_1 \rightarrow p^0$ in the third term, $p_5 \rightarrow k^0, p_1 \rightarrow p^0, \mathbf{k} \rightarrow -\mathbf{k} + \mathbf{q} - \mathbf{p}$ in the fourth term, $p_5 \rightarrow k^0, p_4 \rightarrow p^0, \mathbf{k} \rightarrow \mathbf{p}, \mathbf{p} \rightarrow -\mathbf{k} + \mathbf{q} - \mathbf{p}$ in the fifth term, $p_5 \rightarrow k^0, p_3 \rightarrow p^0, \mathbf{k} \rightarrow -\mathbf{k} + \mathbf{p}, \mathbf{p} \rightarrow -\mathbf{p} + \mathbf{q}$ in the sixth term, and $p_5 \rightarrow k^0, p_2 \rightarrow p^0, \mathbf{k} \rightarrow -\mathbf{p} + \mathbf{q}, \mathbf{p} \rightarrow \mathbf{p} - \mathbf{k}$ in the seventh term of (3.27), in order to arrive at (3.28).

Proceeding as in the previous diagram, for each term in (3.28) the remaining two frequency integrals over k^0 and p^0 are performed next, using the Dirac δ functions in the remaining two spectral functions. Then retaining only those terms which have two statistical distribution factors, we obtain

$$\begin{aligned}
\Sigma_C(i\nu_q, \mathbf{q})|_{\xi=1} &= -e^4 \int_{\mathbf{k}} \int_{\mathbf{p}} \sum_{r,s=\pm 1} \left\{ -\frac{n_F(k) n_B(p)}{2kp} C(kr, \mathbf{k}; i\nu_q - ps, \mathbf{q} - \mathbf{p}; kr - ps, \mathbf{k} - \mathbf{p}) \times \right. \\
& \left. \Delta(i\nu_q - ps; \mathbf{q} - \mathbf{p}) \Delta(i\nu_q - kr, \mathbf{q} - \mathbf{k}) \Delta(kr - ps, \mathbf{k} - \mathbf{p}) \right\}
\end{aligned}$$

$$\begin{aligned}
& + \frac{n_F(k)n_F(p)}{4kp} C(kr, \mathbf{k}; ps, \mathbf{p}; kr + ps - i\nu_q, \mathbf{k} + \mathbf{p} - \mathbf{q}) \times \\
& \quad \Delta(i\nu_q - ps, \mathbf{q} - \mathbf{p}) \Delta(i\nu_q - kr, \mathbf{q} - \mathbf{k}) \Delta(kr + ps - i\nu_q, \mathbf{k} + \mathbf{p} - \mathbf{q}) \\
& + \frac{n_B(k)n_F(p)}{4kp} C(i\nu_q - kr, \mathbf{q} - \mathbf{k}; i\nu_q - ps, \mathbf{q} - \mathbf{p}; i\nu_q - ps - kr, \mathbf{q} - \mathbf{p} - \mathbf{k}) \times \\
& \quad \Delta(i\nu_q - ps, \mathbf{q} - \mathbf{p}) \Delta(i\nu_q - kr, \mathbf{q} - \mathbf{k}) \Delta(kr + ps - i\nu_q, \mathbf{k} + \mathbf{p} - \mathbf{q}) \\
& - \frac{n_F(k)n_B(p)}{2kp} C(kr + ps, \mathbf{k} + \mathbf{p}; i\nu_q - ps, \mathbf{q} - \mathbf{p}; kr, \mathbf{k}) \times \\
& \quad \Delta(kr + ps, \mathbf{k} + \mathbf{p}) \Delta(i\nu_q - ps, \mathbf{q} - \mathbf{p}) \Delta(i\nu_q - kr - ps, \mathbf{q} - \mathbf{k} - \mathbf{p}) \\
& + \frac{n_F(k)n_F(p)}{2kp} C(i\nu_q - ps + kr, \mathbf{q} - \mathbf{p} + \mathbf{k}; ps, \mathbf{p}; kr, \mathbf{k}) \times \\
& \quad \Delta(i\nu_q - ps, \mathbf{q} - \mathbf{p}) \Delta(i\nu_q - ps + kr, \mathbf{q} - \mathbf{p} + \mathbf{k}) \Delta(kr - ps, \mathbf{k} - \mathbf{p}) \Big\} + \dots, \tag{3.30}
\end{aligned}$$

where the ellipsis denotes terms with fewer than two statistical factors, which are subleading in the high temperature expansion. We turn next to the explicit extraction of the leading high temperature behavior of all the two-loop terms in the self-energy.

IV. HIGH TEMPERATURE BEHAVIOR OF THE TWO-LOOP INTEGRALS

In this section we analyze the integrals which result from the evaluation of the three two-loop diagrams of the previous section, extracting the leading order terms in the high temperature expansion $T \gg \nu_q, M, m$, for fermions at rest with respect to the plasma (*i.e.* $\mathbf{q} = 0$), and perform the analytic continuation to real fermion energies $i\nu_q \rightarrow \omega + i0^+$ in order to obtain the real and imaginary parts of the self-energy Σ . The behavior of the high temperature asymptotics for $\mathbf{q} = 0$ is sufficient for our purposes of analyzing the systematics of the two-loop self-energy. When $\mathbf{q} = 0$ only the γ_0 dependent part of the self-energy is non-zero. In this case the integrals over spatial momentum also simplify to give

$$\int_{\mathbf{k}} \int_{\mathbf{p}} \longrightarrow \frac{1}{8\pi^4} \int_0^\infty dk \int_0^\infty dp k^2 p^2 \int_{-1}^1 dx, \tag{4.1}$$

where $k = |\mathbf{k}|$, $p = |\mathbf{p}|$ and $x = \cos \theta = \mathbf{k} \cdot \mathbf{p}/(kp)$.

A. The Bubble Diagram

We start with $\Sigma_{B1}(i\nu_q)$ defined by (3.7)-(3.9) by evaluating the function B for $\mathbf{q} = 0$ and performing the p^0 integral with the help of the δ function from the spectral density $\rho_{M^2}(p^0, \mathbf{p})$. The leading temperature dependence comes from those terms containing a product of two thermal distributions evaluated at *positive*

arguments, *i.e.*, substituting the identities (2.20), we may discard the zero temperature $\theta(\pm E)$ terms and retain only the terms $n_F(|k|)$ and $n_B(|E_p|)$ with $E_p \equiv \sqrt{\mathbf{p}^2 + M^2}$. In this way one obtains from (3.9a)

$$\Sigma_{\text{B1}}(i\nu_q, \mathbf{q} = \mathbf{0}) = \frac{e^4}{2\pi^4} \gamma_0 \lim_{M^2 \rightarrow 0} \frac{\partial}{\partial M^2} \int_0^\infty dk \int_0^\infty dp \int_{-1}^1 dx k^2 p^2 n_F(k) \sum_{r,s=\pm 1} \left\{ \frac{n_B(E_p)}{E_p} \frac{2(i\nu_q(k + rsE_p) - k(sE_p - rp) - M^2) - p(rp - sE_p x)}{[2k(px - rsE_p) - M^2][2i\nu_q sE_p - (i\nu_q)^2 - M^2]} \right\} + \dots, \quad (4.2)$$

where the ellipsis denotes terms with fewer than two statistical factors, which are subleading in the high temperature limit.

To exhibit the singular behavior of (4.2) as the regulator M^2 is removed, one may take the derivative with respect to M^2 inside the integral, and naively take the limit $M^2 \rightarrow 0$. After some straightforward but tedious algebra one obtains in this way,

$$-\frac{e^4}{\pi^4} \gamma_0 \int_0^\infty dk k n_F(k) \int_0^\infty dp \int_{-1}^1 dx \frac{1}{[(i\nu_q)^2 - 4p^2]} \left\{ \left(\frac{p^2}{i\nu_q} + \frac{i\nu_q}{x^2 - 1} \right) \frac{dn_B(p)}{dp} + n_B(p) \left[\frac{2}{x^2 - 1} \left(\frac{p}{i\nu_q} + \frac{i\nu_q}{p} \left(1 + \frac{2}{x^2 - 1} \right) \right) + \frac{i\nu_q p}{(i\nu_q)^2 - 4p^2} \left(1 + \frac{4}{x^2 - 1} \right) \right] \right\}, \quad (4.3)$$

which factorizes into a hard k integral and a soft p integral. This factorization property will persist even when the M^2 regulator is retained, for the leading order terms in the high temperature expansion. However, in several of the terms in (4.3) the soft p integration is infrared divergent at $p = 0$, and is multiplied by an additional collinear divergence from the $x = \cos\theta$ integral at $x = \pm 1$. Thus the most severe type of divergence in (4.3) is the product of an infrared and a collinear divergence, each of which is linear. Hence one may expect generically a quadratic M^{-2} divergence from this singular behavior of the bubble diagram as $M \rightarrow 0$. This is the reason for introducing a photon mass into the calculation to regulate the double pole singularity of the bubble diagram. Since no infrared or collinear divergences are encountered in the one-loop self-energy, the divergence in the two-loop bubble diagram is the clearest indication that a systematic resummation of the perturbative series is needed. This HTL resummation will eventually dress the photon, giving it a Debye mass of order eT , and alter the counting of powers of the coupling constant.

Retaining the mass regulator in Σ_{B1} and performing the sum over $r, s = \pm 1$ in (4.2) one finds

$$\Sigma_{\text{B1}}(i\nu_q) = \frac{e^4}{4\pi^4 i\nu_q} \gamma_0 \frac{\partial}{\partial M^2} \left\{ \int_0^\infty dk k n_F(k) \int_{-1}^1 dx \int_0^\infty dp \frac{p^2}{E_p} n_B(E_p) \times \frac{2(i\nu_q)^2 E_p (px - E_p) - 2pE_p(p - E_p x)(px - E_p) + M^2(i\nu_q)^2 + M^4}{(E_p^2 - \mu_+^2)[(px - E_p)^2 - M^4/(4k^2)]} \right\} \Bigg|_{M^2=0}, \quad (4.4)$$

where $\mu_+ = [(i\nu_q)^2 + M^2]/(2i\nu_q)$. The appearance of $k n_F(k)$ in the first integral shows clearly that the k integration is hard, *i.e.* dominated by $k \sim T$. Since $M \ll T$, the $M^4/k^2 \sim M^4/T^2 \ll M^2$ term in

the denominator can be neglected. Then the hard k integral factorizes completely. Multiplying both the numerator and the denominator by $(px + E_p)^2$, and observing that all terms odd in x vanish by symmetry, we may perform the x integral exactly and obtain

$$\begin{aligned} \Sigma_{\text{B1}}(i\nu_q) = & \frac{e^4 T^2}{24\pi^2 i\nu_q} \gamma_0 \frac{\partial}{\partial M^2} \left\{ [(i\nu_q)^2 + M^2] \int_0^\infty dp \frac{p^2}{E_p} \frac{n_B(E_p)}{E_p^2 - \mu_+^2} \right. \\ & \left. + 2 \int_0^\infty dp p^2 E_p \frac{n_B(E_p)}{E_p^2 - \mu_+^2} - 2i\nu_q \mu_+ \int_0^\infty dp p \frac{n_B(E_p)}{E_p^2 - \mu_+^2} \ln \left[\frac{E_p + p}{E_p - p} \right] \right\} \Big|_{M^2=0}. \end{aligned} \quad (4.5)$$

As we shall show explicitly in Sec. V this is exactly the form of one term which will be reproduced by a single insertion of a hard HTL photon self-energy in the one-loop Σ .

We note that M^2 in the square bracket of the first term in (4.5) comes from the last M^4 term of the numerator in (4.4), which should not be neglected since it will contribute after differentiation with respect to M^2 . The reason for this is the collinear singularity in the x -integral which is regulated by M^2 to give

$$\int_{-1}^1 dx \frac{1}{(px - E_p)^2} = \frac{2}{M^2}. \quad (4.6)$$

This changes the M^4 dependence of this term in (4.5) to M^2 .

The soft p integrals remaining in each of the three terms in (4.5) are analyzed in Appendix B. For the first integral we obtain from (B23), in the high temperature limit, $T \gg M, T \gg \omega$,

$$\Sigma_{\text{B1,a}}(\omega) \simeq \frac{e^4 T^2}{24\pi^2 \omega} \gamma_0 \left[\frac{\pi T}{M} + \ln \left(\frac{M}{\omega} \right) - \frac{1}{2} \ln \left(\frac{T}{\omega} \right) - 2\pi i \frac{T}{\omega} + \dots \right], \quad (4.7)$$

upon analytical continuation $i\nu_q \rightarrow \omega$ to real frequencies. The ellipsis in (4.7) refers to terms which first vanish in the asymptotic high temperature limit $T/M, T/\omega \rightarrow \infty$ (with M/ω fixed), and also remain finite in the second limit in which the regulator is removed, $M/\omega \rightarrow 0$. In other words, terms which are divergent as $M \rightarrow 0$ but subleading in the high temperature expansion have been discarded. It is this particular sequence of limits which is relevant to the comparison to the physics of hard thermal loops, and the fermion self-energy on-shell, in which $\omega \sim M$ are both of order of the soft scale eT , and $e \ll 1$.

The second integral of (4.5) gives after differentiation with respect to M^2 a finite contribution as $M \rightarrow 0$. Using (B24) one obtains only the purely imaginary part of the self-energy

$$\Sigma_{\text{B1,b}}(\omega) \simeq -i\gamma_0 \frac{e^4 T^3}{48\pi\omega^2} + \dots \quad (4.8)$$

in the high temperature expansion.

Lastly the asymptotic behavior of the third integral in (4.5) at high T is studied in Appendix B, and (B26) yields

$$\Sigma_{\text{B1,c}}(\omega) \simeq \frac{e^4 T^2}{24\pi^2 \omega} \gamma_0 \left[-\frac{\omega^2}{2M^2} \left(\ln \frac{T}{\omega} + \ln(4\pi) - \gamma_E \right) + i \frac{\pi\omega T}{M^2} \right]$$

$$+\frac{1}{2} \ln \frac{T}{\omega} \left(\ln \frac{T}{\omega} - 2 \ln \frac{M}{\omega} \right) + \left(\ln(4\pi) - \gamma_E \right) \ln \frac{T}{M} - \frac{1}{2} \ln \frac{T}{\omega} + \dots \Big], \quad (4.9)$$

where γ_E is Euler's constant.

As anticipated by the discussion following (4.3), both the real and imaginary parts of the last contribution to Σ_B diverge quadratically as $M \rightarrow 0$. This severe quadratic infrared/collinear divergence will turn out to cancel against other terms in Σ_B to be evaluated below. The most interesting term is the linearly divergent $1/M$ term in (4.7), both because of its non-analyticity in M^2 and the fact that it gives rise to the dominant term in the real part of Σ , if we anticipate that after HTL resummation M will be of order eT . The existence of this term implies that the NLO correction to the real part of the fermion self-energy will finally be of order e^2T , rather than $e^3T \ln(1/e)$, as one might have supposed from the real part of the NLO one loop self-energy in (2.23). In other words, the form of the divergent terms as $M \rightarrow 0$ in the high temperature expansion of the two-loopbubble self-energy diagram, which are not encountered at one loop, indicate not only the need for resummation of higher loop diagrams in a systematic way, but moreover that these resummed higher loop diagrams will actually give the *dominant* contribution to the NLO behavior of the real part of fermion self-energy (e^2T), compared to the NLO one loop $e^3T \ln(1/e)$ behavior.

Proceeding to the second term Σ_{B2} of (3.8) one evaluates $B(rk, \mathbf{k}; rk + p_0, \mathbf{k} + \mathbf{p}; i\nu_q - p_0, \mathbf{q} - \mathbf{p})$ for $\mathbf{q} = 0$ with the definition in (3.7) and obtains

$$\Sigma_{B2}(i\nu_q) = -\frac{e^4}{2\pi^4} \gamma_0 \frac{\partial}{\partial M^2} \int_0^\infty dk \int_0^\infty dp \int_{-\infty}^\infty dp_0 \int_{-1}^1 dx k^2 p^2 \sum_{r=\pm 1} \left\{ n_F(rk) n_F(p_0 + rk) \epsilon(p_0 + rk) \delta((p_0 + rk)^2 - (\mathbf{k} + \mathbf{p})^2) \frac{2(rk + p_0)(i\nu_q - p_0) + p^2 + px(rp_0 + 2k)}{[E_p^2 - p_0^2][p^2 - (i\nu_q - p_0)^2]} \right\}. \quad (4.10)$$

In this form one can see that because there is no k in the denominator, the k integral is clearly hard, since even taking account of the remaining delta function it would be UV quadratically divergent if not for the statistical factors. Thus $k \sim T$ and the k integral will give a factor of T^2 . On the other hand the p, p_0 integrals are soft due to the appearance of p, p_0 in the denominators, and after differentiation with respect to M^2 are rendered UV finite even without making use of the statistical factors. Hence p and p_0 will be of order ν_q or M and all expressions can be expanded in $p_0/k, p/k$. In the limit $p_0, p \ll k$ the arguments of the Dirac δ are $(p_0 \pm k)^2 - (\mathbf{k} + \mathbf{p})^2 \simeq \pm 2k(p_0 \mp px)$ and after the change of variable $x \rightarrow -x$ in the term coming from $r = -1$ one obtains

$$\Sigma_{B2}(i\nu_q) \simeq -\frac{e^4}{2\pi^4} i\nu_q \gamma_0 \frac{\partial}{\partial M^2} \int_{-\infty}^\infty dp_0 \int_0^\infty dp p^2 \frac{1}{[E_p^2 - p_0^2][p^2 - (i\nu_q - p_0)^2]} \times \int_{-1}^1 dx \int_0^\infty dk k^2 \left[n_F(k) n_F(k + p_0) + (1 - n_F(k))(1 - n_F(k - p_0)) \right] \delta(p_0 - px) \Big|_{M^2=0}. \quad (4.11)$$

Next one can make use of a relation for the product of two Fermi-Dirac distributions in terms of products of a Bose-Einstein and a Fermi-Dirac distribution functions (see *e.g.* Eq.(3.20) of [30]):

$$n_F(x)n_F(x+y) = (1+n_B(y))n_F(x+y) - n_F(x)n_B(y). \quad (4.12)$$

Using this relation with $x = k, y = p_0$ and $x = k, y = -p_0$, respectively, one obtains

$$n_F(k)n_F(k+p_0) + (1-n_F(k))(1-n_F(k-p_0)) = -n_B(-p_0)[n_F(k+p_0) - n_F(k-p_0)] + 1. \quad (4.13)$$

Discarding the vacuum piece, expanding the two terms in the square brackets above for $k \gg p_0$ and keeping the first non-vanishing term one substitutes (4.13) and

$$\int_0^\infty dk k^2 \frac{dn_F(k)}{dk} = -2 \int_0^\infty dk k n_F(k) = -\frac{\pi^2 T^2}{6}, \quad (4.14)$$

into (4.11) to obtain

$$\Sigma_{B_2}(i\nu_q) = -\frac{e^4 T^2}{6\pi^2} i\nu_q \gamma_0 \frac{\partial}{\partial M^2} \int_{-1}^1 dx \int_0^\infty dp x p^3 \int_{-\infty}^\infty dp_0 \frac{\delta(p_0 - xp) n_B(-p_0)}{(E_p^2 - p_0^2)(p^2 - (i\nu_q - p_0)^2)} \Big|_{M^2=0}. \quad (4.15)$$

As we shall show in Sec. V this form is also exactly reproduced by an HTL insertion of a hard HTL photon self-energy in the one-loop Σ .

If one performs the p_0 integral in (4.15), keeping only the thermal contribution which is separated with the help of (2.20), and taking into account the sign function coming from (2.20), one obtains

$$\Sigma_{B_2}(i\nu_q) = \frac{e^4 T^2}{6\pi^2} \gamma_0 \frac{\partial}{\partial M^2} \int_0^1 dx \int_0^\infty dp \frac{x p^3 n_B(xp)}{[p^2(x^2 - 1) - M^2]} \sum_{r=\pm 1} \frac{i\nu_q}{[i\nu_q - rp(1+x)][i\nu_q + rp(1-x)]} \Big|_{M^2=0}. \quad (4.16)$$

Using partial fractioning of the denominator, changing the integration variable p to p/x and then performing the x integral and sum over $r = \pm 1$, one obtains

$$\begin{aligned} \Sigma_{B_2}(i\nu_q) = & \frac{e^4 T^2}{12\pi^2} \gamma_0 \frac{\partial}{\partial M^2} \left\{ i\frac{\pi}{2} \int_0^\infty dp \frac{p^2 n_B(p)}{p^2 - \mu_+^2} - \mu_+ \ln\left(\frac{M^2}{\nu_q^2}\right) \int_0^\infty dp \frac{p n_B(p)}{p^2 - \mu_+^2} \right. \\ & \left. + \frac{\mu_+}{2} \int_0^\infty dp \frac{p n_B(p)}{p^2 - \mu_+^2} \ln\left(\frac{4p^2}{\nu_q^2} + 1\right) - i \int_0^\infty dp \frac{p^2 n_B(p)}{p^2 - \mu_+^2} \operatorname{arccot}\left(\frac{2p}{\nu_q}\right) \right\} \Big|_{M^2=0}, \quad (4.17) \end{aligned}$$

where $\mu_\pm = ((i\nu_q)^2 \pm M^2)/(2i\nu_q)$. The asymptotic analysis of the above integrals is given in Appendix B.

Using (B15), (B16) and the series expansion given in (B17) one obtains after analytical continuation

$$\begin{aligned} \Sigma_{B_2}(\omega) \simeq & \frac{e^4 T^2}{24\pi^2 \omega} \gamma_0 \left[\frac{\omega^2}{2M^2} \left(\ln \frac{T}{\omega} + \ln(4\pi) - \gamma_E \right) - \frac{i\pi\omega T}{M^2} + \ln \frac{T}{\omega} \ln \frac{M}{\omega} - \frac{1}{4} \ln^2 \frac{T}{\omega} \right. \\ & \left. + \frac{1}{2} (1 + \gamma_E - \ln(4\pi)) \left(\ln \frac{T}{\omega} - 2 \ln \frac{M}{\omega} \right) \right], \quad (4.18) \end{aligned}$$

were we have again retained only the terms in the high temperature expansion which contribute at the order of interest or are singular in the $M^2 \rightarrow 0$ limit.

For the last term Σ_{B3} of (3.8) and (3.9c) one evaluates $B(k_0, \mathbf{k}; i\nu_q + k_0 - p_0, \mathbf{k} + \mathbf{p}; p_0, -\mathbf{p})$ and $B(k_0 + p_0 - i\nu_q, \mathbf{k}; k_0, \mathbf{k} + \mathbf{p}; p_0, -\mathbf{p})$ with the definition (3.7), and obtains then

$$\begin{aligned} \Sigma_{B3}(i\nu_q) = & \frac{e^4}{2\pi^4} \gamma_0 \frac{\partial}{\partial M^2} \int_0^\infty dk \int_0^\infty dp \int_{-\infty}^\infty dp_0 \int_{-1}^1 dx k^2 p^2 \frac{\delta(p_0^2 - p^2) \epsilon(p_0)}{[E_p^2 - (p_0 - i\nu_q)^2]} \sum_{r=\pm 1} r \left\{ \right. \\ & \frac{px(2rk + i\nu_q - p_0) - 2kp_0 + rp^2}{[2kr(prx + p_0 - i\nu_q) + i\nu_q(2p_0 - i\nu_q)]} n_F(rk) n_F(-p_0) \\ & \left. - \left[\frac{(r|\mathbf{k} + \mathbf{p}| + p_0 - i\nu_q)(2r|\mathbf{k} + \mathbf{p}|p_0 + kpx + p^2) + rkp_x|\mathbf{k} + \mathbf{p}|}{k^2 - (r|\mathbf{k} + \mathbf{p}| + p_0 - i\nu_q)^2} \right] \frac{n_F(r|\mathbf{k} + \mathbf{p}|)}{|\mathbf{k} + \mathbf{p}|} n_F(p_0) \right\} \Big|_{M^2=0}, \end{aligned} \quad (4.19)$$

where $|\mathbf{k} + \mathbf{p}| = \sqrt{k^2 + p^2 + 2kpx}$. Since the large k behavior of the integrand (without the statistical factors) in both terms is k^2 , the k integral is hard, and $k \sim T$, while p_0 and p are soft, of order ν_q or M . Expanding the expression in the curly bracket of (4.19) for $p_0, p \ll k$, redefining $x \rightarrow -x$ in the terms with $r = -1$ and doing the sum over r yields

$$\begin{aligned} \Sigma_{B3}(i\nu_q) = & \frac{e^4}{2\pi^4} \gamma_0 \frac{\partial}{\partial M^2} \int_0^\infty dk \int_0^\infty dp \int_{-\infty}^\infty dp_0 \int_{-1}^1 dx k^2 p^2 \frac{\delta(p_0^2 - p^2) \epsilon(p_0)}{E_p^2 - (i\nu_q - p_0)^2} \left\{ \right. \\ & \frac{p_0 + px}{p_0 + px - i\nu_q} [n_F(k) + n_F(-k)][n_F(p_0) + n_F(-p_0)] \\ & + i\nu_q \frac{p^2}{2k} \frac{x^2 - 1}{(p_0 + px - i\nu_q)^2} [n_F(k) - n_F(-k)][n_F(-p_0) + n_F(p_0)] \\ & + 2 \frac{dn_F(k)}{dk} \left(px + \frac{i\nu_q px}{px + p_0 - i\nu_q} \right) n_F(p_0) \\ & \left. - \frac{p_0}{2k} [n_F(-p_0) - n_F(p_0)][n_F(k) - n_F(-k)] \right\} \Big|_{M^2=0}. \end{aligned} \quad (4.20)$$

Note, that due to the relations (2.15) the first term in (4.20) is a vacuum piece and the second term contains only one statistical factor and can not contribute at leading order in the high temperature expansion. Disregarding these terms and using (4.14) one obtains

$$\begin{aligned} \Sigma_{B3}(i\nu_q) \simeq & \frac{e^4 T^2}{6\pi^2} \gamma_0 \frac{\partial}{\partial M^2} \left\{ \int_0^\infty dp p^2 \int_{-\infty}^\infty dp_0 \epsilon(p_0) \frac{\delta(p_0^2 - p^2) n_F(p_0)}{E_p^2 - (i\nu_q - p_0)^2} \right. \\ & \left. \times \left[p_0 + i\nu_q p \int_{-1}^1 dx \frac{x}{i\nu_q - p_0 - xp} \right] \right\} \Big|_{M^2=0}. \end{aligned} \quad (4.21)$$

Performing the x and p_0 integrals in Σ_{B3} results in

$$\Sigma_{B3}(i\nu_q) \simeq -\frac{e^4 T^2}{24\pi^2} \gamma_0 \frac{\partial}{\partial M^2} \left\{ 4\mu_- \int_0^\infty dp \frac{p n_F(p)}{p^2 - \mu_-^2} + \mu_+ \int_0^\infty dp \frac{p n_F(p)}{p^2 - \mu_-^2} \ln \left(\frac{4p^2}{\nu_q^2} + 1 \right) \right\}$$

$$+2i\mu_-\mu_+ \int_0^\infty dp \frac{n_F(p)}{p^2 - \mu_-^2} \arctan\left(\frac{2p}{\nu_q}\right) \Big|_{M^2=0}, \quad (4.22)$$

where $\mu_\pm = ((i\nu_q)^2 \pm M^2)/(2i\nu_q)$. This form of the third contribution to Σ_B is also obtained directly from the the insertion of a hard HTL photon self-energy in the one-loop Σ , as we shall show explicitly in Sec. V.

The asymptotic analysis of the above integrals is given in Appendix B. Using (B15) and the series expansion given in (B17) one obtains after analytical continuation to real frequencies,

$$\Sigma_{B3}(\omega) \simeq \frac{e^4 T^2}{48\pi^2 \omega} \gamma_0 \left[-\frac{1}{2} \ln^2 \frac{T}{\omega} + (2 + \gamma_E - \ln \pi) \ln \frac{T}{\omega} \right] + i \cdot \mathcal{O}\left(\frac{e^4 T^2}{\omega} \ln \frac{T}{\omega}\right). \quad (4.23)$$

Here we have again retained only the terms in the high temperature expansion which contribute at the order of interest. The imaginary part neglected in (4.23) is of order $e^3 T \ln(1/e)$ and subleading to the NLO terms of magnitude $e^2 T$ in which we are interested.

The sum of the contributions (4.7), (4.8) and (4.9) from Σ_{B1} , (4.18) from Σ_{B2} , and (4.23) from Σ_{B3} is

$$\Sigma_B(\omega) = \Sigma_{B1}(\omega) + \Sigma_{B2}(\omega) + \Sigma_{B3}(\omega) \simeq \frac{e^4 T^2}{24\pi^2 \omega} \gamma_0 \left[\frac{\pi T}{M} + \left(\frac{1}{2} + \ln 2\right) \ln \frac{T}{\omega} - \frac{5\pi i T}{2\omega} \right]. \quad (4.24)$$

Remarkably, all the M^{-2} and $\ln M$ infrared/collinear divergences cancel in this leading order high temperature form, as well as γ_E and $\ln \pi$, but the M^{-1} divergence remains. This cancellation is in line with the findings of [15] which demonstrates the cancellation of all collinear and infrared divergences in the final result for the imaginary part of the vector-boson self-energy in the limit where the dilepton invariant mass is much bigger than the temperature. In our case, the presence of the photon double pole, which produces a more singular behavior than the fermionic one present in [15], results in the survival of the M^{-1} divergence in the real part, coming from (4.7) in our final result given in (7.1a). The cancellation of the M^{-2} and $\ln M$ terms can be understood by a simple argument, implicit already in the work of Ref. [31], which we discuss in Section VII.

The most important implication of (4.24) is that because of its M^{-1} dependence, the photon mass regulator cannot be consistently taken to zero in the two-loop fermion self-energy. Only the bubble self-energy diagram contains this divergence. The second important feature of the above analysis is that all of the contributions to the two-loop bubble self-energy that are of the same magnitude as the NLO one-loop terms in (2.23), (or larger in the case of the M^{-1} term) are obtained from one hard and one soft momentum loop. The higher order terms which have been neglected are soft-soft. There are no hard-hard contributions to Σ_B at all.

The remaining two-loop linear divergence $\propto M^{-1}$ as $M \rightarrow 0$, not present in the one-loop self-energy indicates the need for a systematic resummation of higher loop contributions and a reorganization of the

perturbative series. Moreover, if we anticipate that after resummation the photon will acquire a Debye mass of order eT , this M^{-1} term indicates that the correction to the real part of the fermion dispersion relation on-shell will be of order e^2T , and not $e^3T \ln(1/e)$, as might have been expected from the NLO one-loop correction to the real part (2.23).

B. The Rainbow Diagram

Taking $\mathbf{q} = 0$ in expressions (3.22) and (3.23) and taking for term Σ_{R2} the derivative with respect to m^2 and the limit $m^2 = 0$ one obtains

$$\begin{aligned} \Sigma_{R1}(i\nu_q, \mathbf{q} = \mathbf{0}) &= \frac{e^4}{8\pi^4} \gamma_0 \int_0^\infty dp \int_0^\infty dk \int_{-1}^1 dx \sum_{r,s=\pm 1} \left[\frac{r k n_F(p) n_B(k)}{2(x-rs)((i\nu_q)^2 - 2kp(x-rs) - 2i\nu_q(rk+sp))} \right. \\ &\quad - n_F(p) n_B(k) \frac{k}{2i\nu_q} \frac{r}{(x-rs)(i\nu_q - 2sp)} + n_F(p) n_F(k) \frac{1}{2i\nu_q} \frac{sp - rk}{(x-rs)(i\nu_q - 2sp)} \\ &\quad + n_B(p) n_B(k) \frac{k^2 p}{i\nu_q} \frac{r}{(i\nu_q - 2sp)((i\nu_q)^2 - 2kp(x-rs) - 2i\nu_q(rk+sp))} \\ &\quad \left. + n_B(p) n_F(k) \frac{kp}{i\nu_q} \frac{kr - (i\nu_q - sp)}{(i\nu_q - 2sp)((i\nu_q)^2 - 2kp(x-rs) - 2i\nu_q(rk+sp))} \right], \end{aligned} \quad (4.25)$$

$$\Sigma_{R2}(i\nu_q, \mathbf{q} = \mathbf{0}) = \frac{e^4 T^2}{4\pi^2} \gamma_0 \int_0^\infty dp \left[\frac{p i\nu_q}{((i\nu_q)^2 - 4p^2)^2} (n_B(p) - n_F(p)) - \frac{p^2}{i\nu_q((i\nu_q)^2 - 4p^2)} \frac{dn_F(p)}{dp} \right]. \quad (4.26)$$

The first term and the very last term, involving $(i\nu_q - sp)$ in (4.25) can be handled in the following way. If k and p are hard momenta in these terms, then the sums over r, s either give integrands which vanish identically, or are odd under $x \rightarrow -x$, so vanish upon integration over x . Hence these terms have no hard-hard contribution and must contain at least one additional power of ω in the numerator, relative to all terms in (2.23). Therefore they are subleading.

Performing the sum over r and s one finds that the sum of the second and third terms of (4.25) is

$$-\frac{e^4}{8\pi^4 i\nu_q} \gamma_0 \int_0^\infty dk k [n_B(k) + n_F(k)] \int_0^\infty dp n_F(p) \frac{p}{[p^2 - (i\nu_q/2)^2]} \int_{-1}^1 \frac{dx}{1-x^2}. \quad (4.27)$$

The imaginary part of this contribution is subleading, *cf.* (B10a), while the real part follows the hard-soft pattern, and does contribute at the same order as the NLO terms in (2.23). Moreover because of the x integral factor, it is collinearly divergent. However, taking into account the remaining terms in (4.25), *i.e.* the fourth term and remaining part of the fifth term involving kr , we observe that in both of these k must be treated as hard, while p is soft. After partial fractioning and using interchange of $x \rightarrow -x$ freely, these

remaining terms may be written in the form [*c.f.* in Appendix B the derivation of (B12) from (B11)]

$$\frac{e^4}{8\pi^4 i\nu_q} \gamma_0 \int_0^\infty dk k [n_B(k) + n_F(k)] \int_0^\infty dp n_B(p) \int_{-1}^1 \frac{dx}{1-x^2} \left[\frac{p}{p^2 - (i\nu_q/2)^2} - \frac{2p}{p^2 - (i\nu_q/(1+x))^2} \right]. \quad (4.28)$$

In view of (B12) and (B14) the real part of this expression cancels at leading order in the high temperature expansion the real part of (4.27), while its imaginary part vanishes at this order. Hence combining all terms of (4.25) gives no collinear divergence for either the real or imaginary parts of the self-energy, and no contribution at the same NLO as (2.23).

For the terms in (4.26), the factorization into a hard and soft momentum integral is again obvious. Performing an integration by parts in the last term of (4.26), one can rewrite (4.26) in the form

$$\Sigma_{R2}(i\nu_q) = \frac{e^4 T^2 i\nu_q}{4\pi^2} \gamma_0 \int_0^\infty dp \frac{p}{((i\nu_q)^2 - 4p^2)^2} [n_B(p) + n_F(p)]. \quad (4.29)$$

Differentiating the integrals $I_\pm(ia)$ defined in Appendix B gives for this contribution

$$\Sigma_R(i\nu_q) = \Sigma_{R2}(i\nu_q) = -i \frac{e^4 T^3}{32\pi (i\nu_q)^2} \gamma_0. \quad (4.30)$$

After analytic continuation $i\nu_q \rightarrow \omega + i0^+$ the R2 term becomes purely imaginary, while Σ_{R1} does not contribute at all at this order comparable to the NLO one-loop self-energy. Hence the contribution to the fermion self-energy of the rainbow diagram is simply

$$\Sigma_R(\omega) \simeq \Sigma_{R2}(\omega) \simeq -i \frac{e^4 T^3}{32\pi \omega^2} \gamma_0. \quad (4.31)$$

at the same order as the NLO imaginary part of (2.23). This leading order contribution of the two-loop rainbow diagram arises explicitly from one hard and one soft loop integral. There are no hard-hard contributions to the rainbow diagram.

C. The Crossed Photon Diagram

Evaluating the crossed photon diagram self-energy (3.30) at $\mathbf{q} = 0$, by using the definition (3.29) one obtains

$$\begin{aligned} \Sigma_C(i\nu_q, \mathbf{q} = \mathbf{0}) &= \frac{e^4}{8\pi^4} \gamma_0 \int_0^\infty dp \int_0^\infty dk \int_{-1}^1 dx \sum_{r,s=\pm 1} \left[2n_B(p)n_F(k) \frac{(rk-sp)(i\nu_q rk + kp(x-rs))}{(i\nu_q)^2(i\nu_q - 2rk)(i\nu_q - 2sp)(x-rs)} \right. \\ &\quad - kp n_F(p)n_F(k) \frac{rk+sp-i\nu_q}{(i\nu_q)^2(i\nu_q - 2rk)(i\nu_q - 2sp)} \frac{-2kp(x-rs)}{((i\nu_q)^2 - 2kp(x-rs) - 2i\nu_q(rk+sp))} \\ &\quad \left. + kp n_B(p)n_B(k) \frac{rk+sp-i\nu_q}{(i\nu_q)^2(i\nu_q - 2rk)(i\nu_q - 2sp)} \frac{(i\nu_q)^2 - 2kp(x-rs) - 2i\nu_q(rk+sp) + (i\nu_q)^2}{(i\nu_q)^2 - 2kp(x-rs) - 2i\nu_q(rk+sp)} \right] \end{aligned}$$

$$\begin{aligned}
& + n_B(p)n_F(k) \frac{rk}{i\nu_q(i\nu_q - 2sp)(x - rs)} \frac{(i\nu_q)^2 - 2kp(x - rs) - 2i\nu_q(rk + sp) - (i\nu_q)^2}{(i\nu_q)^2 - 2kp(x - rs) - 2i\nu_q(rk + sp)} \\
& - 2n_F(p)n_F(k) \frac{rk(kp(x - rs) + i\nu_q sp)}{i\nu_q(i\nu_q - 2sp)((i\nu_q)^2 - 2kp(x - rs) - 2i\nu_q(rk + sp))(x - rs)} \Big]. \quad (4.32)
\end{aligned}$$

In the last term we have changed $x \rightarrow -x$ and $r \rightarrow -r$. Performing partial fractioning in each term one observes that in some cases the x -dependence partially simplifies between the numerator and the denominator. With simple algebraic manipulations one can separate in the integrand x -independent contributions and contributions which are explicitly collinearly divergent, obtaining

$$\begin{aligned}
\Sigma_C(i\nu_q) = & \frac{e^4}{8\pi^4} \gamma_0 \int_0^\infty dk \int_0^\infty dp \int_{-1}^1 dx \left\{ \right. \\
& n_B(p)n_F(k) \left[\frac{4kp}{i\nu_q} \left(\frac{1}{(i\nu_q)^2 - 4k^2} - \frac{1}{(i\nu_q)^2 - 4p^2} \right) - \frac{8kp}{i\nu_q((i\nu_q)^2 - 4p^2)} \frac{1}{x^2 - 1} \right] \\
& + n_F(p)n_F(k) \left[\frac{4kp}{i\nu_q((i\nu_q)^2 - 4p^2)} - \frac{kp}{i\nu_q} \sum_{r,s=\pm 1} \frac{1}{(i\nu_q)^2 - 2kp(x - rs) - 2i\nu_q(rk + sp)} \right. \\
& \quad \left. + 2 \frac{k^2 p}{i\nu_q} \sum_{r,s=\pm 1} \frac{1}{i\nu_q - 2sp} \frac{r}{(i\nu_q)^2 - 2kp(x - rs) - 2i\nu_q(rk + sp)} \right] \\
& + n_B(p)n_B(k) \left[- \frac{4kp}{i\nu_q((i\nu_q)^2 - 4p^2)} - kp \sum_{r,s=\pm 1} \frac{1}{i\nu_q - 2sp} \frac{1}{(i\nu_q)^2 - 2kp(x - rs) - 2i\nu_q(kr + sp)} \right] \\
& + n_B(p)n_F(k) \left[\left(\frac{i\nu_q}{(i\nu_q)^2 - 4(k - p)^2} - \frac{i\nu_q}{(i\nu_q)^2 - 4(k + p)^2} + \frac{8kp}{i\nu_q((i\nu_q)^2 - 4p^2)} \right) \frac{1}{x^2 - 1} \right. \\
& \quad \left. - 2k^2 p \sum_{r,s=\pm 1} \frac{1}{i\nu_q - 2sp} \frac{1}{i\nu_q - 2(rs + sp)} \frac{r}{(i\nu_q)^2 - 2kp(x - rs) - 2i\nu_q(rk + sp)} \right] \\
& + n_F(p)n_F(k) \left[\frac{i\nu_q}{2} \left(\frac{1}{(i\nu_q)^2 - 4(k - p)^2} - \frac{1}{(i\nu_q)^2 - 4(k + p)^2} \right) \frac{1}{x^2 - 1} \right. \\
& \quad - 2 \frac{k^2 p}{i\nu_q} \sum_{r,s=\pm 1} \frac{1}{i\nu_q - 2sp} \frac{r}{(i\nu_q)^2 - 2kp(x - rs) - 2i\nu_q(rk + sp)} \\
& \quad \left. - 4 \frac{k^2 p^2}{i\nu_q} \sum_{r,s=\pm 1} \frac{1}{i\nu_q - 2sp} \frac{1}{i\nu_q - 2(rs + sp)} \frac{rs}{(i\nu_q)^2 - 2kp(x - rs) - 2i\nu_q(rk + sp)} \right] \Big\}. \quad (4.33)
\end{aligned}$$

Note that whenever possible we have exploited the interchanging of $p \leftrightarrow k$ and $x \rightarrow -x$. Note, also, that we have catalogued all the terms as they arise in order from the previous expression (4.32), although actually the last term in the fourth line with two Fermi-Dirac statistical factors exactly cancels the term in the ninth line of (4.33). Also noteworthy is that the terms with $(x^2 - 1)^{-1}$ factors, which are collinearly logarithmically divergent cancel whenever they multiply spatial momentum integrals which factorize into separate integrals over k and p , namely the last terms of the second line and the sixth line respectively.

We shall show that the leading order terms in the high temperature expansion of (4.33) come from

precisely the remaining x -independent factorizable terms. Performing the interchange $k \leftrightarrow p$ in the first term inside the large round parentheses of the second line of (4.33) one can combine these terms to obtain

$$\begin{aligned}\Sigma_{\text{C}}(i\nu_q) &= \frac{e^4}{4\pi^4 i\nu_q} \gamma_0 \int_0^\infty dk k [n_B(k) + n_F(k)] \int_0^\infty dp \frac{p}{p^2 - (i\nu_q)^2/4} [n_B(p) - n_F(p)] \\ &= \frac{e^4 T^2}{16\pi^2 i\nu_q} \gamma_0 \int_0^\infty dp \frac{p}{p^2 - (i\nu_q)^2/4} [n_B(p) - n_F(p)].\end{aligned}\quad (4.34)$$

These leading factorizable terms contain no remaining collinear divergences. Note, that we obtained the product of the same integrals which already have appeared in the LO and NLO expressions of the HTL approximation to the 1-loop fermion self-energy (2.19). The first integral over k in (4.34) is clearly dominated by hard $k \sim T$, and given by (2.21), while the second integral is given in Appendix B and is soft. Through the analytical continuation $i\nu_q \rightarrow \omega + i0^+$, using (B6) and (B7), one obtains from these factorizable hard/soft terms

$$\Sigma_{\text{C}}(\omega) = \frac{e^4 T^2}{16\pi^2 \omega} \gamma_0 \left[-\ln \frac{T}{\omega} + i\pi \frac{T}{\omega} \right], \quad (4.35)$$

which contains both real and imaginary parts.

It remains to show that all the remaining non-factorizable terms in (4.33) are subleading to (4.35). We show first that these remaining terms do not contain any contributions at all when both k and p are hard. The remaining non-factorizable terms are of two kinds, *viz.* those involving the integrand

$$\frac{i\nu_q}{(i\nu_q)^2 - 4(k-p)^2} - \frac{i\nu_q}{(i\nu_q)^2 - 4(k+p)^2} \quad (4.36)$$

multiplied by the collinearly divergent integral $\int_{-1}^1 dx/(1-x^2)$ and either $n_B(p)n_F(k)$ or $n_F(p)n_F(k)$, and the following four terms, involving sums over r and s ,

$$\begin{aligned}& \sum_{r,s=\pm 1} \left\{ n_F(p)n_F(k) \left[-\frac{kp}{i\nu_q} \frac{1}{(i\nu_q)^2 - 2kp(x-rs) - 2i\nu_q(rk+sp)} \right. \right. \\ & -4 \frac{k^2 p^2}{i\nu_q} \frac{1}{i\nu_q - 2sp} \frac{1}{i\nu_q - 2(rk+sp)} \frac{rs}{(i\nu_q)^2 - 2kp(x-rs) - 2i\nu_q(rk+sp)} \left. \right] \\ & + n_B(p)n_B(k) \left[-kp \frac{1}{i\nu_q - 2sp} \frac{1}{(i\nu_q)^2 - 2kp(x-rs) - 2i\nu_q(kr+sp)} \right] \\ & \left. + n_B(p)n_F(k) \left[-2k^2 p \frac{1}{i\nu_q - 2sp} \frac{1}{i\nu_q - 2(rk+sp)} \frac{r}{(i\nu_q)^2 - 2kp(x-rs) - 2i\nu_q(rk+sp)} \right] \right\}. \quad (4.37)\end{aligned}$$

For the first kind of terms in (4.33), namely those involving a difference like (4.36), it is clear that there is no hard-hard contribution, since the integrand (4.36) vanishes for $k \gg \omega$ or $p \gg \omega$. In fact, the integral over k for these terms is dominated by soft k for which we can replace the Fermi-Dirac distribution $n_F(k)$ by $1/2$. Then the integral can be performed with the result

$$\int_0^\infty dk n_F(k) \left[\frac{i\nu_q}{(i\nu_q)^2 - 4(k-p)^2} - \frac{i\nu_q}{(i\nu_q)^2 - 4(k+p)^2} \right] \rightarrow \frac{1}{4} \ln \left[\frac{i\nu_q + 2p}{i\nu_q - 2p} \right]. \quad (4.38)$$

The real part of this integrand vanishes for $i\nu_q \rightarrow \omega \rightarrow 0$, but is proportional to $1/p$ for large p , the final integration over p with a second $n_F(p)$ gives a contribution to Σ_C proportional to $e^4\omega \ln(T/\omega)$, which is subleading. In the cases where the final integration over p involves the Bose-Einstein distribution $n_B(p)$, there is an enhancement of T/ω and the contribution of the integral is proportional to e^4T , which is still subleading. Therefore the contributions of the terms involving the difference (4.36) are subleading compared to (2.23) and hence NNLO.

For the second kind of terms, that is those of (4.37), we observe that they again do not contain any hard-hard contributions, for when both k and p are hard, then one can ignore $i\nu_q \rightarrow \omega$ relative to k and p in factors of the denominators in (4.37). In that limit, the third term vanishes upon summing over r, s , while the first and fourth terms of (4.37) are explicitly odd under $x \rightarrow -x$, and vanish under integration over x . By symmetrizing the remaining second term of (4.37) under $x \leftrightarrow -x$, we find that it becomes proportional to

$$\int_0^\infty dk n_F(k) \int_0^\infty dp n_F(p) \left[\frac{kp}{k^2 - p^2} \right] = 0 \quad (4.39)$$

by antisymmetry under interchange of k and p .

All terms in (4.37) vanish in the hard-hard limit, *i.e.* when ω is neglected in the denominators. The integral over these terms must be proportional to at least one factor of ω/T , relative to (4.35) with one of the momenta soft. Thus all the leading contributions from the high temperature expansion of the two-loop crossed photon self-energy diagram are obtained from the explicitly factorizable terms in (4.33), and given completely by (4.35), which exhibit the pattern of one loop integration momentum hard, and the other soft, just as in the bubble and rainbow diagrams considered previously.

V. THE HARD-SOFT PATTERN AND EFFECTIVE HTL INSERTIONS

By explicit analysis of the two-loop self-energy we have found that the leading contributions in the high temperature limit which should be compared with the NLO one-loop contributions arise in all two-loop diagrams where one loop momentum is hard ($\sim T$) while the other is soft ($\sim \omega \sim eT$ for imaginary parts or over the range $0 \leq k < T$ for real parts giving rise to logarithms). On the other hand, the basic one-loop HTL self-energies and vertices are derived precisely by assuming the internal loop momentum is hard, relative to the external momenta flowing into them which are assumed soft. Hence by replacing one of the loops (the hard one) of each two-loop diagram by an HTL self-energy or vertex part, and evaluating the resulting effective *one-loop* soft integrals, we must obtain exactly the same result as our direct analysis of the leading high temperature behavior of the two-loop diagram. This reduction of two-loop diagrams with

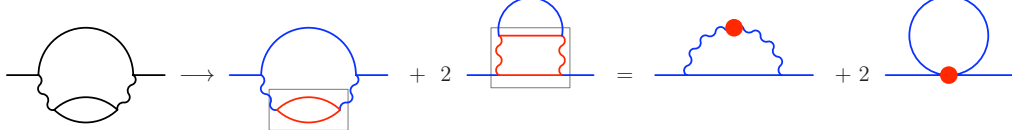


FIG. 6: Reduction of the two-loop bubble diagram to effective one-loop diagrams with HTL insertions. The framed part of the diagram represent the hard loop which are replaced by an effective HTL self-energy or vertex part.

one loop hard and the other soft is illustrated graphically in Figs. 6, 8 and 10. In this section we shall *prove* that the initially rather different looking expressions obtained by the insertion of one HTL self-energy or vertex in the one-soft-loop diagrams of Figs. 6, 8, 10 yields precisely the same results as that obtained in Section IV for each diagram. This furnishes a non-trivial check by a completely different method on the detailed analysis of the two-loop fermion self-energy in Section IV.

The non-vanishing three- and four-point functions in the LO HTL approximation are given in Minkowski space by [3, 8]

$$\Sigma^{\text{HTL}}(P) = m_f^2 \int \frac{d\Omega}{4\pi} \frac{\Psi}{P \cdot V + i\epsilon}, \quad (5.1)$$

$$\Pi_{\mu\nu}^{\text{HTL}}(Q) = m_D^2 \left[-\delta_{0\mu}\delta_{0\nu} + Q_0 \int \frac{d\Omega}{4\pi} \frac{V_\mu V_\nu}{V \cdot Q + i\epsilon} \right], \quad (5.2)$$

$$\Gamma_\mu^{\text{HTL}}(P_1, P_2) = m_f^2 \int \frac{d\Omega}{4\pi} \frac{V_\mu \Psi}{(P_1 \cdot V + i\epsilon)(P_2 \cdot V + i\epsilon)}, \quad (5.3)$$

$$\Gamma_{\mu\nu}^{\text{HTL}}(P_1, P_2, Q) = m_f^2 \int \frac{d\Omega}{4\pi} \frac{V_\mu V_\nu \Psi}{((P_1 + Q) \cdot V + i\epsilon)((P_2 - Q) \cdot V + i\epsilon)} \left(\frac{1}{P_1 \cdot V + i\epsilon} + \frac{1}{P_2 \cdot V + i\epsilon} \right), \quad (5.4)$$

where $m_f = eT/\sqrt{8}$ is the fermion thermal mass, $m_D = eT/\sqrt{3}$ is the Debye screening mass for photons, $d\Omega = d(\cos\theta)d\phi$ is the measure for angular integration and $V = (1, \mathbf{v})$ with $\mathbf{v}^2 = 1$.

The HTL two-electron proper vertices obey the simple Ward identities [3]

$$(P_1 - P_2)^\mu \Gamma_\mu^{\text{HTL}}(P_1, P_2) = \Sigma^{\text{HTL}}(P_2) - \Sigma^{\text{HTL}}(P_1), \quad (5.5)$$

$$Q^\nu \Gamma_{\mu\nu}^{\text{HTL}}(P, P, Q) = \Gamma_\mu^{\text{HTL}}(P, P - Q) - \Gamma_\mu^{\text{HTL}}(P + Q, P), \quad (5.6)$$

$$Q^\mu Q^\nu \Gamma_{\mu\nu}^{\text{HTL}}(P, P, Q) = \Sigma^{\text{HTL}}(P + Q) - 2\Sigma^{\text{HTL}}(P) + \Sigma^{\text{HTL}}(P - Q), \quad (5.7)$$

while the HTL two-photon polarization function is transverse:

$$Q^\nu \Pi_{\mu\nu}^{\text{HTL}}(Q) = 0. \quad (5.8)$$

A. The HTL Reduced Bubble Diagram

Fig. 6 shows the diagrams arising when one loop is hard and another is soft in the original two-loop bubble diagram and the hard loop is replaced by the corresponding effective HTL two and four-point function. The last tadpole diagram does not contribute because there is no 4-electron effective HTL vertex. The contribution of the one-loop diagram with the insertion of the LO HTL photon polarization Π (5.2) is

$$\Sigma_{\Pi}(Q) = -e^2 \int_P \gamma_{\alpha} G(Q-P) \gamma_{\beta} D^{\alpha\mu}(P) \Pi_{\mu\nu}^{\text{HTL}}(P) D^{\nu\beta}(P). \quad (5.9)$$

Working out the Dirac structure in Feynman gauge, we obtain two terms corresponding to the two structures of the HTL photon polarization in (5.2)

$$\begin{aligned} \gamma^{\alpha}(\not{Q} - \not{P})\gamma^{\beta} \delta_{0\alpha} \delta_{0\beta} &= (Q-P)_{\rho} \gamma^0 \gamma^{\rho} \gamma^0 = (Q-P)_0 \gamma^0 - (\mathbf{q} - \mathbf{p}) \cdot \boldsymbol{\gamma}, \\ (Q-P)_{\mu} \gamma^{\alpha} \gamma^{\mu} \gamma^{\beta} V_{\alpha} V_{\beta} &= 2(Q-P)^{\alpha} \gamma^{\beta} V_{\alpha} V_{\beta} - (\not{Q} - \not{P}) \not{V} \cdot \not{V} = 2(Q-P) \cdot V \not{V}. \end{aligned}$$

Using the relations above and setting $\mathbf{q} = 0$, one can write

$$P_0 \left(\frac{Q \cdot V}{V \cdot P + i\epsilon} - 1 \right) = (Q-P)_0 + \mathbf{v} \cdot \mathbf{p} Q_0 \frac{1}{V \cdot P + i\epsilon},$$

and hence,

$$\begin{aligned} \Sigma_{\Pi}(Q_0, \mathbf{q} = \mathbf{0}) &= -\frac{2}{3} e^4 T^2 Q_0 \gamma_0 \frac{\partial}{\partial M^2} \int \frac{d\Omega}{4\pi} \int_P \mathbf{v} \cdot \mathbf{p} D_{M^2}(P) S(P) D(Q-P) \Big|_{M^2=0} \\ &\quad - i \frac{e^4 T^2}{3} \gamma_0 \frac{\partial}{\partial M^2} \int_P (Q_0 - P_0) \tilde{D}(Q-P) D_{M^2}(P) \Big|_{M^2=0}, \end{aligned} \quad (5.10)$$

where $S(P)$ appearing here is defined by

$$S(P) \equiv \frac{i}{P \cdot V + i\epsilon}, \quad (5.11)$$

and D_{M^2} is defined by (2.29). In imaginary time $S(i\omega_n, \mathbf{p}) = -i\Delta_S(i\omega_n, \mathbf{p})$, (ω_n is bosonic) and the spectral representation of $\Delta_S(i\omega_n, \mathbf{p})$ is

$$\Delta_S(i\omega_n, \mathbf{p}) = \frac{1}{\mathbf{v} \cdot \mathbf{p} - i\omega_n} = \int_{-\infty}^{\infty} \frac{dp_0}{2\pi} \frac{\rho_S(p_0, \mathbf{p})}{p_0 - i\omega_n}, \quad \rho_S(p_0, \mathbf{p}) = 2\pi \delta(p_0 - \mathbf{v} \cdot \mathbf{p}). \quad (5.12)$$

In imaginary time, since ω_n is bosonic and $\nu_q - \omega_n$ is fermionic, the Matsubara sum for the second term in (5.10) is given by (2.13). For the first term in (5.10) we need the Matsubara sum

$$T \sum_n \prod_{i=1}^3 \frac{1}{p_i^0 - i\omega_i} = -\frac{1}{p_1^0 - p_2^0} \left[\frac{n_B(-p_2^0)}{p_3^0 + p_2^0 - i\nu_q} - \frac{n_B(-p_1^0)}{p_3^0 + p_1^0 - i\nu_q} \right] - \frac{n_F(p_3^0)}{(p_1^0 + p_3^0 - i\nu_q)(p_2^0 + p_3^0 - i\nu_q)}, \quad (5.13)$$

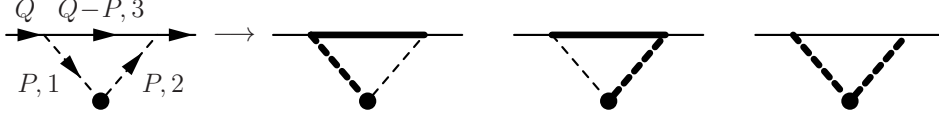


FIG. 7: The diagram corresponding to the first momentum integral of (5.10) when it is decomposed into Gaudin tree graphs. The dashed (solid) line means bosonic (fermionic) propagator. See Fig. 3 for other conventions on the lines.

which was evaluated knowing that ω_1, ω_2 are bosonic while ω_3 is fermionic. The corresponding Gaudin tree graphs are shown in Fig. 7.

Using in (5.10) the spectral representation of the propagators and the result of the Matsubara sums given in (2.13) and (5.13), one obtains

$$\Sigma_{\Pi}(i\nu_q) = \Sigma_{\Pi 1}(i\nu_q) + \Sigma_{\Pi 2}(i\nu_q) + \Sigma_{\Pi 3}(i\nu_q), \quad (5.14)$$

with

$$\begin{aligned} \Sigma_{\Pi 1}(i\nu_q) &= \frac{e^4 T^2}{6\pi^2} \gamma_0 \frac{\partial}{\partial M^2} \left\{ \int_0^\infty dp p^2 \int_{-\infty}^\infty dp_0 \varepsilon(p_0) \frac{\delta(p_0^2 - E_p^2) n_B(-p_0)}{p^2 - (i\nu_q - p_0)^2} \right. \\ &\quad \left. \times \left[i\nu_q - p_0 + i\nu_q p \int_{-1}^1 dx \frac{x}{p_0 - xp} \right] \right\} \Big|_{M^2=0}, \end{aligned} \quad (5.15a)$$

$$\Sigma_{\Pi 2}(i\nu_q) = -\frac{e^4 T^2}{6\pi^2} i\nu_q \gamma_0 \frac{\partial}{\partial M^2} \int_{-1}^1 dx \int_0^\infty dp x p^3 \int_{-\infty}^\infty dp_0 \frac{\delta(p_0 - xp) n_B(-p_0)}{(E_p^2 - p_0^2)(p^2 - (i\nu_q - p_0)^2)} \Big|_{M^2=0}, \quad (5.15b)$$

$$\begin{aligned} \Sigma_{\Pi 3}(i\nu_q) &= \frac{e^4 T^2}{6\pi^2} \gamma_0 \frac{\partial}{\partial M^2} \left\{ \int_0^\infty dp p^2 \int_{-\infty}^\infty dp_0 \varepsilon(p_0) \frac{\delta(p_0^2 - p^2) n_F(p_0)}{E_p^2 - (i\nu_q - p_0)^2} \right. \\ &\quad \left. \times \left[p_0 + i\nu_q p \int_{-1}^1 dx \frac{x}{i\nu_q - p_0 - xp} \right] \right\} \Big|_{M^2=0}, \end{aligned} \quad (5.15c)$$

where $x = \cos \theta$ and the three x -dependent terms come from the first term of (5.10), while the two terms independent of x come from the second term of (5.10).

For $\Sigma_{\Pi 1}$ the comparison between the HTL expression (5.15a) and the corresponding first contribution to the two-loop bubble diagram Σ_{B1} is immediate, since by performing the x and p_0 integrals in (5.15a) one obtains exactly (4.5). For the other two contributions, $\Sigma_{\Pi 2}$ and $\Sigma_{\Pi 3}$, the expressions (5.15b) and (5.15c) derived by one HTL insertion on a soft loop coincide exactly with the leading order contributions (4.15) and (4.21) of the corresponding terms in the two-loop bubble self-energy, Σ_{B2} and Σ_{B3} respectively. The hard k integral in all terms of Σ_B has converted into an HTL photon self-energy insertion, with the final p integral remaining soft, thus proving explicitly the reduction of the two-loop bubble to the one soft loop illustrated in Fig. 6.

As a technical aside, we remark that there is a graphical correspondence between the Gaudin tree graphs of the two-loop bubble diagram and those of the corresponding HTL reduced diagrams, namely the first

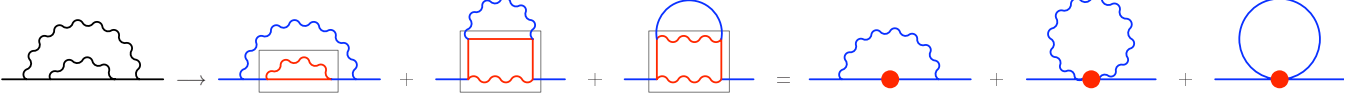


FIG. 8: Reduction of the two-loop rainbow diagram to effective one-loop diagrams with HTL insertions. The framed part of the diagram represent the hard loop which are replaced by an effective HTL self-energy or vertex part.

four diagrams of Fig. 3 correspond to the first diagram of Fig. 7, the fifth diagram of Fig. 3 corresponds to the second diagram of Fig. 7 and the last two diagrams of Fig. 3 correspond to the third diagram of Fig. 7. The second correspondence between $\Sigma_{\Pi 2}$ and $\Sigma_{B 2}$ is not obvious graphically because the fifth diagram of Fig. 3 gives a product of two Fermi-Dirac statistical factors coming from the independent frequencies corresponding to the thin lines of the fermionic bubble, whereas the second diagram of Fig. 7 contains just one Bose-Einstein statistical factor coming from the only independent frequency in this one-loop diagram represented by its one thin, dashed bosonic line. The detailed correspondence of these terms is revealed only by the analysis described in Sec. IV between (4.10) and (4.15), and relies upon the interesting relation (4.13) between a product of two Fermi-Dirac statistical factors and a mixed product of one Fermi-Dirac and one Bose-Einstein factor. The Fermi-Dirac factor contributes to the hard-loop HTL insertion, leaving behind just the soft-loop Bose-Einstein factor required to match the expression in (5.15b).

In this way the equivalence of the high temperature asymptotic contributions of the two-loop bubble diagram with the corresponding HTL reduced diagram in Fig. 6 is proven.

B. The HTL Reduced Rainbow Diagram

Fig. 8 shows the three diagrams obtained by considering a hard and a soft loop in the original two-loop rainbow diagram. The last tadpole diagram does not give contribution to the fermion self-energy at the NLO HTL order because there is no 4-electron HTL effective vertex. The tadpole diagram containing the two-electron–two-photon 4-point function $\Gamma_{\mu\nu}^{\text{HTL}}$ vanishes in Feynman gauge, since cf. (5.4) one has the contraction, $g^{\mu\nu}V_\mu V_\nu = V_\mu V^\mu = 1 - \mathbf{v} \cdot \mathbf{v} = 0$.

The contribution of the remaining effective one-loop diagram with the insertion of the LO HTL fermion self-energy given in (5.1) reads

$$\Sigma_\Sigma(Q) = -e^2 \int_P \gamma_\alpha G(P) \Sigma^{\text{HTL}} G(P) \gamma_\beta D^{\mu\alpha}(Q - P). \quad (5.16)$$

In Feynman gauge the Dirac algebra gives

$$\gamma_\alpha \not{P} \not{V} \not{P} \gamma^\alpha = -P^2 \gamma_\alpha \not{V} \gamma^\alpha + 2P \cdot V \gamma_\alpha \not{P} \gamma^\alpha = 2P^2 \not{V} - 4P \cdot V \not{P}.$$

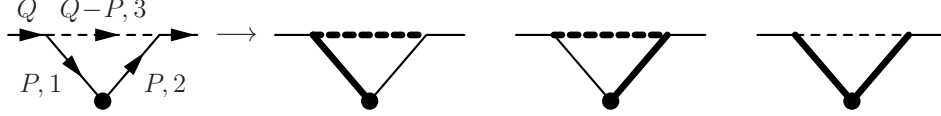


FIG. 9: The diagram corresponding to the first momentum integral of (5.17) when it is decomposed in Gaudin tree graphs. The dashed (solid) line means bosonic (fermionic) propagator. See Fig. 3 for other conventions on the lines.

Using the above expression in (5.16), the integral reduces to the sum of two terms:

$$\Sigma_{\Sigma}(Q) = \frac{e^4 T^2}{4} \int \frac{d\Omega}{4\pi} \int_P \Psi S(P) \tilde{D}(P) D(Q-P) + i \frac{e^4 T^2}{2} \frac{\partial}{\partial m^2} \int_P G_{m^2}(P) D(Q-P) \Big|_{m^2=0}. \quad (5.17)$$

The propagators $S(P)$ and $G_{m^2}(P)$ were defined in (5.12) and (3.13). In imaginary time $S(i\omega_n, \mathbf{p}) = -i\tilde{\Delta}_S(i\omega_n, \mathbf{p})$, (ω_n is fermionic) and $\tilde{\Delta}_S(i\omega_n, \mathbf{p})$ has the same spectral representation as $\Delta_S(i\omega_n, \mathbf{p})$ in (5.12).

The second term in (5.17) is exactly the term Σ_{R2} encountered in the calculation of the two-loop rainbow given by (3.15b). This can be seen immediately by applying (3.20) to the first integral in (3.15b).

Since with the direct two-loop calculation we have seen that at leading order in the high temperature expansion the non-vanishing contribution comes only from Σ_{R2} , it remains to show that the first term of (5.17) does not contribute at this order. In imaginary time this term is

$$\Sigma_{\Sigma 1}(i\nu_q, \mathbf{q}) = -\frac{e^4 T^2}{4} \int \frac{d\Omega}{4\pi} \int_{\mathbf{p}} \left(\prod_{i=1}^3 \int \frac{dp_i^0}{2\pi} \right) \rho(p_1^0, \mathbf{p}_1) \rho_S(p_2^0, \mathbf{p}_2) \rho(p_3^0, \mathbf{p}_3) T \sum_n \prod_{i=1}^3 \frac{1}{p_i^0 - i\omega_i}, \quad (5.18)$$

where $\mathbf{p}_1 = \mathbf{p}_2 = \mathbf{p}$, $\mathbf{p}_3 = \mathbf{q} - \mathbf{p}$, $\omega_1 = \omega_2 = \omega_n$, and $\omega_3 = \nu_q - \omega_n$. Since ω_1 and ω_2 are fermionic Matsubara frequencies, the result of the sum is

$$T \sum_n \prod_{i=1}^3 \frac{1}{p_i^0 - i\omega_i} = \frac{1}{p_1^0 - p_2^0} \left[\frac{n_F(-p_2^0)}{p_3^0 + p_2^0 - i\nu_q} - \frac{n_F(-p_1^0)}{p_3^0 + p_1^0 - i\nu_q} \right] + \frac{n_B(p_3^0)}{(p_1^0 + p_3^0 - i\nu_q)(p_2^0 + p_3^0 - i\nu_q)}, \quad (5.19)$$

where the three terms correspond to the Gaudin tree graphs of Fig. 9.

Substituting (5.19) into (5.18), performing the frequency integrals, and taking $\mathbf{q} = 0$, one obtains the three terms

$$\Sigma_{\Sigma 1}(i\nu_q, \mathbf{q} = \mathbf{0}) = \Sigma_{\Sigma 1a}(i\nu_q) + \Sigma_{\Sigma 1b}(i\nu_q) + \Sigma_{\Sigma 1c}(i\nu_q), \quad (5.20)$$

where

$$\Sigma_{\Sigma 1a}(i\nu_q) = \frac{e^4 T^2}{16\pi^2} \gamma_0 \int_{-1}^1 dx \frac{1}{x^2 - 1} \int_0^\infty dp \frac{n_F(-px)}{p^2 - (i\nu_q - px)^2}, \quad (5.21a)$$

$$\Sigma_{\Sigma 1b}(i\nu_q) = -\frac{e^4 T^2}{32\pi^2 i\nu_q} \gamma_0 \int_{-1}^1 dx \frac{1}{1 - x^2} \int_0^\infty dp n_F(p) \frac{p}{p^2 - (i\nu_q/2)^2}, \quad (5.21b)$$

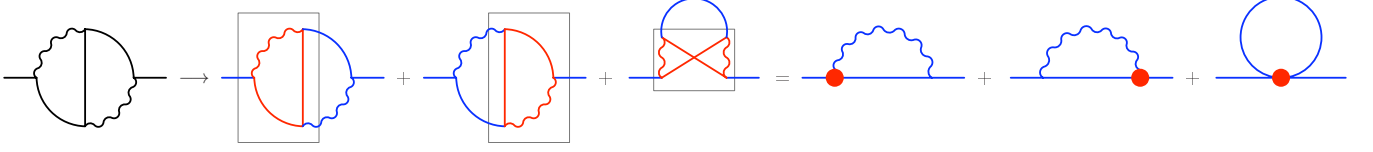


FIG. 10: Reduction of the two-loop crossed photon diagram to effective one-loop diagrams with HTL insertions. The framed part of the diagram represent the hard loop which are replaced by an effective HTL vertex part.

$$\Sigma_{\Sigma 1c}(i\nu_q) = \frac{e^4 T^2}{32\pi^2 i\nu_q} \gamma_0 \int_{-1}^1 dx \frac{1}{1-x^2} \int_0^\infty dp \left[\frac{p n_B(p)}{p^2 - (i\nu_q/2)^2} - 2 \frac{p n_B(p)}{p^2 - (i\nu_q/(1+x))^2} \right]. \quad (5.21c)$$

For $\Sigma_{\Sigma 1a}$ one observes that in the UV the integrand is well-behaved allowing the use of $n_F(-px) \simeq 1/2$. Then the momentum integral gives

$$\frac{1}{2} \int_0^\infty dp \frac{1}{p^2 - (i\nu_q - px)^2} = \frac{\pi}{4i\nu_q} + \frac{i}{4i\nu_q} \ln \frac{1-x}{1+x}. \quad (5.22)$$

After analytical continuation one sees that the imaginary part contains an odd function in x whose integral vanishes. The real part is collinearly divergent, but nevertheless it is subleading because it does not contain the factor $\ln(T/\omega)$.

Using (B6) and (B14), the real part of $\Sigma_{\Sigma 1c}$ cancels at leading order in the high temperature expansion against the real part of $\Sigma_{\Sigma 1b}$. As for the imaginary part, as shown in Appendix B neither $\Sigma_{\Sigma 1b}$ nor $\Sigma_{\Sigma 1c}$ acquires a contribution at leading order in the high temperature expansion [see (B10a) and (B14)]. This completes the proof that the first term in (5.17) does not contribute at leading order in the high temperature expansion. Hence the only contribution of the reduced HTL rainbow diagram in Fig. 8 at leading order in the high temperature expansion is given by the second term of (5.17), which agrees exactly with the corresponding rainbow diagram contribution of (4.31).

C. The HTL Reduced Crossed Photon Diagram

The reduction of the two-loop crossed photon diagram into diagrams containing one HTL insertion and one soft loop is shown in Fig. 10. The last diagram in Fig. 10 does not contribute to the fermion self-energy at NLO HTL order because there is no 4-electron HTL effective vertex. The contribution of the two remaining diagrams in Fig. 10 in which one of the original loop integral is replaced by the effective HTL vertex given by (5.3) are equal and give

$$\Sigma_\Gamma(Q) = -2ie^2 \int_P \gamma_\alpha G(Q-P) \Gamma_\nu^{\text{HTL}}(Q-P, Q) D^{\nu\alpha}(P). \quad (5.23)$$

In Feynman gauge ($\xi = 1$) one has $\gamma_\alpha(Q - P)V^\alpha \Psi = 2(Q - P) \cdot V \Psi$ and the angular and momentum integrals factorize:

$$\Sigma_\Gamma(Q) = i \frac{e^4 T^2}{2} \int \frac{d\Omega}{4\pi} \frac{\Psi}{Q \cdot V} \int_P \tilde{D}(Q - P) D(P). \quad (5.24)$$

In imaginary time, using the spectral representation of the propagators and performing the Matsubara sum coming from the momentum integral of (5.24), one obtains

$$\Sigma_\Gamma(i\nu_q, \mathbf{q}) = -\frac{e^4 T^2}{2} \gamma_0 \int \frac{d\Omega}{4\pi} \frac{\Psi}{Q \cdot V} \int_{\mathbf{p}} \int_{-\infty}^{\infty} \frac{dp_0}{2\pi} \int_{-\infty}^{\infty} \frac{dr_0}{2\pi} \rho(p_0, \mathbf{p}) \rho(r_0, \mathbf{q} - \mathbf{p}) \frac{n_F(r_0) + n_B(-p_0)}{p_0 + r_0 - i\nu_q}. \quad (5.25)$$

For $\mathbf{q} = 0$ one has $Q \cdot V = i\nu_q$ and one frequency integral can be performed by undoing the spectral representation of the propagator, while the other frequency integral can be performed by the use the Dirac δ -function in the spectral function. Retaining only the terms with two statistical factors, one obtains

$$\Sigma_\Gamma(i\nu_q) = \frac{e^4 T^2}{16\pi^2 i\nu_q} \gamma_0 \int_0^\infty dp \frac{p}{p^2 - (i\nu_q)^2/4} [n_B(p) - n_F(p)], \quad (5.26)$$

which is exactly the result of (4.34).

Thus, the full leading order high temperature contributions of the perturbative two-loop fermion self-energy coincide with those of the corresponding one-loop reduced HTL diagrams, according to Figs. 6, 8, and 10, just as required by the hard-soft pattern exhibited in the two-loop self-energy.

VI. GAUGE PARAMETER DEPENDENCE AT TWO LOOPS

Having computed the full two-loop electron self-energy in the Feynman gauge $\xi = 1$ we consider the dependence of the self-energy upon the gauge parameter ξ at two-loops. For $\xi = 1$ we have shown that all the leading order terms in the high temperature expansion of the two-loop self-energy exhibit a factorized hard-soft pattern. This pattern should continue to hold for $\xi \neq 1$, because in Euclidean time the additional factor of $(1 - \xi)K^\mu K^\nu / K^2$ in the photon propagator is homogeneous of order zero under rescaling $K^\mu \rightarrow \lambda K^\mu$. Hence it neither enhances nor suppresses the loop momentum Matsubara sum and integration with respect to the $\xi = 1$ case, and we expect the same hard-soft pattern to hold. Assuming this to be the case, we can analyze the ξ dependence of the remaining soft loop integration in the reduced HTL description of the last section.

One immediate effect of the factorization into one hard, one soft loop is that all ξ dependence drops out of the internal hard thermal loop, so that it is impossible to find any quadratic dependence on ξ in the leading high temperature terms of the two-loop self-energy, despite the fact that the original diagrams contain two photon propagators. The remaining ξ dependence can at most be linear. In this section we

analyze the linear ξ dependent terms in the two-loop self-energy, assuming the hard-soft pattern and HTL reduction to effective one-loop diagrams.¹ We note also that owing to the transversality of the HTL photon polarization $\Pi_{\mu\nu}^{\text{HTL}}$, the HTL reduced bubble diagram has no ξ parameter dependence at all.

For the rainbow diagram the first framed self-energy correction diagram of Fig. 8 gives

$$\xi\Sigma_{\Sigma}(Q) = (1 - \xi)ie^2 \int_K \left[\gamma_{\mu} \frac{1}{\not{Q} - \not{K}} \Sigma^{\text{HTL}}(Q - K) \frac{1}{\not{Q} - \not{K}} \gamma_{\nu} \right] \frac{K^{\mu}K^{\nu}}{(K^2)^2}, \quad (6.1)$$

while the second framed diagram of Fig. 8 gives the tadpole contribution

$$\xi\Sigma_T(Q) = (1 - \xi)ie^2 \int_K \Gamma_{\mu\nu}^{\text{HTL}}(Q, Q, K) \frac{K^{\mu}K^{\nu}}{(K^2)^2}. \quad (6.2)$$

In these expressions $\Gamma_{\mu}^{\text{HTL}}(P_1, P_2)$ and $\Gamma_{\mu\nu}^{\text{HTL}}(Q, Q, K)$ are the HTL vertices defined by (5.3) and (5.4).

For the crossed photon diagram the reduction of one of the loops into a HTL vertex yields the ξ dependent terms

$$\xi\Sigma_{\Gamma}(Q) = (1 - \xi)ie^2 \int_K \left[\gamma_{\mu} \frac{1}{\not{Q} - \not{K}} \Gamma_{\nu}^{\text{HTL}}(Q - K, Q) + \Gamma_{\mu}^{\text{HTL}}(Q, Q - K) \frac{1}{\not{Q} - \not{K}} \gamma_{\nu} \right] \frac{K^{\mu}K^{\nu}}{(K^2)^2} \quad (6.3)$$

from the first two framed diagrams of Fig. 10, while the third framed diagram of Fig. 10 gives no contribution, since the corresponding LO HTL 4-fermion vertex vanishes.

Since the HTL vertex functions obey the Ward Identities (5.5), (5.6), and (5.7), we may contract the $K^{\mu}K^{\nu}$ vectors into these vertices to express all the ξ dependent terms in terms of the HTL self-energy Σ^{HTL} in the form

$$\begin{aligned} \xi\Sigma_2(Q) &\equiv \xi\Sigma_{\Gamma}(Q) + \xi\Sigma_{\Sigma}(Q) + \xi\Sigma_T(Q) \\ &= (1 - \xi)ie^2 \int_K \frac{1}{(K^2)^2} \left\{ \left[\not{Q} \frac{1}{\not{Q} - \not{K}} - 1 \right] [\Sigma^{\text{HTL}}(Q - K) - \Sigma^{\text{HTL}}(Q)] \right. \\ &\quad \left. + [\Sigma^{\text{HTL}}(Q - K) - \Sigma^{\text{HTL}}(Q)] \left[\frac{1}{\not{Q} - \not{K}} \not{Q} - 1 \right] \right\} \\ &\quad + (1 - \xi)ie^2 \int_K \frac{1}{(K^2)^2} \left[\not{Q} \frac{1}{\not{Q} - \not{K}} - 1 \right] \Sigma^{\text{HTL}}(Q - K) \left[\frac{1}{\not{Q} - \not{K}} \not{Q} - 1 \right] \\ &\quad + (1 - \xi)ie^2 \int_K \frac{1}{(K^2)^2} \left\{ \Sigma^{\text{HTL}}(Q + K) - 2\Sigma^{\text{HTL}}(Q) + \Sigma^{\text{HTL}}(Q - K) \right\} \\ &= (1 - \xi)ie^2 \int_K \frac{1}{(K^2)^2} \left\{ -\not{Q} \frac{1}{\not{Q} - \not{K}} \Sigma^{\text{HTL}}(Q) - \Sigma^{\text{HTL}}(Q) \frac{1}{\not{Q} - \not{K}} \not{Q} \right. \\ &\quad \left. + \not{Q} \frac{1}{\not{Q} - \not{K}} \Sigma^{\text{HTL}}(Q - K) \frac{1}{\not{Q} - \not{K}} \not{Q} + \Sigma^{\text{HTL}}(Q + K) \right\}, \quad (6.4) \end{aligned}$$

¹ Some preliminary work on the gauge parameter dependence was reported in [16], with however a differing result for the real part, which we calculate fully here.

for the sum of these two-loop ξ dependent contributions. In order to find the magnitude of this two-loop gauge dependent self-energy, we substitute the LO HTL condition, $\mathcal{Q} = \Sigma^{\text{HTL}}(Q)$ and add the result to the one-loop ξ dependent self-energy (2.27), to obtain

$$\begin{aligned} \xi \Sigma_{\text{on-shell}}(Q) \equiv [\xi \Sigma_1(Q) + \xi \Sigma_2(Q)]_{\text{on-shell}} &= (1 - \xi) i e^2 \int_K \frac{1}{(K^2)^2} \left\{ -\mathcal{Q} \frac{1}{\mathcal{Q} - \mathcal{K}} \mathcal{Q} - (\mathcal{Q} + \mathcal{K}) \right. \\ &\quad \left. + \mathcal{Q} \frac{1}{\mathcal{Q} - \mathcal{K}} \Sigma^{\text{HTL}}(Q - K) \frac{1}{\mathcal{Q} - \mathcal{K}} \mathcal{Q} + \Sigma^{\text{HTL}}(Q + K) \right\}_{\text{on-shell}} \end{aligned} \quad (6.5)$$

for the sum.

We note that the relative sign of the first two terms in (6.5) is opposite that for one-loop ξ dependent self-energy (2.27). Following the familiar methods these two terms can be written in the forms

$$-(1 - \xi) i e^2 \int_K \frac{1}{(K^2)^2} \mathcal{Q} \frac{1}{\mathcal{Q} - \mathcal{K}} \mathcal{Q} = -\frac{(1 - \xi) e^2}{2\pi^2} (i\nu_q)^2 \gamma_0 F_1, \quad (6.6a)$$

$$-(1 - \xi) i e^2 \int_K \frac{1}{(K^2)^2} (\mathcal{Q} + \mathcal{K}) = -\frac{(1 - \xi) e^2}{2\pi^2} (i\nu_q) \gamma_0 F_2, \quad (6.6b)$$

for $\mathbf{q} = \mathbf{0}$, where

$$F_1 \equiv \frac{\partial}{\partial M^2} \int_0^\infty k^2 dk \int_{-\infty}^\infty \frac{dk_0}{2\pi} \rho_{M^2}(k_0, \mathbf{k}) \int_{-\infty}^\infty \frac{dp_0}{2\pi} p_0 \rho(p_0, -\mathbf{k}) \left[\frac{n_B(-k_0) + n_F(p_0)}{k_0 + p_0 - i\nu_q} \right], \quad (6.7a)$$

$$F_2 \equiv \frac{\partial}{\partial M^2} \int_0^\infty k^2 dk \int_{-\infty}^\infty \frac{dk_0}{2\pi} \rho_{M^2}(k_0, \mathbf{k}) n_B(k_0), \quad (6.7b)$$

with the limit $M \rightarrow 0$ (if it exists) to be taken after integration is understood. After performing the integrations over all variables which are *not* arguments of the statistical distributions, and an integration by parts in the fermionic term, we find that the thermal part of F_1 may be expressed in the form

$$\begin{aligned} F_1 &= -\frac{1}{8i\nu_q} \int_0^\infty \frac{dE}{E^2 - (i\nu_q/2)^2} \frac{d}{dE} [E^2 n_F(E)] \\ &\quad - \frac{1}{8(i\nu_q)^2} \int_0^\infty dE E n_B(E) \left[\frac{E + i\nu_q}{(E + i\nu_q/2)^2} - \frac{E - i\nu_q}{(E - i\nu_q/2)^2} \right] \\ &\quad - \frac{1}{8i\nu_q} \int_M^\infty \frac{dE n_B(E)}{\sqrt{E^2 - M^2}} \left[\frac{E + i\nu_q}{E + i\nu_q/2} + \frac{E - i\nu_q}{E - i\nu_q/2} \right], \end{aligned} \quad (6.8)$$

where the finite M regulator must be retained only in the last integral. Likewise for F_2 ,

$$F_2 = -\frac{1}{2} \int_M^\infty \frac{dE n_B(E)}{\sqrt{E^2 - M^2}}. \quad (6.9)$$

The high temperature asymptotic forms of each of the integrals in F_1 and F_2 may be obtained by the methods of Appendix B, with the results

$$F_1 = -\frac{1}{4\omega} \left[\frac{\pi T}{M} - \ln \frac{\omega}{M} - \frac{3i\pi T}{2\omega} \right] + \dots \quad (6.10a)$$

$$F_2 = -\frac{1}{4} \left[\frac{\pi T}{M} - \ln \frac{T}{M} \right] + \dots \quad (6.10b)$$

after continuation to real time, $i\nu_q \rightarrow \omega + i0^+$. Thus each of the first two terms in (6.5) contain both linear and logarithmic divergences as the photon regulator mass $M \rightarrow 0$. These add in (6.5) but cancel when combined with the opposite relative sign in (2.27), to yield the finite result (2.34) for the high T asymptotic form of the gauge dependent part of the one-loop self-energy.

For the third and fourth terms in (6.5) one uses the definition of Σ^{HTL} given in (5.1), performs the Dirac algebra, using

$$\mathcal{Q}(\mathcal{Q} - \mathcal{K}) \mathcal{V}(\mathcal{Q} - \mathcal{K}) \mathcal{Q} = 2(Q - K) \cdot V [(Q - K)^2 \mathcal{Q} - K^2 \mathcal{Q} + Q^2 \mathcal{K}] + (Q - K)^2 [Q^2 \mathcal{V} - 2Q \cdot V \mathcal{Q}] \quad (6.11)$$

and the Matsubara sums, to obtain for $\mathbf{q} = \mathbf{0}$,

$$(1 - \xi) i e^2 \int_K \frac{1}{(K^2)^2} \mathcal{Q} \frac{1}{\mathcal{Q} - \mathcal{K}} \Sigma^{\text{HTL}}(Q - K) \frac{1}{\mathcal{Q} - \mathcal{K}} \mathcal{Q} = \frac{(1 - \xi) e^2}{\pi^2} m_f^2 (i\nu_q) \gamma_0 \left(G_1 - G_2 + i\nu_q G_3 - \frac{i\nu_q}{4} G_4 \right), \quad (6.12)$$

and

$$(1 - \xi) i e^2 \int_K \frac{1}{(K^2)^2} \Sigma^{\text{HTL}}(Q + K) = -\frac{(1 - \xi) e^2}{4\pi^2} m_f^2 \gamma_0 H, \quad (6.13)$$

where

$$G_1 \equiv \frac{\partial}{\partial M^2} \int_0^\infty k^2 dk \int_{-\infty}^\infty \frac{dk_0}{2\pi} \rho_{M^2}(k_0, \mathbf{k}) \int_{-\infty}^\infty \frac{dp_0}{2\pi} \rho(p_0, -\mathbf{k}) \left[\frac{n_B(-k_0) + n_F(p_0)}{k_0 + p_0 - i\nu_q} \right], \quad (6.14a)$$

$$G_2 \equiv \frac{\partial}{\partial m^2} \int_0^\infty k^2 dk \int_{-\infty}^\infty \frac{dk_0}{2\pi} \rho(k_0, \mathbf{k}) \int_{-\infty}^\infty \frac{dp_0}{2\pi} \rho_{m^2}(p_0, -\mathbf{k}) \left[\frac{n_B(-k_0) + n_F(p_0)}{k_0 + p_0 - i\nu_q} \right], \quad (6.14b)$$

$$G_3 \equiv \frac{\partial}{\partial M^2} \frac{\partial}{\partial m^2} \int_0^\infty k^2 dk \int_{-\infty}^\infty \frac{dk_0}{2\pi} k_0 \rho(k_0, \mathbf{k}) \int_{-\infty}^\infty \frac{dp_0}{2\pi} \rho_{m^2}(p_0, -\mathbf{k}) \left[\frac{n_B(-k_0) + n_F(p_0)}{k_0 + p_0 - i\nu_q} \right], \quad (6.14c)$$

$$G_4 \equiv \frac{\partial}{\partial M^2} \int_0^\infty k^2 dk \int_{-\infty}^\infty \frac{dk_0}{2\pi} \rho_{M^2}(k_0, \mathbf{k}) \int_{-\infty}^\infty \frac{dp_0}{2\pi} \rho(p_0, -\mathbf{k}) \int_{-1}^1 dx \int_{-\infty}^\infty dr_0 \delta(r_0 + kx) \times \left\{ \frac{n_B(k_0)}{(k_0 + p_0 - i\nu_q)(k_0 + r_0 - i\nu_q)} + \frac{1}{p_0 - r_0} \left[\frac{n_F(p_0)}{k_0 + p_0 - i\nu_q} - \frac{n_F(r_0)}{k_0 + r_0 - i\nu_q} \right] \right\}, \quad (6.14d)$$

and

$$H \equiv \frac{\partial}{\partial M^2} \int_0^\infty k^2 dk \int_{-\infty}^\infty \frac{dk_0}{2\pi} \rho_{M^2}(k_0, \mathbf{k}) \int_{-1}^1 dx \int_{-\infty}^\infty dr_0 \delta(r_0 + kx) \left[\frac{n_B(-k_0) + n_F(r_0)}{k_0 + r_0 + i\nu_q} \right], \quad (6.15)$$

The Matsubara sum needed to obtain (6.14d) is given by a formula analogous to (5.19). corresponding to the Gaudin tree graphs of Fig. 9. In order to deal with the double poles in both the bosonic and fermionic propagators we have made use of the massive regulator (2.29) as before, with M the bosonic mass and m the fermionic one, the limits $M, m \rightarrow 0$ (if they exist) to be taken at the end.

The integrals in (6.14) and (6.15) are similar to those we have encountered above and in the previous Feynman gauge analysis. The most efficient method of evaluating them is to write them as a sum of terms and in each term use the delta functions to evaluate all the integrals which do not involve the Bose-Einstein or Fermi-Dirac statistical functions, leaving this single frequency integral for last, using relations (2.15) to retain only the thermal parts as integrals over positive range. In this way we obtain

$$G_1 = -\frac{1}{8(i\nu_q)^2} \int_0^\infty dE E [n_F(E) + n_B(E)] \left[\frac{1}{(E + i\nu_q/2)^2} + \frac{1}{(E - i\nu_q/2)^2} \right] + \frac{1}{8} \int_M^\infty \frac{dE}{\sqrt{E^2 - M^2}} \frac{n_B(E)}{E^2 - (i\nu_q/2)^2}, \quad (6.16a)$$

$$G_2 = \frac{1}{8(i\nu_q)^2} \int_0^\infty dE E [n_F(E) + n_B(E)] \left[\frac{1}{(E + i\nu_q/2)^2} + \frac{1}{(E - i\nu_q/2)^2} \right] - \frac{1}{8} \int_m^\infty \frac{dE}{\sqrt{E^2 - m^2}} \frac{n_F(E)}{E^2 - (i\nu_q/2)^2}, \quad (6.16b)$$

$$G_3 = \frac{1}{16(i\nu_q)^2} \int_0^\infty dE n_B(E) \left[\frac{1}{(E + i\nu_q/2)^2} - \frac{1}{(E - i\nu_q/2)^2} \right] + \frac{1}{8(i\nu_q)^3} \int_0^\infty dE E^2 n_B(E) \left[\frac{1}{(E + i\nu_q/2)^3} + \frac{1}{(E - i\nu_q/2)^3} \right] - \frac{1}{8(i\nu_q)^3} \int_0^\infty dE E n_F(E) \left[\frac{E + i\nu_q}{(E + i\nu_q/2)^3} + \frac{E - i\nu_q}{(E - i\nu_q/2)^3} \right] + \frac{1}{16(i\nu_q)^2} \int_m^\infty \frac{dE n_F(E)}{\sqrt{E^2 - m^2}} \left[\frac{E + i\nu_q}{(E + i\nu_q/2)^2} - \frac{E - i\nu_q}{(E - i\nu_q/2)^2} \right], \quad (6.16c)$$

$$G_4 = -\frac{1}{8(i\nu_q)^2} \int_0^\infty dE n_B(E) \left\{ \frac{1}{(E + i\nu_q/2)^2} \ln \left(\frac{2E + i\nu_q}{i\nu_q} \right) - \frac{1}{(E - i\nu_q/2)^2} \ln \left(\frac{2E - i\nu_q}{-i\nu_q} \right) \right\} - \frac{1}{8(i\nu_q)^2} \int_M^\infty \frac{dE n_B(E)}{\sqrt{E^2 - M^2}} \left[\frac{E + i\nu_q}{(E + i\nu_q/2)^2} - \frac{E - i\nu_q}{(E - i\nu_q/2)^2} \right] + \frac{1}{8(i\nu_q)^2} \int_0^\infty dE n_F(E) \left\{ \frac{1}{(E + i\nu_q/2)^2} \ln \left[\frac{4E^2}{-2iE\nu_q - (i\nu_q)^2} \right] - \frac{1}{(E - i\nu_q/2)^2} \ln \left[\frac{4E^2}{2iE\nu_q - (i\nu_q)^2} \right] \right\} + \frac{1}{8(i\nu_q)^2} \int_0^\infty dE n_F(E) \left[\frac{1}{(E + i\nu_q/2)^2} - \frac{1}{(E - i\nu_q/2)^2} \right], \quad (6.16d)$$

and

$$H = \frac{1}{4i\nu_q} \int_M^\infty \frac{dE n_B(E)}{\sqrt{E^2 - M^2}} \left[\frac{E + i\nu_q}{E + i\nu_q/2} + \frac{E - i\nu_q}{E - i\nu_q/2} \right] + \frac{1}{2i\nu_q} \int_0^\infty \frac{dE E n_F(E)}{E^2 - (i\nu_q/2)^2}, \quad (6.17)$$

where we have set M and m to zero wherever the integrals are finite after differentiation, retaining the regulator masses only when they are needed.

The high temperature asymptotic forms of the integrals (6.16) and (6.17), evaluated by the methods of Appendix B are

$$G_1 = \frac{1}{4\omega^2} \left[-\frac{\pi T}{M} + \ln \frac{\omega}{M} + \frac{2\pi i T}{\omega} \right] + \dots \quad (6.18a)$$

$$G_2 = \frac{1}{4\omega^2} \ln \frac{\omega}{m} + \dots \quad (6.18b)$$

$$G_3 = \frac{1}{4\omega^3} \left[\ln \frac{\omega}{m} + \frac{i\pi T}{\omega} \right] + \dots \quad (6.18c)$$

$$G_4 = -\frac{1}{2\omega^3} \left[\frac{\pi T}{M} - \ln \frac{\omega}{M} - \frac{3\pi i T}{\omega} \right] + \dots \quad (6.18d)$$

and

$$H = \frac{1}{2\omega} \left[\frac{\pi T}{M} - \ln \frac{\omega}{M} - \frac{i\pi T}{\omega} \right] + \dots \quad (6.19)$$

upon analytic continuation to real time.

Assembling the results for the asymptotic forms (6.10), (6.18) and (6.19) in (6.5), (6.6), (6.12) and (6.13), with $\omega = m_f = eT/\sqrt{8}$, we find finally

$$\xi \Sigma_{\text{on-shell}}(Q) = (1 - \xi) \frac{e^2}{8\pi^2} \gamma_0 \left[-m_f \ln \frac{T}{m_f} + \frac{5i\pi T}{2} \right] + \dots \quad (6.20)$$

where we have everywhere neglected terms of order $e^2 m_f \sim e^3 T$ subdominant to the logarithm in the real part and $e^2 T$ in the imaginary part. Although all dependence on the regulator masses M and m have dropped out of the sum of terms in (6.5), neither the real nor imaginary parts of the gauge dependent self-energy vanish, even when the on-shell LO HTL condition is used. In addition to the infrared divergence encountered in the two-loop bubble diagram, this residual gauge parameter dependence in a physical quantity such as the fermion lifetime in the plasma indicates that a resummation of the perturbative series in e^2 is necessary in high temperature QED. Such a resummation was performed for QED in [20, 21] within the HTL resummation program. After HTL resummation both the electron damping rate and the electron mass were calculated at NLO and shown to be independent of the gauge fixing parameter ξ .

VII. SUMMARY AND DISCUSSION

We have presented a thorough analysis of the leading order contributions to the high temperature limit of the two-loop electron self-energy at rest with respect to the plasma ($\mathbf{q} = 0$). The three two-loop self-energy diagrams illustrated in Fig. 2 yield (4.24), (4.31), and (4.35) at leading order for $T \gg \omega$ in Feynman gauge, *i.e.*,

$$\Sigma_{\text{B}}(\omega) \Big|_{\xi=1} \simeq \frac{e^4 T^2}{24\pi^2 \omega} \gamma_0 \left[\frac{\pi T}{M} + \left(\frac{1}{2} + \ln 2 \right) \ln \frac{T}{\omega} - \frac{5i\pi}{2} \frac{T}{\omega} \right], \quad (7.1a)$$

$$\Sigma_{\text{R}}(\omega) \Big|_{\xi=1} \simeq -i \frac{e^4 T^3}{32\pi\omega^2} \gamma_0, \quad (7.1b)$$

$$\Sigma_C(\omega)\Big|_{\xi=1} \simeq \frac{e^4 T^2}{16\pi^2 \omega} \gamma_0 \left[-\ln \frac{T}{\omega} + i\pi \frac{T}{\omega} \right]. \quad (7.1c)$$

As explained in the Introduction, the photon mass M was introduced to regulate the infrared and/or collinear divergences in the self-energy bubble diagram. All terms which are either independent of temperature or vanish in the high temperature limit T/ω , $T/M \rightarrow \infty$ have been omitted from (7.1). Terms which remain finite in the subsequent limit of removing the regulator, $M/\omega \rightarrow 0$ have also been omitted.

The first important observation about the leading high temperature behavior of the two-loop self-energy given in (7.1) is that it is more infrared singular, both as $\omega \rightarrow 0$ and $M \rightarrow 0$ than the corresponding one-loop LO and NLO self-energy,

$$\Sigma_{1\text{-loop}}(\omega, \mathbf{0}) = \frac{e^2 T^2}{8\omega} \gamma_0 + \xi \frac{e^2 \omega}{8\pi^2} \gamma_0 \ln \frac{T}{\omega} + i(1 - 3\xi) \frac{e^2 T}{16\pi} \gamma_0, \quad (7.2)$$

calculated in (2.23) and (2.24) and Refs. [10, 11] in covariant ξ gauges. Since to LO, $\omega = m_f = eT/\sqrt{8}$, the NLO one-loop self-energy gives a correction to its real part of order $e^3 \ln(1/e)$, and an imaginary part of order $e^2 T$. Using the lowest order value for $\omega = m_f$ for an electron on-shell and at rest in the plasma, we observe that the leading order terms in the high temperature expansion at two loops, given by (7.1b) and (7.1c) are comparable to the NLO terms from one-loop, again $e^3 \ln(1/e)$ in its real part, and $e^2 T$ in its imaginary part for this value of $\omega \sim eT$. The higher power of e^2 in the numerator of the two-loop self-energy is compensated by the more singular behavior of the denominators (7.1) when $\omega \sim eT$. The $1/M$ term in the real part of the bubble contribution (7.1a) violates the rule of finite NLO contribution to the real part of Σ of order $e^3 \ln(1/e)$, and gives a true, uncanceled infrared divergence as the photon mass regulator $M \rightarrow 0$ in bare perturbation theory. The singular infrared behavior of (7.1), and the uncanceled linear divergence as $M \rightarrow 0$ in (7.1a) clearly demonstrate the breakdown of the usual perturbative loop expansion, even for very weak coupling $e \ll 1$.

The gauge dependent terms of the self-energy up to two-loop order on-shell are given by (6.20), *viz.*

$$\xi \Sigma_{\text{on-shell}}(Q) = [\xi \Sigma_1(Q) + \xi \Sigma_2(Q)]_{\text{on-shell}} = (1 - \xi) \frac{e^2}{8\pi^2} \gamma_0 \left[-m_f \ln \frac{T}{m_f} + \frac{5i\pi T}{2} \right], \quad (7.3)$$

and are also of the same order as the NLO one-loop result (7.2). This non-cancellation of the gauge parameter dependence even on-shell is a second indication of the breakdown of weak coupling perturbation theory at high temperatures, the need for resummation and eventual restructuring of the usual (bare) perturbative loop expansion.

In our direct evaluation of the two-loop self-energy in bare perturbation theory, the photon mass M is a regulator, introduced to define the double pole terms in (3.1), and should be taken to zero. However, anticipating the result of HTL resummation of the NLO terms, we can estimate instead that after

resummation M will be replaced by the photon Debye mass, so that $M \sim eT$ finally. With this estimate we observe that the $1/M$ term in (7.1a) gives a contribution to the real part of the self-energy on-shell which is of order e^2T , parametrically *larger* than the $e^3 \ln(1/e)$ correction of both the NLO one-loop terms and the other leading order two-loop terms. Thus, the electron effective thermal mass at next-to-leading order in the HTL approximation is of order $\mathcal{O}(e^2T)$, *not* of order $e^3T \ln(1/e)$ as one might expect from the NLO one-loop result, and *both* the real and imaginary parts of the full resummed self-energy contain order e^2T corrections. In fact, the resummation within the HTL effective theory has been calculated in both its imaginary and real parts, and a gauge parameter independent result of order $\mathcal{O}(e^2T)$ for both has been obtained [20, 21].

The origin of this result can be understood intuitively also in the following way. From (2.19) in the LO HTL one-loop self-energy there is a contribution proportional to the Bose-Einstein statistical factor of the photon of the form

$$\frac{e^2}{2\pi^2\omega}\gamma_0 \int_0^\infty dk \frac{k}{e^{k/T} - 1}. \quad (7.4)$$

Because the Bose-Einstein distribution behaves like T/k at small k , this hard integral converges linearly as $k \rightarrow 0$, and as we have noted is dominated by $k \sim T$. However at two loops the bubble diagram has an additional photon propagator, and photon self-energy mass insertion proportional to $\Pi^{\text{HTL}}/k^2 \sim e^2T^2/6k^2$ relative to the one-loop contribution (7.4). Thus we should expect an integral with an additional power of $e^2T^2/6k^2$ in the integrand, and the two-loop bubble to make a contribution to Σ of

$$\frac{e^4T^2}{12\pi^2\omega}\gamma_0 \int_0^\infty \frac{dk}{k} \frac{1}{e^{k/T} - 1} \sim \frac{e^4T^3}{12\pi^2\omega} \int_0^\infty \frac{dk}{k^2} \rightarrow \infty.$$

which is now dominated by *soft* momenta and in fact diverges linearly at small k . When this linear IR divergence is cut off by the introduction of a photon mass regulator M , so that k^2 is replaced by $k^2 + M^2$, we therefore expect a non-analytic contribution of order of

$$\frac{e^4T^3}{12\pi^2\omega}\gamma_0 \int_0^\infty \frac{dk}{k^2 + M^2} = \frac{e^4T^3}{24\pi\omega M}\gamma_0, \quad (7.5)$$

which is indeed what we find in (7.1a). Notice that this estimate does not allow for a M^{-2} or $\ln M$ term, and is consistent with earlier approximations to the bubble diagram, *c.f.* [31]. There is no divergence, logarithmic or otherwise, from the corresponding HTL insertion of a fermion self-energy and double fermion propagators in the rainbow diagram. Hence there is no need for any fermion mass regulator in any two-loop self-energy diagram. From (7.1a) or (7.5) the order e^2T contribution to the real part of the self-energy in the HTL resummed evaluation of [21] has its origin in the appearance of a non-analytic linear $1/M$ dependence on the photon Debye mass $M \sim m_f \sim eT$ of the two-loop (and higher) bubble self-energy diagram(s).

Since the HTL resummation program requires a hard-soft factorization at ℓ loops, in which exactly one of the loops is soft and the rest are hard, the hard-soft pattern we have verified explicitly at $\ell = 2$ is a necessary condition for HTL resummation method to work, and provides a non-trivial check on its consistency. At $\ell > 2$ loops the HTL resummation contains a geometric series of multiple hard photon and electron self-energy insertions on the basic one-loop topology of Fig. 1, but in which the bare vertex is corrected only to one hard loop order. Thus for $\ell > 2$ HTL resummation when expanded in bare perturbative diagrams contains only a subset of all self-energy diagrams with $\ell - 1$ hard loops and one soft loop. To demonstrate that the HTL resummation captures all contributions of comparable order for $\omega \sim eT$, one would have to show that for $\ell > 2$ all the contributions to Σ at order e^2T arise from

- factorized ℓ loop diagrams with exactly $\ell - 1$ hard loops imbedded in one remaining soft loop; but
- only the subset of diagrams of this kind that can be represented as multiple insertions of either the HTL photon or electron self-energy, with no more than the one-loop HTL vertex insertion.

Thus the diagrams of different topology, such as a double rainbow two-loop vertex correction on the basic one-loop topology should give a subleading correction to the self-energy at $\ell = 3$ and be negligible compared to e^2T for an on-shell fermion at rest. The HTL resummation program essentially assumes that this holds.

Let us emphasize again that there are *no* hard-hard contributions at order e^2T in the two-loop self-energy as enumeration of the generic power counting rules given in [3, 8] might lead one to expect, and moreover that this absence of hard-hard contributions at two-loop order is in fact a *necessary* condition for HTL resummation. The soft-soft contributions to the two-loop self-energy are non-vanishing but subdominant to the NLO one-loop terms in Σ , and will enter at higher orders in the consistent expansion in e .

Our method has been based on isolating the leading order singularities as $\omega \rightarrow 0$ of the asymptotics of the high temperature expansion, at each loop order separately, and then comparing the magnitude of these contributions when the fermion is on-shell at $\omega \simeq eT/\sqrt{8}$. This suggests that collecting all the contributions which are subdominant to the NLO ones we have been considering, *i.e.* the NNLO order contributions, would require *two* soft loops and $\ell - 2$ strictly hard ones of order T , which would require either at least a three-loop computation, or an inductive general argument to verify explicitly. If this is the case, then collecting infrared singularities order by order in the high temperature expansion at each ℓ becomes possible, and a reordering of the usual loop expansion can be carried out in a completely systematic and gauge invariant way. At NLO this reordering is just one-loop HTL resummation, while at higher orders it may require additional resummation of both self-energy and vertex parts.

The HTL resummation procedure works when all energies and momenta in the remaining loops are soft $\sim eT$. This one-soft-loop HTL resummed contribution should always give the order $\omega/T \sim e$ corrections to the leading order HTL self-energy. On the other hand, uncritical use of HTL resummation has no justification *a priori* when extended to higher orders in ω/T in the high temperature expansion, or in loop integrals containing hard momenta, and may lead to incomplete or incorrect results when misapplied in this way. This seems to be the case in the use of HTL resummed propagators in the photon polarization function for the calculation of the photon damping rate in QED, or photon and dilepton production in QCD [32–34]. In the photon self-energy (unlike the fermion self-energy considered in this paper) the NLO result *vanishes*, because of the appearance of the statistical factor $1 - 2n_F(\omega/2) \simeq \omega/4T$ which produces a further suppression [33]. Because of this suppression the first non-zero contribution to the photon damping rate in QED and the complete calculation of the photon and dilepton production rate in QCD both require additional diagrams and depend upon additional physical processes (bremsstrahlung) than those captured in the one-loop HTL resummed photon polarization tensor $^*\Pi_{\mu\nu}$. Based on the results of this paper, we would conjecture that a completely analogous calculation of the two-loop perturbative photon polarization in QED would give a vanishing contribution from both hard-hard and hard-soft loops, and yield a non-zero contribution only when both loops are soft, which is down by $(\omega/T)^2 \sim e^2$ and is NNLO compared to the LO one-loop result $e^2 T^2$. Hence it cannot be captured by the usual HTL resummation.

Once HTL resummation has been carried out, one obtains a new HTL improved self-energy which contains the correct physics to NLO, at the soft scale eT . Thus we would expect that the main results of our detailed two-loop study for fermions at rest $\mathbf{q} = \mathbf{0}$ should continue to hold for fermions which are slow moving, $|\mathbf{q}| \lesssim eT$. However, there is no necessity for the expansion in \mathbf{q}^2/ω^2 to be analytic at $\mathbf{q}^2 = 0$. Non-analytic behavior has been reported in scalar QED [35, 36], but the spinor QED or QCD cases have not been fully investigated to our knowledge. It is known that even the HTL resummed fermion self-energy is inadequate to describe the damping rate or energy loss of a fast moving fermion with $|\mathbf{q}| \gg eT$ [13, 37], and a further or different sort of resummation is required [29]. The appearance of additional logarithmic terms of the form $\ln(\mathbf{q}^2/\omega^2)$ for $|\mathbf{q}| \gg eT$ does not mean that HTL resummation is inconsistent, but only that it must be properly applied. This example of the damping rate of a fast moving fermion, as those mentioned above of the photon damping rate in QED and both the photon production and dilepton production rates in a hot QCD plasma simply lie outside of the range of strict applicability of HTL resummation, which is valid for soft external four-momenta only.

To investigate the breakdown of HTL resummation, the systematic method which we have used in this paper for the two-loop perturbative self-energy could be applied to the HTL one-loop resummed self-

energy (photon or fermion) as well. Thus, if this HTL resummed self-energy is given *off-shell* for all ω and \mathbf{q} , one could examine its high temperature limit, or equivalently, its infrared singularities at $\mathbf{q} = \mathbf{0}$ and $\omega \rightarrow 0$, as well as its behavior at large $|\mathbf{q}| \gg eT$. Then, depending on the result one could examine terms at two and higher loops in the effective HTL theory to determine when they become of the same magnitude as the LO HTL results. It is known that the breakdown of the HTL resummation program is associated with the appearance of collinear divergences [38] and requires an additional resummation of ladder-like diagrams corresponding to multi-loop vertex corrections not contained in the usual HTL resummed self-energy [39]. Such ladder sums are also required to compute transport coefficients in hot gauge theories [40, 41]. Quantitative control of the breakdown of the HTL resummation program by the extension of the methods utilized in this paper to determine the most infrared sensitive contributions at each HTL resummed loop order can provide detailed guidance to its proper generalization to more complete resummation algorithms in hot gauge theories.

If one finds that higher order terms beyond NLO can be resummed in a consistent gauge invariant way, this would provide the theoretical justification for a systematic extension of the HTL program to higher orders, including also resummed vertex parts and ladder diagrams, which might enable the extension of resummation methods to lower energy and momentum scales and the hydrodynamic limit, where weak coupling methods are usually thought to fail entirely, particularly in QCD.

Physically, taking account of infrared and collinear singularities by a reordering of the loop expansion and resummation of self-energies and proper vertices relate the dressed quasiparticles and many-body interactions in the medium to the single particle excitations of the theory in the absence of a medium, *i.e.* in the vacuum at zero temperature and density. The dispersion relations of the dressed quasiparticles for low frequencies and soft momenta are required to describe the collective modes of the plasma in the hydrodynamic limit, and to determine transport coefficients such as electrical conductivity, and shear and bulk viscosity. A thorough understanding of the quasiparticle degrees of freedom at high temperatures or densities and the interactions they undergo in thermodynamic equilibrium or under slight departures therefrom is thus an entry point into the systematic study of non-equilibrium processes in the plasma and self-consistent methods for studying them systematically as well.

Acknowledgments

E. M. would like to thank Margaret E. Carrington for invaluable discussions, and in particular for sharing with us her detailed calculations of the two-loop self-energy in the real time formalism, which

indicated the non-cancellation of the ξ dependence in the imaginary part of Σ up to two-loop order, prior to the initiation of this work. Zs. Sz. would like to thank Los Alamos National Laboratory for its hospitality and visitor support under LDRD Grant 20060049DR. E. M. would like to thank A. Patkós for his hospitality and visitor support from the Eötvös Loránd University, Budapest, Hungary. Both authors thank the KITP at UCSB, and organizers of the KITP Program, Nonequilibrium Dynamics in Particle Physics and Cosmology, Jan.-Mar. 2008, during which a significant segment of this research was carried out, supported in part by the National Science Foundation under Grant No. NSF PHY05-51164. Zs. Sz. was supported by the Hungarian Scientific Research Fund (OTKA) under Postdoctoral Grant No. PD 050015 and also T068108 and K77534.

Appendix A: Gaudin's Method for Matsubara sums

The Gaudin method [22] relies on a systematic decomposition of a product of N fractions, each linearly depending upon Matsubara frequencies and corresponding to a finite temperature propagator, into sums of products of fractions, in each of which the only Matsubara frequencies which appear are the *independent* ones to be summed. Since the number of such independent Matsubara frequencies in a Feynman diagram with ℓ loops is ℓ , no matter how many propagators (N) it may contain, the independent Matsubara sums are more easily performed in this method when $\ell < N$.

The necessary systematic decomposition of the original product of denominators containing the Matsubara frequencies in a given Feynman diagram can itself be represented graphically. For simplicity and definiteness we consider only the case of one external Euclidean frequency ν as in the case of the multi-loop Feynman self-energy diagrams for Σ treated in the text.

To each Feynman multi-loop diagram one associates a set of Gaudin graphs \mathcal{G} . The set is composed of tree diagrams specified by all the possible ways of connecting every vertex of the original Feynman diagram without forming any closed loop. In each of these Gaudin graphs the propagator lines which belong to the tree can be drawn with thick lines and form a set denoted by \mathcal{T}_g . The complement of this set, namely the propagator lines of the original Feynman diagram not contained in the given Gaudin tree graph is denoted by $\bar{\mathcal{T}}_g$. If the total number of propagator lines in the original graph is N , we must have

$$N_{\mathcal{T}_g} + N_{\bar{\mathcal{T}}_g} = N, \quad (\text{A1})$$

where $N_{\mathcal{T}_g}$ is the number of lines in the Gaudin tree graph $g \in \mathcal{G}$, and $N_{\bar{\mathcal{T}}_g}$ the number of lines in its complement. For an original Feynman diagram with ℓ loops, in fact $N_{\bar{\mathcal{T}}_g} = \ell$. The propagator lines in $\bar{\mathcal{T}}_g$ will be treated as the lines with the independent Matsubara frequencies to be summed ω_k , $k = 1, \dots, N_{\bar{\mathcal{T}}_g}$, while

the frequencies in \mathcal{T}_g , denoted Ω_j , $j = 1, \dots, N_{\mathcal{T}_g}$ are treated as dependent. The frequency $\Omega_j(i\nu, p_1^0, \dots, p_\ell^0)$ of each line of \mathcal{T}_g is expressed in terms of the independent real frequencies p_k^0 , $k = 1, \dots, \ell$ by simply replacing each $i\omega_k$ with p_k^0 and the external imaginary frequency $i\nu$, using energy conservation at each vertex.

The general Gaudin decomposition formula then reads

$$\prod_{i=i}^N \frac{e^{i\omega_i \tau_i}}{p_i^0 - i\omega_i} = \sum_{g \in \mathcal{G}} \left[e^{i\nu T_e} \prod_{j \in \mathcal{T}_g} \frac{1}{p_j^0 - i\Omega_j(i\nu, p_k^0)} \prod_{k \in \bar{\mathcal{T}}_g} \frac{e^{i\omega_k T_k}}{p_k^0 - i\omega_k} \right]. \quad (\text{A2})$$

The time arguments in the exponentials are introduced as regulators so that the sums over the independent Matsubara frequencies in Eqs. (A3) and (A4) below converge. These time arguments are somewhat arbitrary and will be taken to zero at the end. They are needed only to guarantee that all sums converge, and results of Matsubara sums which are absolutely convergent will not depend on how the τ_i are assigned. For definiteness one may choose the following rules to fix the τ_i

- Specify the orientation of each line of a diagram, label it with integer number (k) and associate to each line a positive number τ_k . A possible choice is $\tau_k = k\epsilon$, with ϵ positive.
- T_k for a given line is calculated by choosing a loop containing that line and adding the τ_i of all the lines of the loop, formed with the line $k \in \bar{\mathcal{T}}_g$ and lines of the tree \mathcal{T}_g , with \pm sign if the orientation of the line agrees with/is opposite to the orientation of the line $k \in \bar{\mathcal{T}}_g$.
- T_e is determined by the τ 's of the lines of \mathcal{T}_g which connects the two external lines. In this case the reference orientation is the orientation of the external line.

To perform the sums over the independent Matsubara frequencies set $\tau_k = k\epsilon$, let $\epsilon \rightarrow 0^+$ and apply the summation formulas

$$T \sum_n \frac{e^{i\omega_n \tau}}{p^0 - i\omega_n} = \varepsilon(\tau) n_B(\varepsilon(\tau) p^0) e^{p^0 \tau}, \quad \text{for } \omega_n = 2\pi n T, \quad (\text{A3})$$

$$T \sum_n \frac{e^{i\omega_n \tau}}{p^0 - i\omega_n} = -\varepsilon(\tau) n_F(\varepsilon(\tau) p^0) e^{p^0 \tau}, \quad \text{for } \omega_n = (2n + 1)\pi T, \quad (\text{A4})$$

valid for $-\beta < \tau < \beta$. This associates a statistical factor to each line of $\bar{\mathcal{T}}_g$. The $e^{i\omega_n \tau}$ factors are necessary as regulators so that the Matsubara sums are well defined and convergent. After the sums have been performed, the limit $\epsilon \rightarrow 0, \tau \rightarrow 0$ may be taken.

The simplification of the Gaudin method over other methods for performing the sums results from the fact that the frequencies of the last product in (A2) are disentangled and independent of each other. For

each of them the Matsubara sum may be performed separately, using only the fundamental formulas (A3) and (A4), each independent sum yielding its own statistical factor depending on whether that line is bosonic or fermionic. With all Matsubara sums performed, the finite temperature amplitude is expressed in terms of N timelike momentum integrals over p_i^0 , $i = 1, \dots, N_{\mathcal{T}_g}$ and p_j^0 , $j = 1, \dots, N_{\bar{\mathcal{T}}_g}$ and ℓ spatial momentum integrals. The first set of $N - \ell$ timelike integrations can be performed immediately by undoing the spectral representation of the propagators. For subtleties and a more extensive discussion of the Gaudin method the reader is referred to Ref. [23].

Appendix B: Asymptotic analysis of integrals

We present here the high temperature expansion of various integrals which were encountered in the text. We start with the evaluation of the integral

$$\begin{aligned} I_{\pm}(ia) &\equiv \int_0^{\infty} dx g_{\pm}(x) \frac{1}{x^2 - (ia)^2} \\ &= \frac{1}{2ia} \int_0^{\infty} dx g_{\pm}(x) \left[\frac{1}{x - ia} - \frac{1}{x + ia} \right], \end{aligned} \quad (\text{B1})$$

where $g_{\pm}(x) \equiv x/(\exp(x) \pm 1)$. This integral appears in the calculation of the one-loop self-energy at NLO in the HTL approximation, and is typical of the various integrals over soft momenta that are encountered in the two-loop self-energy. Its real part emerging after analytical continuation to real frequencies

$$ia = \frac{i\nu_q}{2T} \rightarrow \frac{\omega}{2T} + i0^+ \quad (\text{B2})$$

was evaluated only numerically in [10].

We note first that although $\omega \ll T$, we cannot set $a = 0$ in the integrand, since then $g_{\pm}(x)/x^2 \sim x^{-2}$ as $x \rightarrow 0$ and the integral would be linearly divergent. As we will see, the linear divergence survives in the imaginary part of I_{-} after analytic continuation but not in the real part, giving a logarithmic dependence on T/ω instead. Indeed integrating (B1) by parts twice, we obtain

$$\begin{aligned} I_{\pm}(ia) &= \frac{1}{2ia} g_{\pm}(0) [\ln(ia) - \ln(-ia)] - \frac{1}{2} g'_{\pm}(0) [\ln(ia) + \ln(-ia)] \\ &\quad - \frac{1}{2ia} \int_0^{\infty} dx g''_{\pm}(x) [(x + ia) \ln(x + ia) - (x - ia) \ln(x - ia)]. \end{aligned} \quad (\text{B3})$$

Under the analytic continuation (B2),

$$\ln(ia) \rightarrow \ln\left(\frac{\omega}{2T}\right), \quad \ln(-ia) \rightarrow \ln\left(\frac{\omega}{2T}\right) - i\pi, \quad (\text{B4})$$

so that

$$I_{\pm} \left(\frac{\omega}{2T} + i0^+ \right) = \frac{i\pi T}{\omega} g_{\pm}(0) + g'_{\pm}(0) \left[\ln \left(\frac{T}{\omega} \right) + \frac{i\pi}{2} \right] + \dots, \quad (\text{B5})$$

where the ellipsis denotes (real) constant terms, and terms that vanish as $\omega/T \rightarrow 0$.

Using then $g_+(0) = 0$, $g_-(0) = 1$, and $g'_{\pm}(0) = \pm 1/2$, we find that to leading order in the high temperature expansion

$$-\text{Re} \int_0^{\infty} dp \frac{p n_B(p)}{p^2 - (\omega + i0^+)^2/4} = \text{Re} \int_0^{\infty} dp \frac{p n_F(p)}{p^2 - (\omega + i0^+)^2} = \frac{1}{2} \ln \frac{T}{\omega}, \quad (\text{B6})$$

$$\text{Im} \int_0^{\infty} dp \frac{p n_B(p)}{p^2 - (\omega + i0^+)^2/4} = \frac{\pi T}{\omega}. \quad (\text{B7})$$

Note that for $T \gg \omega$ only the integral with the Bose-Einstein statistical factor has an imaginary part. These results to leading logarithmic order may also be obtained more rapidly by simply substituting the first two terms of the Taylor expansion of $g_{\pm}(x)$ into (B1), and cutting off the logarithmic UV divergence by a cutoff of order of T .

An analytic calculation which captures the large temperature behavior of (B1) beyond the leading order given in (B6) and (B7) can be performed with the standard technique presented in detail in Appendix C of [42]. Using the identities

$$\frac{1}{\exp(x) \pm 1} = \pm \frac{1}{2} \mp \sum_{n=-\infty}^{\infty} \frac{x}{x^2 + \omega_{\pm}^2(n)}, \quad (\text{B8})$$

where $\omega_+(n) = (2n+1)\pi$ and $\omega_-(n) = 2n\pi$, one separates the integral given in the first line of (B1) into two integrals which are regularized by inserting x^{ϵ} in the integrands. Interchanging the order of the summation and integration one uses partial fractioning and exploits the properties of the sums to write

$$I_{\pm}(ia) = \lim_{\epsilon \rightarrow 0} \left\{ \pm \frac{1}{2} \int_0^{\infty} dx \frac{x^{1+\epsilon}}{x^2 + a^2} + l_{\pm} \int_0^{\infty} dx \frac{x^{\epsilon}}{x^2 + a^2} \right. \\ \left. \pm 2a^2 \int_0^{\infty} dx \frac{x^{\epsilon}}{x^2 + a^2} \sum_{n=l_{\pm}}^{\infty} \frac{1}{\omega_{\pm}^2(n) - a^2} \mp 2 \sum_{n=l_{\pm}}^{\infty} \frac{\omega_{\pm}^2(n)}{\omega_{\pm}^2(n) - a^2} \int_0^{\infty} dx \frac{x^{\epsilon}}{x^2 + \omega_{\pm}^2(n)} \right\}, \quad (\text{B9})$$

where $l_{\pm} = -(-1 \pm 1)/2$. The second term is the contribution of the static Matsubara mode $n = 0$ in $I_-(a)$. In the second and third terms the limit $\epsilon \rightarrow 0$ can be taken. In the last term one does the integral and then one expands the summand around $a = 0$ in order to be able to do the sum over n . Note, that for bosons this expansion can be safely done once we separated the static mode. The limit $\epsilon \rightarrow 0$ is taken at the very end which results in the cancellation of the $1/\epsilon$ type singularity present in the first and last terms of (B9). With these sequence of steps one obtains

$$I_+(ia) = -\frac{1}{2} \left(\ln \frac{2a}{\pi} + \gamma_E \right) + \frac{\pi a}{8} - \frac{7\zeta(3)}{8\pi^2} a^2 + \mathcal{O}(a^3), \quad (\text{B10a})$$

$$I_-(ia) = \frac{\pi}{2a} + \frac{1}{2} \left(\ln \frac{a}{2\pi} + \gamma_E \right) - \frac{\pi a}{24} + \frac{\zeta(3)}{8\pi^2} a^2 + \mathcal{O}(a^3), \quad (\text{B10b})$$

where $a = \nu_q/(2T)$ and γ_E is the first Stieltjes constant (Euler's constant).

We can use the result (B5) or (B10) for the integral (B1) to evaluate the integral appearing in (4.28) and (5.21c) at leading order in the high temperature expansion. One defines the integral

$$L_{\pm}(i\nu_q) \equiv \int_{-1}^1 dx \int_0^{\infty} dp k p f_{\pm}(p) \sum_{r,s=\pm 1} \frac{r}{(i\nu_q - 2sp)((i\nu_q)^2 - 2kp(x - rs) - 2i\nu_q(rk + sp))}, \quad (\text{B11})$$

where $f_-(x) = n_B(x)$ and $f_+(x) = n_F(x)$. In the limit $k \gg p, \nu_q$ one approximates $-2kp(x - rs) - 2i\nu_q(rk + sp) - rskp - riv_q/2 \simeq -2k[p(x - rs) + riv_q]$, then one uses partial fractioning and the change $x \rightarrow -x$ in some terms to rewrite the integral in the following form:

$$L_{\pm}(i\nu_q) \simeq \int_{-1}^1 dx \frac{1}{1-x^2} \int_0^{\infty} dp \left[\frac{pf_{\pm}(p)}{p^2 - (i\nu_q/2)^2} - 2 \frac{pf_{\pm}(p)}{p^2 - (i\nu_q/(1+x))^2} \right]. \quad (\text{B12})$$

Then one uses (B6) and (B7) to write

$$L_{\pm}(\omega + i0^+) \simeq \int_{-1}^1 dx \frac{1}{1-x^2} \left[-l_{\pm} x \frac{i\pi T}{\omega} \pm \frac{1}{2} \left(2 \ln \frac{\omega}{T(1+x)} - \ln \frac{\omega}{2T} \right) \right], \quad (\text{B13})$$

where $l_{\pm} = -(-1 \pm 1)/2$. The imaginary part vanishes since the integrand is odd in x . Keeping in the real part the terms which are leading order in the temperature one has

$$L_{\pm}(\omega + i0^+) \simeq \mp \frac{1}{2} \ln \frac{T}{\omega} \int_{-1}^1 dx \frac{1}{1-x^2} + 0i. \quad (\text{B14})$$

With the same method one can perform the asymptotic analysis of the integrals appearing in (4.17) and (4.22). Introducing a new variable of integration $x = p/T$, the notation $a = \nu_q/(2T)$, $b_{\pm} = (\nu_q^2 \pm M^2)/(2\nu_q T)$ and taking the derivative with respect to M^2 of the various terms in (4.17) and (4.22) one obtains

$$\frac{\partial}{\partial M^2} \left\{ \mu_+ \int_0^{\infty} dx g_{\pm}(x) \frac{\ln(1 + \frac{x^2}{a^2})}{x^2 + b_{\pm}^2} \right\} \Big|_{M=0} = \frac{1}{2i\nu_q} \left\{ \mp \left(2 + a \frac{\partial}{\partial a} \right) I_{\pm}(ia) \right. \quad (\text{B15a})$$

$$\left. + \left(1 \mp a \frac{\partial}{\partial a} \right) \int_0^{\infty} dx g_{\pm}(x) \frac{\ln \left(1 + \frac{x^2}{a^2} \right)}{x^2 + a^2} \right\}, \quad (\text{B15b})$$

$$\frac{\partial}{\partial M^2} \left\{ \int_0^{\infty} dx x g_-(x) \frac{\cot^{-1}(\frac{x}{a})}{x^2 + b_-^2} \right\} \Big|_{M=0} = \frac{a}{\nu_q^2} \left[\frac{1}{2a} \frac{\partial}{\partial a} (a^2 I_-(ia)) - \frac{\partial}{\partial a} \int_0^{\infty} dx x g_-(x) \frac{\cot^{-1}(\frac{x}{a})}{x^2 + a^2} \right], \quad (\text{B15c})$$

$$\frac{\partial}{\partial M^2} \left\{ 2i \frac{\mu_- \mu_+}{T} \int_0^{\infty} \frac{dx}{e^x + 1} \frac{\tan^{-1}(\frac{x}{a})}{x^2 + b_+^2} \right\} \Big|_{M=0} = \frac{i}{4T} \left\{ \frac{\partial}{\partial a} I_+(ia) - 2a \frac{\partial}{\partial a} \int_0^{\infty} \frac{dx}{e^x + 1} \frac{\tan^{-1}(\frac{x}{a})}{x^2 + a^2} \right\}, \quad (\text{B15d})$$

$$\frac{\partial}{\partial M^2} \left\{ 4\mu_- I_+(ib_+) \right\} \Big|_{M=0} = -\frac{2}{i\nu_q} \left(1 + a \frac{\partial}{\partial a} \right) I_+(ia), \quad (\text{B15e})$$

$$\frac{\partial}{\partial M^2} \left\{ \int_0^{\infty} dx g_-(x) \frac{x}{x^2 + b_-^2} \right\} \Big|_{M=0} = -\frac{a}{\nu_q^2} \frac{\partial}{\partial a} \int_0^{\infty} dx g_-(x) \frac{x}{x^2 + a^2}, \quad (\text{B15f})$$

where again $g_{\pm}(x) = x/(\exp(x) \pm 1)$. The only term where one cannot take the limit $M^2 = 0$ is

$$\frac{\partial}{\partial M^2} \left\{ b_- \ln \frac{M^2}{\nu_q^2} I_-(ib_-) \right\} = \left[\frac{a}{M^2} - \frac{a}{\omega^2} \left(1 + \ln \frac{M^2}{\nu_q^2} \right) \left(1 + a \frac{\partial}{\partial a} \right) \right] I_-(ia) + \mathcal{O}(M^2). \quad (\text{B16})$$

Here we expanded in powers of M . In the expressions above $I_{\pm}(ia)$ is given by (B1).

Then the method described between (B8) and (B10a) gives the following series:

$$\int_0^{\infty} dx g_+(x) \frac{\ln \left(1 + \frac{x^2}{a^2} \right)}{x^2 + a^2} = \frac{1}{2} \ln^2 a + \left(\gamma_E - \ln \frac{\pi}{2} \right) \ln a + C_1 - \frac{a\pi}{4} (1 - \ln 2) + \mathcal{O}(a^2), \quad (\text{B17a})$$

$$\int_0^{\infty} dx g_-(x) \frac{\ln \left(1 + \frac{x^2}{a^2} \right)}{x^2 + a^2} = \frac{\pi}{a} \ln 2 - \frac{1}{2} \ln^2 a - (\gamma_E - \ln(2\pi)) \ln a + C_2 + \frac{a\pi}{12} (1 - \ln 2) + \mathcal{O}(a^2), \quad (\text{B17b})$$

$$\int_0^{\infty} \frac{dx}{e^x + 1} \frac{\tan^{-1} \left(\frac{x}{a} \right)}{x^2 + a^2} = \frac{\pi^2}{16a} + \frac{\pi}{8} \ln a + C_3 + \frac{a\pi}{8} \left(\ln 2 - \frac{7}{\pi^3} \zeta(3) \right) + \mathcal{O}(a^2), \quad (\text{B17c})$$

$$\int_0^{\infty} dx x g_-(x) \frac{\cot^{-1} \left(\frac{x}{a} \right)}{x^2 + a^2} = \frac{\pi}{2} \ln 2 + \frac{a}{2} \left(-1 + \gamma_E + \frac{\pi^2}{8} + \ln \frac{a}{2\pi} \right) + \mathcal{O}(a^2), \quad (\text{B17d})$$

$$\int_0^{\infty} dx g_-(x) \frac{x}{x^2 + a^2} = \frac{a\pi}{4} - \ln a + \mathcal{O}(a^2), \quad (\text{B17e})$$

where the constants are given in terms of the first two Stieltjes constants γ_E and γ_1 and the Glaisher's constant G as $C_1 = \frac{\pi^2}{8} - \gamma_E \ln \frac{\pi}{2} - \frac{1}{2} \ln^2 2 - \frac{1}{2} \ln \frac{4}{\pi} \ln \pi - \gamma_1$, $C_2 = -\frac{\pi^2}{8} - \frac{1}{2} \ln^2(2\pi) + \gamma_E \ln(2\pi) + \gamma_1$, and $C_3 = \frac{\pi}{24}(3\gamma_E + 4 \ln 2 - 36 \ln G)$.

In order to derive (4.7), (4.8), and (4.9) first we define two integrals,

$$J_-(\mu_-) \equiv \int_0^{\infty} \frac{dp}{E_p} \frac{n_B(E_p)}{p^2 - \mu_-^2} = \frac{\pi T}{2\mu_+^2} \left[\frac{1}{(-\mu_-^2)^{1/2}} - \frac{1}{M} \right] - \frac{1}{2\mu_- \mu_+} \left[\ln \frac{M}{i\nu_q} + i \frac{\pi}{2} \right] + \mathcal{O} \left(\frac{1}{Tm}, \frac{1}{T\mu_-} \right), \quad (\text{B18})$$

$$T_B^{\beta}(M) \equiv \frac{1}{2\pi^2} \int_0^{\infty} dp p^2 \frac{n_B(E_p)}{E_p} = \frac{T^2}{12} - \frac{MT}{4\pi} - \frac{M^2}{8\pi^2} \ln \left(c \frac{M}{T} \right) + \mathcal{O} \left(\frac{M^4}{T^2} \right), \quad (\text{B19})$$

where $\mu_{\pm} = ((i\nu_q)^2 \pm M^2)/(2i\nu_q)$, $E_p^2 = p^2 + M^2$, and $\ln(c) = \gamma_E - 1/2 - \ln(4\pi)$. The integrals were evaluated in the high temperature expansion with the method described between (B8) and (B10a). The first term in the expression of $J_-(\mu_-)$ is the contribution of the static Matsubara mode and can be obtained also with the approximation $n_B(E_p) \simeq T/E_p$.

Then using that

$$\int_0^{\infty} dp \frac{n_B(E_p)}{E_p} = -2 \int_0^{\infty} dp p^2 \frac{\partial}{\partial p^2} \frac{n_B(E_p)}{E_p} = -2 \frac{\partial}{\partial M^2} \int_0^{\infty} dp p^2 \frac{n_B(E_p)}{E_p} = -4\pi^2 \frac{\partial}{\partial M^2} T_B^{\beta}(M), \quad (\text{B20})$$

the first two integrals in (4.5) can be written as

$$\int_0^{\infty} dp \frac{p^2}{E_p} \frac{n_B(E_p)}{E_p^2 - \mu_+^2} = -4\pi^2 \frac{\partial T_B^{\beta}(M)}{\partial M^2} + \mu_-^2 J_-(\mu_-), \quad (\text{B21})$$

$$\int_0^{\infty} dp \frac{p^2 E_p n_B(E_p)}{E_p^2 - \mu_+^2} = 2\pi^2 \left[1 - 2\mu_+^2 \frac{\partial}{\partial M^2} \right] T_B^{\beta}(M) + \mu_+^2 \mu_-^2 J_-(\mu_-). \quad (\text{B22})$$

Using the expressions given in (B18) and (B19) one obtains

$$\frac{\partial}{\partial M^2} \left[((i\nu_q)^2 + M^2) \int_0^\infty dp \frac{p^2}{E_p} \frac{n_B(E_p)}{E_p^2 - \mu_+^2} \right] \simeq \pi T \left[\frac{1}{M} - \frac{2i}{i\nu_q} \right] + \ln \frac{M}{i\nu_q} - \frac{1}{2} \ln \frac{T}{i\nu_q} + C, \quad (\text{B23})$$

$$\frac{\partial}{\partial M^2} \int_0^\infty dp \frac{p^2 E_p n_B(E_p)}{E_p^2 - \mu_+^2} \simeq \frac{1}{8} - i \frac{\pi T}{4i\nu_q}, \quad (\text{B24})$$

where $C = (1 + \gamma_E - \ln(4\pi))/2$ and the expressions on the right hand sides were expanded for small M . After analytical continuation ($i\nu_q \rightarrow \omega + i0^+$) one obtains (4.7) and (4.8).

For the last term of (4.5) one may introduce $x = E_p/T$ as a new variable of integration and obtain

$$I_B \equiv \frac{\partial}{\partial M^2} \left\{ (\nu_q^2 - M^2) \int_\mu^\infty dx \frac{x}{e^x - 1} \frac{1}{x^2 + b^2} \ln \left[\frac{x + \sqrt{x^2 - \mu^2}}{x - \sqrt{x^2 - \mu^2}} \right] \right\}, \quad (\text{B25})$$

where $\mu = M/T$ and $b = (\nu_q^2 - M^2)/(2\nu_q T)$. In order to obtain the contribution of (B25) for $M, |i\nu_q| \ll T$ at leading order in the high- T expansion one splits the integral into two pieces by introducing the point \bar{x} satisfying $0 < \mu, b \ll \bar{x} \ll 1$. For $x > \bar{x}$ one expands the logarithm for large x and use the method described between (B8) and (B10a). For $x < \bar{x}$ one expands $x/(e^x - 1) \simeq 1 - x/2$ and one scales the variables with μ . Writing the logarithm as a difference of two logarithms one introduces in the resulting two integrals the argument of the respective logarithm as a new variable of integration. The integrals can be done with the symbolic program Mathematica. Adding the two parts the \bar{x} dependence cancels and the result is

$$I_B = -\frac{\pi\nu_q T}{M^2} + \frac{\nu_q^2}{2M^2} \left[\ln \frac{T}{\nu_q} + \ln(4\pi) - \gamma_E \right] + \frac{1}{2} \ln \left(\frac{T}{\nu_q} \right) \ln \left(\frac{\nu_q T}{M^2} \right) + (\ln(4\pi) - \gamma_E) \ln \frac{T}{M} - \frac{1}{2} \ln \frac{T}{\nu_q} + C_B + \mathcal{O} \left(\frac{\nu_q}{T}, \frac{M}{T} \right), \quad (\text{B26})$$

where $C_B = \frac{\gamma_E}{2} - \gamma_1 + \frac{\pi^2}{12} + \frac{1}{2} \ln^2(4\pi) - (\gamma_E + \frac{1}{2}) \ln(4\pi)$. After analytical continuation one obtains (4.9).

The high temperature asymptotics of integrals of the form

$$F = \int_0^\infty \frac{dE}{\sqrt{E^2 - M^2}} n_B(E) f(E), \quad (\text{B27})$$

with $f(E)$ a regular differentiable function of E at $E = 0$, encountered in Sec. VI can be handled by similar methods. Introducing an intermediate scale \bar{E} , such that $M \ll \bar{E} \ll T$, one can write

$$F = \int_M^{\bar{E}} \frac{dE}{\sqrt{E^2 - M^2}} \left(\frac{T}{E} - \frac{1}{2} + \dots \right) (f(0) + Ef'(0) + \dots) + \int_{\bar{E}}^\infty \frac{dE}{E} n_B(E) f(E) + \dots, \quad (\text{B28})$$

where the ellipsis gives terms of order M/T or smaller. Performing the first integral exactly and integrating the second by parts twice gives

$$F = Tf(0) \left[\frac{\pi}{2M} - \frac{1}{\bar{E}} \right] + \left[Tf'(0) - \frac{1}{2} \right] \ln \frac{\bar{E}}{M} - n_B(E) f(E) \Big|_{\bar{E}}^\infty$$

$$\begin{aligned}
& + \frac{d}{dE} [En_B(E)f(E)] \ln \frac{E}{T} \Big|_{\bar{E}}^{\infty} + \int_{\bar{E}}^{\infty} dE \frac{d^2}{dE^2} [En_B(E)f(E)] \ln \frac{E}{T} \\
& = \frac{\pi T}{2M} f(0) + T f'(0) \ln \frac{T}{M} - \frac{f(0)}{2} \ln \frac{T}{M} + T f'(0) + \mathcal{O}(1)
\end{aligned} \tag{B29}$$

in the high temperature limit. This gives the results (6.10) and is used in obtaining (6.18) and (6.19). A result analogous to (B29) is easily obtained for the Fermi-Dirac distribution n_F . Finally we note that the same method of introducing an intermediate scale, $|\nu_q| \ll \bar{E} \ll T$ may be used to extract the asymptotic behavior of the finite integrals in Eqs. (6.16) as well.

References

- [1] R. D. Pisarski, Phys. Rev. Lett. **63**, 1129 (1989).
- [2] M. H. Thoma, *Applications of High Temperature Field Theory to Heavy Ion Collisions*, in *Quark-gluon plasma 2*, edited by R. C. Hwa, World Scientific: Singapore (1995).
- [3] M. Le Bellac, *Thermal Field Theory*, Cambridge University Press: Cambridge (1996).
- [4] J.-P. Blaizot and E. Iancu, Phys. Rept. **359**, 355 (2002).
- [5] J. I. Kapusta and Ch. Gale, *Finite-Temperature Field Theory: Principles and Applications*, 2nd Edition, Cambridge University Press: Cambridge (2006).
- [6] E. Braaten and R. D. Pisarski, Phys. Rev. Lett. **64**, 1338 (1990).
- [7] J. Frenkel and J. C. Taylor, Nucl. Phys. **B334**, 199 (1990).
- [8] E. Braaten and R. D. Pisarski, Nucl. Phys. **B337**, 569 (1990).
- [9] E. Braaten and R. D. Pisarski, Phys. Rev. D **42**, 2156 (1990).
- [10] I. Mitra, Phys. Rev. D **62**, 045023 (2000).
- [11] S.-Y. Wang, Phys. Rev. D **70**, 065011 (2004).
- [12] M. Qader, S. S. Masood and K. Ahmed, Phys. Rev. D **46**, 5633 (1992).
- [13] T. Altherr, E. Petitgirard and T. del Rio Gaztelurrutia, Phys. Rev. D **47**, 703 (1993).
- [14] H. Schulz, Nucl. Phys. **B413**, 353 (1994).
- [15] A. Majumder and C. Gale, Phys. Rev. C **65**, 055203 (2002).
- [16] M. E. Carrington and E. Mottola, Nucl. Phys. **A785**, 142 (2007).
- [17] R. Kobes, G. Kunstatter and K. Mak, Phys. Rev. D **45**, 4632 (1992).
- [18] E. Braaten and R. D. Pisarski, Phys. Rev. D **46**, 1829 (1992).
- [19] F. Flechsigg and H. Schulz, Phys. Lett. **B349**, 504 (1995).
- [20] M. E. Carrington, Phys. Rev. D **75**, 045019 (2007).
- [21] M. E. Carrington, A. Gynther and D. Pickering, Phys. Rev. D **78**, 045018 (2008).
- [22] M. Gaudin, Nuov. Cim. **38**, 844 (1965).
- [23] J.-P. Blaizot and U. Reinosa, Nucl. Phys. **A764**, 393 (2006).

- [24] A. Peshier, K. Schertler and M. H. Thoma, *Annals Phys.* **266**, 162 (1998).
- [25] M. E. Peskin and D. V. Schroeder, *An Introduction to Quantum Field Theory*, Westview Press: New York (1995).
- [26] H. A. Weldon, *Phys. Rev. D* **28**, 2007 (1983).
- [27] V. V. Klimov, *Sov. J. Nucl. Phys.* **33**, 934 (1981).
- [28] H. A. Weldon, *Phys. Rev. D* **26**, 1394 (1982).
- [29] J.-P. Blaizot and E. Iancu, *Phys. Rev. D* **55**, 973 (1997).
- [30] R. Baier, B. Pire and D. Schiff, *Phys. Rev. D* **38**, 2814 (1988).
- [31] G. Gattoff and J. Kapusta, *Phys. Rev. D* **41**, 611 (1990).
- [32] P. Aurenche, F. Gelis, R. Kobes, and E. Petitgirard, *Z. Phys. C* **75**, 315 (1997).
- [33] H. Zaraket, [hep-ph/9810246], in *Proceedings of the 5th Thermal Field Theory Workshop, Regensburg, 1998*, edited by U. Heinz.
- [34] P. Aurenche, F. Gelis, and H. Zaraket, *JHEP* **0207**, 063 (2002).
- [35] M. H. Thoma and C. T. Traxler, *Phys. Lett. B* **378**, 233 (1996).
- [36] A. Abada and K. Bouakaz, *JHEP* **0601**, 161 (2006).
- [37] R. D. Pisarski, *Phys. Rev. D* **47**, 5589 (1993).
- [38] U. Kraemmer, A. K. Rebhan and H. Schulz, *Ann. Phys. N. Y.* **238**, 286 (1995); A. K. Rebhan, hep-ph/960841.
- [39] P. Aurenche, F. Gelis, G. D. Moore, and H. Zaraket, *JHEP* **0212**, 006 (2002).
- [40] S. Jeon, *Phys. Rev. D* **52**, 3591 (1995); S. Jeon and L. G. Yaffe, *Phys. Rev. D* **53**, 5799 (1996).
- [41] J.-S. Gagnon and S. Jeon, *Phys. Rev. D* **75**, 025014 (2007); *ibid.* **76**, 105019 (2007).
- [42] L. Dolan and R. Jackiw, *Phys. Rev. D* **9**, 3320 (1974).